A STUDY OF THE CHEMICAL CLEAVAGE OF BENZYLIC-SILICON BONDS

By

PAULY KAVALAKATT

A thesis

Submitted to the School of Graduate Studies

in Partial Fulfilment of the

Requirements for the Degree of

Master of Science

McMaster University

MASTER OF SCIENCE (2002) McMASTER UNIVERSITY

(Chemistry) Hamilton, Ontario

TITLE: A Study Of The Chemical Cleavage Of Benzylic-Silicon Bonds

AUTHOR: Pauly Kavalakatt

SUPERVISOR: Professor H. D. H. Stöver

NUMBER OF PAGES: 162

Abstract

The key objective of this research was to study the rates of the chemical cleavage of benzyl-silicon bonds in small model molecules, oligomers, polymers, copolymers, and crosslinked microspheres and microgels.

Substrate species including benzyltrimethylsilane (BTMS), *p*-isopropylbenzyltrimethylsilane (ISO-BTMS), oligomeric and polymeric vinylbenzyltrimethylsilane (VBTMS), and their copolymers with styrene and methyl methacrylate as well as microspheres and microgels of bis(vinylbenzyl)dimethylsilane (BVBDMS) were synthesized using Grignard reaction, free radical polymerization, and precipitation polymerization.

Narrow dispersed microspheres were synthesized from bis(vinylbenzyl)dimethylsilane (BVBDMS) by precipitation polymerization in acetonitrile. The reactivities of *para/para, meta/meta,* and *meta/para* isomers of BVBDMS in precipitation polymerization were found to be similar and to obey first-order kinetics. Their apparent rate of polymerization is comparable with that of *meta* and *para* divinylbenzene isomers under identical polymerization conditions. FT-IR analysis of BVBDMS microspheres shows that there are only few pendant double bonds in the particles. This is likely due to the similar reactivity of isolated double bonds of BVBDMS.

Two nucleophilic (hydroxide and fluoride ion) and one oxidative (ceric ammonium nitrate) reagents have been used to cleave the benzylic-silicon bonds of the substrates. The cleavage reactions were quantitatively monitored by ^{1}H-NMR / ^{29}Si-NMR or FT-

IR to derive the reaction kinetic parameters. The reaction behavior of most of the substrates differed from that expected based on the *Flory's principle of equal reactivity.*

Among the hydroxide ion initiated cleavage reactions, the small molecules and the oligomeric analogs obeyed first-order kinetics, but the homopolymer and the copolymers deviated from first-order kinetics. This could be due to the low concentration of hydroxide ion in the polymer matrix, arising from the exclusion of polar hydroxide ion from the hydrophobic polymer matrix. The *p*-isopropylbenzyltrimethylsilane exhibited a lower pseudo first-order rate than benzyltrimethylsilane. This is attributed to an electron releasing substituent effect. Methyl methacrylate can accelerate the reaction on poly(vinylbenzyltrimethylsilane-*co*-methyl methacrylate) by increasing the overall copolymer polarity. The reverse is true for the corresponding styrene copolymers owing to the steric hindrance offered by the phenyl ring of styrene, and the enhanced hydrophobic repulsion against the access of hydroxide ion into the polymer matrix. An electrophilically assisted process was proposed as a principal reaction mechanism for this cleavage reaction. It was found that the only nucleophile attacking on silicon would be the hydroxide ion in KOH/EtOH/THF promoted reactions.

Fluoride ion initiated cleavage reactions of substrates containing benzylic-silicon bonds were found to follow first-order kinetics. The reaction on small molecules was not studied due to their very rapid reaction at room temperature. The homopolymer of vinylbenzyltrimethylsilane exhibited a higher rate of reaction than the corresponding oligomer. However, the change in the reaction rate within a copolymer series, differing

in molecular weight and composition, was not significant. Poly(VBTMS-*co*-MMA) exhibited a rate higher than that of styrene copolymers for polarity or steric reasons.

Oxidative cleavage of benzylic-silicon bond by ceric ammonium nitrate (CAN) was found to obey first-order kinetics at 1:3 substrate to cerium(IV) ratio, and did not show any deviation in reaction order even at higher CAN concentration. The electron releasing isopropyl group reduces the oxidation potential of *p*-isopropylbenzyltrimethylsilane (ISO-BTMS), resulting in an enhanced reaction rate compared to benzyltrimethylsilane (BTMS). This rate accelerating substituent effect, together with a much higher negative value (- 5.4) of Hammett reaction constant ρ is in accordance with the radical-cation mechanism operating in ceric ammonium nitrate promoted oxidation reactions. Significant loss of silane functionality was observed in reactions with polymeric substrates. This is attributed to the benzylic radical coupling reactions. The possibility of polymer backbone cleavage is ruled out for the following reasons: A) lack of significant molecular weight reduction in the oxidation products of polymeric substrates. B) about 100 times easier breaking of benzylic-silicon bond as trimethylsilyl cation than a hydrogen from carbon as proton, and the steric congestion offered by the polymer chain favors the benzylic radical formation only at the primary carbon, not on *tertiary* methine (C-H) on the chain.

Acknowledgements

First and formost, I am deeply grateful to Dr. H. D. H. Stöver, my supervisor, for his supervision, instruction, encouragement, and support in completing this project. His patience, kindness, enthusiasm and high level of knowledge are well appreciated.

Sincere appreciation is also extended to the following people for their sincere support during the course of this project.

Dr. Don Hughes, Dr. Brian Sayer, Mr. George Timmins for their assistance in using the NMR and IR facilities, and interpreting some data.

Dr. M. A. Brook and Dr. J. Warkenton for their involvement in some scientific discussions related to this project.

All staff members of chemistry departmental office for their all sort of help provided. Especially, I am grateful to Carol Dada for her valuable help and sincere advice.

The financial support of the Natural Science and Engineering Research Council of Canada, Ontario Center of Materials Research, the Department of Chemistry and McMaster University are gratefully acknowledged.

Finally, my hearty thanks go to my wife Shyja who put in a lot of patience.

Table of Contents

Abstract iii

Acknowledgements vi

Table of Contents vii

List of Figures xii

List of Tables xvii

List of Abbreviations xx

CHAPTER 1. INTRODUCTION

1.1 Properties of the silicon-carbon bond 1

1.2 Properties of the trimethylsilyl group 2

1.2.1 β-effect 4

1.2.2 α-effect 9

1.3 Characteristics of benzylic-silicon bond 10

1.4 Types of reactions of benzylic-silicon compounds 14

1.4.1 Nucleophilic reactions 15

1.4.2 Electrophilic reactions 17

1.4.3 Oxidative reactions 19

1.5 An overview of chemical reactivity of macromolecules and small homologs 19

1.5.1 Effect of local concentration 20

1.5.2 Effect of reaction medium on functional group reactivity 21

1.5.3 Effect of morphology 23

1.5.4 Effect of neighboring groups 25

1.5.4.1 Electrostatic effect 25

1.5.4.2 Steric hindrance 27

1.5.4.3 Tacticity 28

1.5.5 Reactivity of the polymer gel 32

Aim of Research 34

CHAPTER 2. EXPERIMENTAL METHODS

2.1 General procedures 35

2.2 Materials 35

2.3 Instrumentation and analytical procedures 35

2.4 General Synthesis of benzyltrimethylsilane (BTMS), *p*-isopropyl benzyltrimethylsilane (ISO-BTMS), *m/p*-vinylbenzyltrimethylsilane (*m/p*VBTMS) and bis(vinylbenzyl)dimethylsilane (BVBDMS) - Grignard Reaction 37

2.5 Oligomerization of *m/p*-vinylbenzyltrimethylsilane 41

2.6 Free radical solution polymerization of *m/p*-vinylbenzyltrimethylsilane 41

2.7 Copolymerization of *m/p*-vinylbenzyltrimethylsilane with styrene and methyl methacrylate 42

2.8 Selective cleavage of benzylic-silicon bondsby KOH/EtOH/THF 43

2.9 Selective cleavage of benzylic-silicon bonds by tetrabutyl ammonium fluoride/THF

2.10 Selective cleavage of benzylic-silicon bonds by ceric ammonium nitrate/acetic acid/benzene 45

2.11 Precipitation polymerization of bis(vinylbenzyl)dimethylsilane (BVBDMS) 46

2.11.1 Determination of apparent rate of polymerization 48

2.11.2 Cleavage of bis(vinylbenzyl)dimethylsilane microspheres / microgel by tetrabutyl ammonium fluoride/THF 48

2.11.3 Cleavage of bis(vinylbenzyl)dimethylsilane (BVBDMS) microspheres by ceric ammonium nitrate/acetic acid/benzene 49

CHAPTER 3. RESULTS AND DISCUSSION

3.1 Synthesis of small molecules and linear polymer model compounds 50

3.1.1 Structure and composition of styrene and methyl methacrylate copolymers of vinylbenzyltrimethylsilane 54

3.2 Synthesis of cross-linked model compounds 61

3.2.1 Mechanism of particle formation 64

3.2.2 Kinetic considerations 69

3.3 Cleavage of Benzylic-Silicon bonds by KOH / EtOH / THF 83

3.3.1 Proposed reaction mechanism 84

3.3.2 Cleavage of small model molecules by KOH/EtOH/THF 88

3.3.3 Cleavage of polymer analogs by KOH/EtOH/THF 97

3.3.4 Equilibrium behavior of trimethylsilanol 111

3.4 Cleavage of Benzylic-Silicon Bond by Tetrabutyl Ammonium Fluoride/ THF (TBAF/THF) 115

3.4.1 Cleavage on linear polymer models by TBAF/THF 116

3.4.2 Degradation of cross-linked bis(vinylbenzyl)dimethylsilane (BVBDMS) network by TBAF/THF 120

3.4.2.1 Cleavage of bis(vinylbenzyl)dimethylsilane (BVBDMS) microgel (PP04) by TBAF/THF 120

3.4.2.2 Cleavage of bis(vinylbenzyl)dimethylsilane (BVBDMS) microspheres by TBAF/THF 124

3.5 Cleavage of Benzylic-Silicon Bond by Ceric Ammonium Nitrate / Acetic acid / Benzene (CAN/AcOH/Bz) 127

3.5.1 Oxidation of small molecules and polymer analogs by CAN/AcOH/Bz 128

3.5.2 Oxidation mechanism 143

3.5.3 Oxidative degradation of bis(vinylbenzyl)trimethylsilane (BVBDMS) microspheres 153

3.6 CONCLUSIONS 156

3.7 REFERENCES 159

List of Figures

Figure 1.1 σ-π conjugation 6

Figure 1.2 Schematic representation of (p-d)π bonding 9

Figure 1.3 Charge-transfer frequencies of TCNE complexes with various tin compounds

Figure 1.4 Charge-transfer frequencies of TCNE complexes with various organic compounds 13

Figure 1.5 Cleavage of benzylic-silicon bond by intramolecular electrophilic substitution 18

Figure 1.6 Gel and macro reticular structure of cross linked polymer matrix 33

Figure 3.1.1 Typical Grignard synthesis 50

Figure 3.1.2 ^{1}H-NMR spectra of A) vinylbenzylchloride (*m/p*VBC) B) vinylbenzyltrimethylsilane (*m/p*VBTMS) C) Poly(*m/p*-vinylbenzyltrimethylsilane) 52

Figure 3.1.3 Comparison of ^{1}H NMR spectra of copolymers of VBTMS and MMA with different feed ratio A) 1:1 VM11 B) 1:2 VM12 C) 1:5 VM15 58

Figure 3.1.4 Comparison of ^{1}H NMR spectra of copolymers of VBTMS and Styrene with different feed ratio A) 1:1 VS11 B) 1:2 VS12 C) 1:5 VS15 59

Figure 3.1.5 Comparison of ^{13}C NMR spectra of copolymers of VBTMS and MMA with different feed ratio A) 1:1 VM11 B) 1:2 VM12 C) 1:5 VM15 60

Figure 3.2.1 Synthesis of bis(vinylbenzyl)dimethylsilane (BVBDMS) microspheres. 62

Figure 3.2.2 ^{1}H-NMR spectrum of bis(vinylbenzyl)dimethylsilane (BVBDMS). 62

Figure 3.2.3 Gas chromatogram (Bottom) and the resolved dimethylsilyl ^{1}H-NMR peak (Top) of bis(vinylbenzyl)dimethylsilane (BVBDMS) to show *m/p, m/m & p/p* isomeric ratio. 63

Figure 3.2.4 Schematic representation of microsphere formation in precipitation polymerization. 65

Figure 3.2.5 Narrow dispersed bis(vinylbenzyl)dimethylsilane (BVBDMS) microspheres (with magnified) made in neat acetonitrile. 67

Figure 3.2.6 Effect of Acetonitrile/Toluene volume ratio on bis(vinylbenzyl)dimethylsilane (BVBDMS) particle formation. 68

Figure 3.2.7 Particle size build up during precipitation polymerization of bis(vinylbenzyl)dimethylsilane (BVBDMS). 69

Figure 3.2.8 GC calibration plot for three isomeric bis(vinylbenzyl)dimethylsilane (BVBDMS). 71

Figure 3.2.9 Conversion-Time plot of precipitation polymerization of bis(vinylbenzyl)dimethylsilane (BVBDMS)(GC). 71

Figure 3.2.10 First-order plot of conversion precipitation polymerization for A) *p/p* B) *m/m* C) *m/p* isomers of bis(vinylbenzyl)dimethylsilane (BVBDMS) 72

Figure 3.2.11 FT-IR spectra of A) BVBDMS cross-linker B) BVBDMS sol fraction C) BVBDMS microspheres. 75

Figure 3.2.12 FT-IR spectra of A) DVB monomer B) DVB microspheres. 76

Figure 3.3.1 Effect of [KOH] on cleavage rate of ISO-BTMS (^{29}Si). 88

Figure 3.3.2 Typical GC calibration graph for BTMS and ISO-BTMS with decane as an internal standard. 89

Figure 3.3.3 Conversion-Time plot of alkali cleavage of BTMS and ISO-BTMS (GC). 89

Figure 3.3.4 First-order plot of alkali cleavage of BTMS and ISO-BTMS (GC). 90

Figure 3.3.5 ^{29}Si INVERSEGATE spectra of BTMS after A. 40% B. 52.5% C. 84% of cleavage by KOH/EtOH/THF at 72 °C. 92

Figure 3.3.6 ^{29}Si INVERSEGATE spectra of ISO-BTMS after A. 46% B. 57% C. 85% of cleavage by KOH/EtOH/THF at 90 °C. 93

Figure 3.3.7 Conversion-Time plot & First-order plot (^{29}Si) of linear monomer and crosslinker. 95

Figure 3.3.8 Arrhenius plot for KOH cleavage of BTMS and ISO-BTMS(^{29}Si). 96

Figure 3.3.9 ^{1}H-NMR spectra of homopolymer poly(*m/p*-VBTMS) after A) 13.8% B) 17.6 % C) 28% of cleavage by KOH/EtOH/THF. 99

Figure 3.3.10 Conversion-Time plot of KOH cleavage of ISO-BTMS(GC), oligomer(^{1}H-NMR), homopolymer(^{1}H-NMR), and copolymer(^{1}H-NMR). 100

Figure 3.3.11 First-order plot of KOH cleavage of ISO-BTMS(GC), oligomer(^{1}H-NMR), homopolymer(^{1}H-NMR) and copolymer(^{1}H-NMR). 100

Figure 3.3.12 Deviation from first-order behavior towards hydroxide ion cleavage. 103

Figure 3.3.13 Kinetic behavior of styrene and methyl methacrylate copolymers towards KOH cleavage. 104

Figure 3.3.14 ^{1}H-NMR spectra of poly(VBTMS-*co*-styrene) VS11 after A) 0% B) 13% C) 15% D) 17% cleavage by KOH. 107

Figure 3.3.15 ^{1}H-NMR spectra of poly(VBTMS-*co*-MMA) after A) 14.5% B) 38% C) 69% cleavage by KOH. 108

Figure 3.4.1 Conversion-Time plot of TBAF cleavage reaction. 117

Figure 3.4.2 First-order plot of TBAF cleavage reaction. 117

Figure 3.4.3 ^{1}H-NMR spectra of VBTMS-oligomer at A) 35.5% B) 46% C) 54% of cleavage by TBAF. 118

Figure 3.4.4 Schematic representation of reaction site in the cross-linked network of bis(vinylbenzyl)dimethylsilane (BVBDMS) microspheres or microgel. 121

Figure 3.4.5 FT-IR spectra of TBAF cleaved bis(vinylbenzyl)dimethylsilane (BVBDMS) microgel. 123

Figure 3.4.6 First-order plot of TBAF reaction on bis(vinylbenzyl)dimethylsilane (BVBDMS) particles (PP01). 125

Figure 3.4.7 SEM micrographs of degraded bis(vinylbenzyl)dimethylsilane (BVBDMS) particles by TBAF. 126

Figure 3.5.1 Major oxidation products of CAN oxidation of benzylic-silicon substrate
Figure 3.5.2 ^{1}H-NMR spectra of CAN oxidized oligomeric vinyibenzyltrimethylsilane at A) 0% B) 32% C) 53% D) 82% of oxidation. 131

Figure 3.5.3 Total % cleavage-time plot of CAN oxidative cleavage reactions of benzyltrimethylsilane-BTMS(GC), 4-isopropylbenzyltrimethylsilane-ISO-BTMS(GC), vinylbenzyltrimethylsilane-oligomer(^{1}H-NMR), poly(*m/p*-vinylbenzyltrimethylsilane)-homopolymer(^{1}H-NMR). 132

Figure 3.5.4 First-order plot of CAN oxidative cleavage reactions of benzyltrimethylsilane-BTMS(GC), 4-isopropylbenzyltrimethylsilane-ISO-BTMS(GC), vinylbenzyltrimethylsilane-oligomer(^{1}H-NMR), poly(*m/p*-vinylbenzyltrimethylsilane)-homopolymer(^{1}H-NMR). 132

Figure 3.5.5 Total oxidation-time (Top) and total % cleavage-time plots (Bottom) plots of CAN reactions of styrene and MMA copolymers of VBTMS(^{1}H-NMR) 138

Figure 3.5.6 ^{1}H-NMR spectra of oxidized Poly(VBTMS) as an evidence for crosslinking

Figure 3.5.7 First-order kinetic behavior of Styrene and MMA copolymers of VBTMS (^{1}H-NMR) towards CAN oxidation. 142

Figure 3.5.8 Typical mechanism of CAN oxidation of a benzylsilyl substrate 144

Figure 3.5.9 Possible CAN oxidation products of a benzylsilyl substrate. 145

Figure 3.5.10 Ring oxidation mechanism. 147

Figure 3.5.11 Possible mechanism of polymer backbone cleavage and substituent oxidation of 4-isopropylbenzyltrimethylsilane (ISO-BTMS). 150

Figure 3.5.12 SEM micrographs of CAN degraded bis(vinylbenzyl)dimethylsilane (BVBDMS) microspheres after the reaction time A) 0 hr B) 2 hrs C) 4 hrs D) 9 hrs 155

List of Tables

Table 1.1 Approximate bond dissociation energies (D) for Si-X and C-X bonds and the relative electronegativity 1

Table 1.2 Inductive σ_I and resonance σ_R components of substituent constant σ in 4-substituted styrenes 11

Table 1.3 Excess σ and π-carbon charge densities for 4-$CH_2Si(CH_3)_3$-styrene, relative to styrene 14

Table 1.4 Relative rates of benzyl-Si bond cleavage of $XC_6H_5CH_2SiMe_3$ by 39 wt.% water-methanol at 49.7 °C 16

Table 1.5 Rate factors for electrophilic substitution of benzyl-silicon compounds 18

Table 1.6 Comparison of rates of alkaline and acid hydrolysis of poly(methyl acrylate) with low molecular weight esters 28

Table 1.7 Individual rate constants of chlorination of polyethylene and its analogs 30

Table 1.8 Effect of neighboring groups on the rate constants of polymer–analogous reactions of polymethacrylic esters at 145 °C 31

Table 3.1.1 Synthetic details of poly(VBTMS-*co*-styrene) and poly(VBTMS-*co*-methyl methacrylate) 53

Table 3.1.2 Free radical copolymerization parameters of vinylbenzyltrimethylsilane (VBTMS) 55

Table 3.1.3 Probabilities of environments for methyl methacrylate copolymers of vinylbenzyltrimethylsilane (Poly(VBTMS-*co*-MMA)) 56

Table 3.2.1 Effect of co-solvent composition on precipitation polymerization of bis(vinylbenzyl)dimethylsilane (BVBDMS) 65

Table 3.2.2 Comparison of precipitation polymerization rates of DVB-55 and bis(vinylbenzyl)dimethylsilane (BVBDMS) 73

Table 3.2.3 Effect of *p*-substituents on overall rate of radical polymerization of substituted-styrenes 78

Table 3.2.4 ^{13}C-chemical shifts of β-Carbon of vinyl group of substituted styrenes 79

Table 3.2.5 Correlation of ^{13}C chemical shift and reactivity ratio of monomeric pairs in free radical polymerization 80

Table 3.3.1 Product isotope effect of base cleavage of substituted BTMS 85

Table 3.3.2 Effect of [KOH] on first-order specific rate constant of ISO-BTMS 88

Table 3.3.3 Comparison of pseudo first-order rate constants of KOH cleavages 95

Table 3.3.4 Activation parameters for KOH cleavage of benzylic-silicon bond 97

Table 3.3.5 Kinetic data of styrene and methyl methacrylate copolymers towards KOH cleavage 101

Table 3.3.6 Cleavage reaction-product analysis 111

Table 3.4.1 Pseudo first-order rate constant data for TBAF cleavage of polymeric substrates 119

Table 3.4.2 Kinetic data of TBAF cleavage reaction on bis(vinylbenzyl)dimethylsilane (BVBDMS_ microgel (PP04) 122

Table 3.4.3 Kinetic data of TBAF cleavage reaction on bis(vinylbenzyl)dimethylsilane (BVBDMS) particle (PP01) 124

Table 3.5.1 Kinetic data of CAN cleavage on different substrates 134

Table 3.5.2 Stoichiometry of CAN oxidation reaction on poly(VBTMS) 148

Table 3.5.3 Evidence for absence of backbone degradation of linear polymer analogs 153

Table 3.5.4 Effect of CAN oxidation time on particle size of bis(vinylbenzyl)dimethylsilane (BVBDMS) particles 154

List of Abbreviations

AIBN.....2,2'-Azobisisobutyronitrile

BVBDMS.....bis(vinylbenzyl)dimethylsilane

BTMS.....Benzyltrimethylsilane

ISO-BTMS.....*p*-isopropylbenzyltrimethylsilane

CAN .....Ceric ammonium nitrate

GC.....Gas chromatography

IR.....Infrared spectroscopy

MMA.....Methyl methacrylate

Sty.....Styrene

P.I.E.....Product isotope effect

Mn.....Number average molecular weight

Mw .....Weight average molecular weight

NMR.....Nuclear magnetic resonance

TBAF.....Tetrabutyl ammonium fluoride

Tg.....Glass transition temperature

VBC.....Vinylbenzylchloride

VBTMS.....Vinylbenzyltrimethylsilane

PMMA.....Poly(methyl methacrylate)

P.D.....Poly dispersity

DVB.....Divinylbenzene

TMSCl.....Trimethylchlorosilane

CHAPTER 1. INTRODUCTION

1.1 Properties of the silicon-carbon bond

Organosilicon compounds are defined as species having silicon-carbon bonds. There are few exceptions as in the derivatives of silane. By substituting a silicon moiety in place of a hydrogen atom of an organic substrate, one can activate the substrate to a reaction, direct the course of a reaction or protect the substrate from unwanted reactions. Hence, the study of the properties of silicon-carbon bonds have been of great interest over the past years.

Most of the properties of silicon in an organic compound are highly related to its bond strength with different elements and its relative electronegativity. Table 1.1 shows the approximate bond dissociation energies (D) for Si-X and C-X bonds and the relative electronegativity data.[1,2]

Table 1.1 Approximate bond dissociation energies (D) for Si-X and C-X bonds and the relative electronegativity.[1,2]

Bond Si-X	D kJ/mol	Bond C-X	D kJ/mol	Element	Electronegativity
Si-C	318	C-C	334	H	2.79
Si-H	339	C-H	420	Si	1.64
Si-O	531	C-O	340	C	2.35
Si-N	320	C-N	335	N	3.16
Si-I	322	C-I	213	O	3.52
Si-F	807	C-F	452	F	4.0

It can be seen from Table 1.1 that whereas the silicon's bonds to fluorine and oxygen are stronger than the corresponding bonds between carbon and these elements, its bonds to carbon and hydrogen are weaker. Silicon always appears more electropositive than carbon, resulting in strong polarization of Si-C bonds. This makes the Si-C bonds more susceptible to heterolytic bond scission rather than to homolytic fission, either by nucleophilic attack at silicon or by electrophilic attack at carbon. Both C-Si and C-H bonds break in the same direction ($C^{-}Si^{+}$, $C^{-}H^{+}$), which is a good indication of the likely behavior of both bonds. Just as Ar-H bonds are broken by treatment with electrophiles such as bromine, so also are Ar-Si bonds. The lower bond strength of the C-Si bonds compared to the C-H bonds suggests that when a C-H bond is cleaved by a particular ionic reagent, the corresponding C-Si bond will be broken even more readily by the same reagent. Comparison of their reactivities towards nucleophiles / bases shows that the Si-C bond is more reactive towards oxygen and halogen nucleophiles, whereas the C-H bond is more reactive towards carbon and nitrogen nucleophiles.

1.2 Properties of the trimethylsilyl group

Size and shape[3]**:** Silicon has a covalent radius of 1.17 Å, significantly larger than that of carbon (0.77 Å). The Si-C bond length in trimethylsilyl group is 1.9 Å, but may vary with the element on the fourth silicon bond. The trimethylsilyl group has bond angles similar to those found in the *t*-butyl group. Silicon, being larger, has more room for the groups bonded to it. Therefore, there is less steric strain within the trimethylsilyl group though the group is larger and exerts stronger steric effects than the *t*-butyl group. Hwu *et al.*[4] have shown that the trimethylsilyl cationic species can be regarded as a '*Bulky*

proton'. They used the bulkiness of the trimethylsilyl group to differentiate two carbonyl groups in different steric environments through acid catalyzed dioxolanation reactions. When the acid catalysts, containing a trimethylsilyl moiety equivalent to proton, were used to ketalize or acetalize the compounds containing two types of carbonyl groups[4] (Scheme 1), very high product selectivity was achieved, with ketal or acetal functions being introduced only at the less sterically hindered site.

Scheme 1

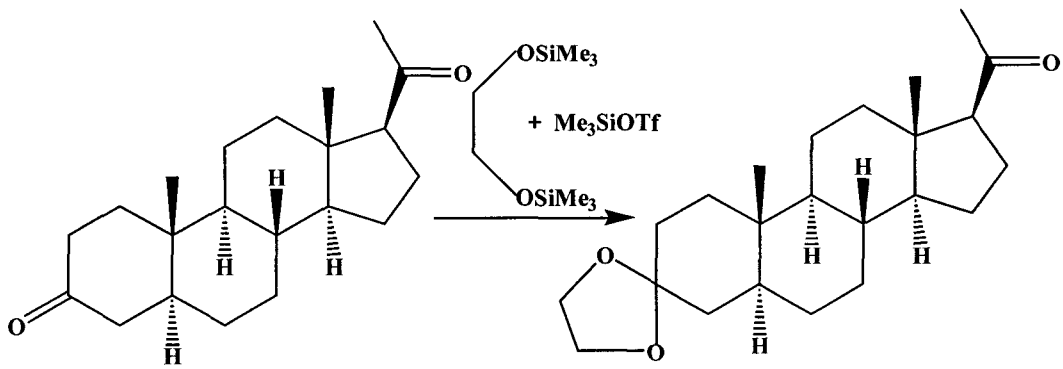

5α-pregnane-3,20-dione **Selectivity 100:0**

In oxygen-silicon compounds, the trimethylsilyl group functions as a substitute for the proton of an alcohol or enol[5]. Like protons, silyl groups are very easy to put on and remove. Hence, in synthetic organic chemistry, the trimethylsilyl group is widely used as protecting groups for alcohols, amines and esters. Both O-H and O-Si bonds formally dissociate in the same direction. Since the O-Si bonds are stronger than O-H bonds, silicon-oxygen bonds break more slowly than the corresponding hydrogen-oxygen bonds. Hence, in silicon-oxygen chemistry the trimethylsilyl group is regarded as a *'Feeble proton'*.[5]

On the other hand, in silicon-carbon chemistry, the trimethylsilyl group[5] is regarded as a *Super proton'*. The significantly lower bond energy (100 kJ/mol) of a silicon-carbon bond compared with a carbon-hydrogen bond allows the silyl groups to be displaced much more easily from carbon than a proton from the corresponding carbon, especially in the case of oxygen and halogen nucleophiles.

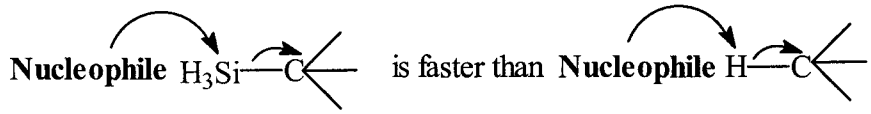

Thus, Chan *et al.* [6] used β-elimination of haloalkanes to give allenes (Scheme 2).

Scheme 2

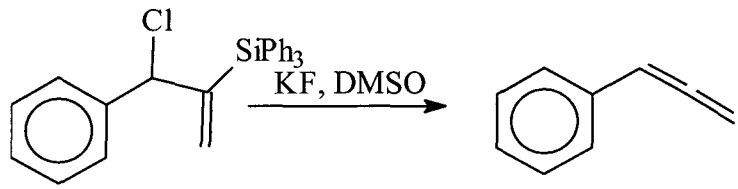

1.2.1 β-effect

There are reactions in organosilicon chemistry where the cleavage of silicon-carbon bonds is favored as a consequence of an unusual property of silicon, called β-silicon effect – the ability to stabilize and to promote the generation of a carbonium ion at the β-position. Many aliphatic β-functionalized organosilanes exhibit abnormally high reactivity compared to either the α- or γ-substituted compounds. Sommer[7] *et al.* reported that β-chloroethyltrichlorosilane was so reactive towards bases that it could be titrated with sodium hydroxide, producing ethylene (Scheme 3). They also found that

2-hydroxypropyltrialkylsilanes[8] underwent rapid conversion to propene on treatment with dilute sulfuric acid (Scheme 3).

Scheme 3[7,8]

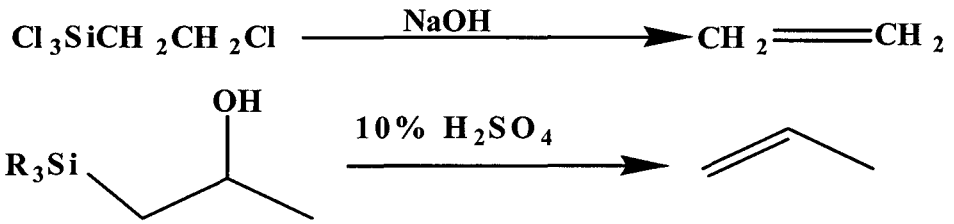

Allylsilanes and propargylsilanes usually undergo addition or substitution reactions with electrophiles.[9,10] In most of these electrophilic reactions, the substitution involving Si-C bond cleavage dominates over addition (Scheme 4).

Scheme 4

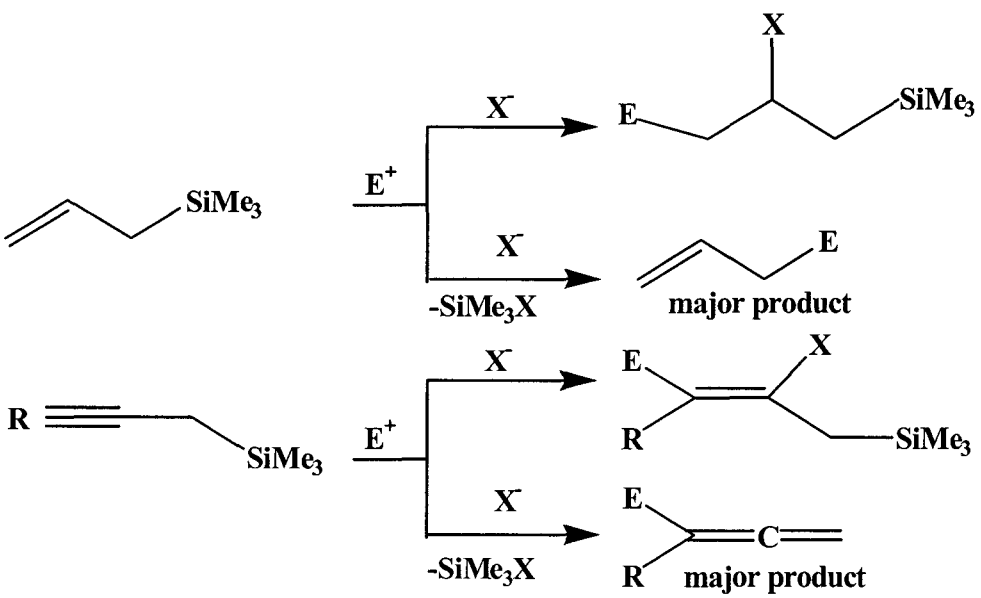

Another manifestation of the β-effect is the *anti*-Markovnikov addition of hydrogen halides to vinylsilanes where the formation of the β-carbonium ion is preferred over the α-cation, leading to addition rather than substitution[11] (Scheme 5, where X = Cl, Br).

Scheme 5

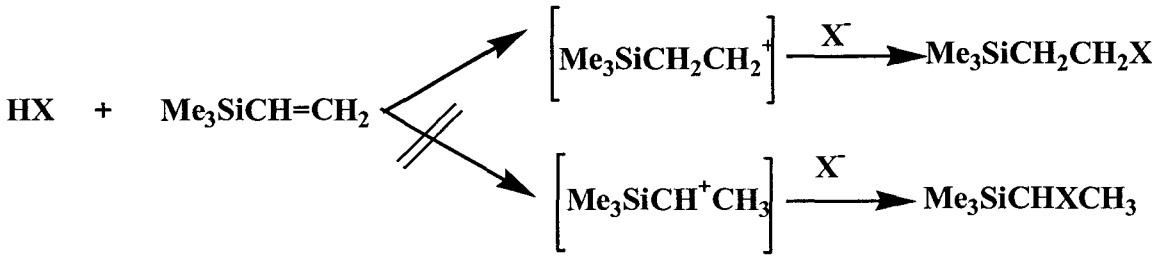

The β- silicon effect has been shown to be due to hyperconjugation, or σ-π conjugation (vertical stabilization), where an overlap between the bonding σ-level of the C-Si bond with the adjacent p-orbital of the carbonium ion is described[1,12] (Figure 1.1).

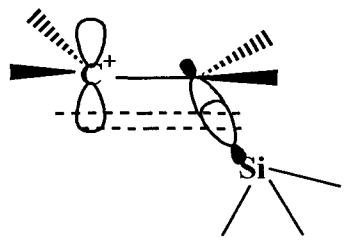

Figure 1.1 σ-π Conjugation

The proposed orbital overlap can be understood in terms of a high degree of polarization in the direction of the more electronegative carbon, as in $C^{\delta-}$ $Si^{\delta+}$. The Si-C bonding orbital is higher in energy than the C-H or C-C bonding orbitals, and the energy match with the empty p-orbital is therefore better. This results in an enhanced ability of C-Si σ orbitals to stabilize an adjacent electron-poor center e.g., β-carbonium

ions) by orbital overlap. The C-Si σ orbital overlap with the positive center results in the donation of electron density from silicon, and leads to a weakening of the C-Si bond. This promotes C-Si bond cleavage and hence makes the silyl group behave as a 'super proton' in many reactions.

When the silyl group is directly attached to an aromatic system as in silylbenzenes, the β-effect controls the reaction site during electophilic substitution reaction. In most cases, the β-effect results in an enhanced rate of electrophilic attack at the *ipso* position[12], followed by desilylation (overall substitution) (Scheme 6). In most electrophilic aromatic substitutions of aryltrimethylsilanes, except in nitration using specific nitrating agents such as nitronium tetrafluoroborate, the desilylation is faster than the deprotonation.

Scheme 6

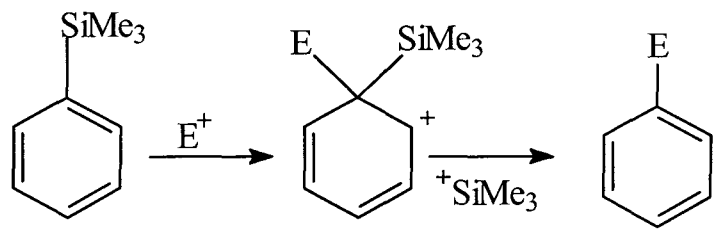

The Hammett substituent constants, σ_m and σ_p, for *meta* and *para* Me_3Si– groups average as - 0.05 and - 0.03, whereas the corresponding values for *t*-Bu groups are - 0.09 and - 0.15. The negligible σ_p value of Me_3Si– group compared to *t*-Bu group is explained in terms of its electron withdrawing resonance interaction with the aromatic ring through (p-d)π bonding.[12] This is also evidenced from the negative σ_I and the

positive σ_R (inductive and resonance components of substituent constant σ) values of Me_3Si– group as - 0.08 and 0.06. Thus, the Me_3Si– group attached to an aromatic ring donates the electron density by induction, and withdraws the electron density by resonance.

Similarly, most vinylsilanes give addition products that undergo subsequent elimination to give overall substitution involving C-Si bond cleavage. The β-effect plays a significant role in controlling the stereochemistry of this addition. Very often, *anti*-addition is the course of reaction analogous to the reaction of alkenes with halonium ion. However, depending on the factors such as solvent polarity, type of silyl substituents and extent of hyperconjugative stabilization of carbonium ion, *syn*-addition is also reported (Scheme 7). For example, bromination of β-silylstyrenes in polar solvents was reported as *syn*-addition by Brook[13] *et al.* on account of an open carbonium ion transition state with maximum hyperconjugative stabilization formed by minimal rotation of the C-C bond, followed by the bromide ion attack from the least hindered side (*anti* to β-silyl group).

Scheme 7

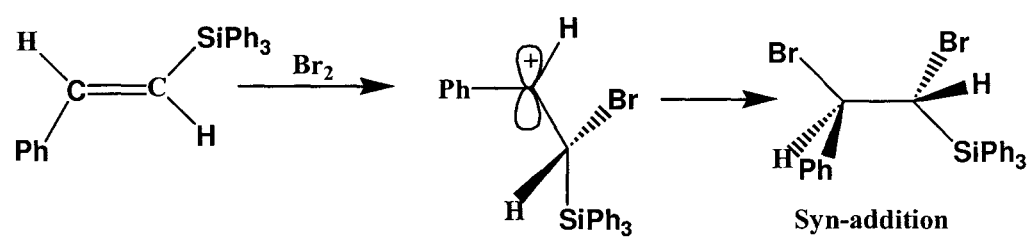

1.2.2 α-Effect

Trimethylsilyl groups can act as a π-electron withdrawing group and stabilize α-carbanions. The accepted explanation is that the relatively low-lying unoccupied 3d-orbitals can participate in (p-d)π bonding, as shown in Figure 1.2, where the electron density from the p-orbital on X can be partially transferred onto silicon through a donor-acceptor interaction with the vacant 3d-orbitals. The unexpected shortness of the silicon-oxygen and silicon-chlorine bonds, reduced basicity of R_3SiNR_2 and enhanced acidity of R_3SiOH[1] are attributed to this effect.

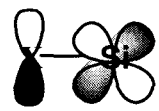

Figure 1.2 Schematic representation of (p-d)π bonding.

There are a number of reactions in organosilicon chemistry involving the ability of silicon to stabilize adjacent negative charges in anions such as R_3SiX^- (X = CH_2, NR, O, S). In the series $(Me_3Si)_nH_{3-n}CH$, the ease of metallation increases as *n* increases from 0 to 3[14]. Hopkinson and Lien[15] calculated the proton affinities of $C_2H_5^-$ and $H_3SiCH_2^-$ as 448.7 kcal/mol and 416.3 kcal/mol by using *ab initio* method. The difference of 31.5 kcal/mol accounts for the stabilization of the adjacent carbanion by the SiH_3 group, relative to the methyl group. An α-methyl group was found to weakly destabilize neighboring carbanions by 2.2 kcal/mol, relative to hydrogen. Pitt[16] *et al.* found that the p_π charge density in $H_3SiCH_2^-$ was lower than that of $H_3CCH_2^-$

The activating and directive influence of silicon on α-carbanion formation is illustrated in organometallic addition to vinylsilanes[17]. The fast metal-halogen exchange of $Me_3SiCHBrR$ by butyl lithium is the typical example,[12] showing the α-effect of silicon. The directive influence of silicon on carbanion formation is shown in Scheme 8[17]. Introduction of a CH_2 group as in 3 leads to a substitution product whereas in 1 and 2, the α-effect results in addition products[15].

Scheme 8

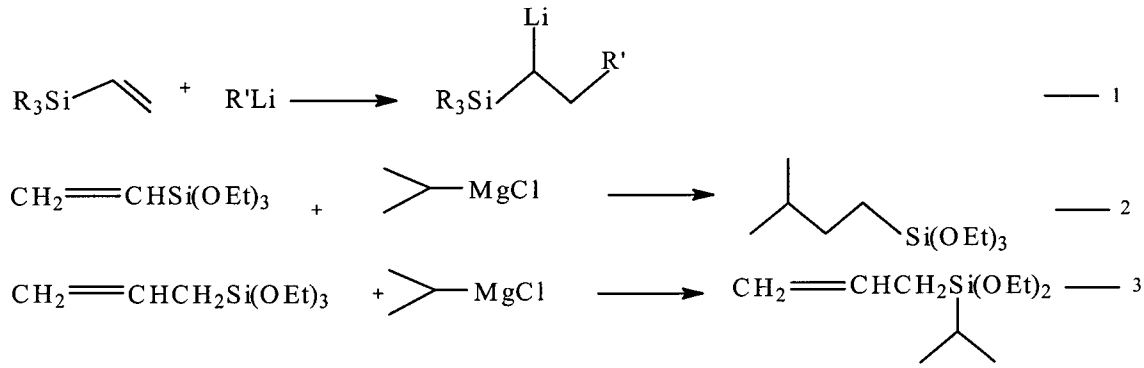

1.3 Characteristics of benzylic-silicon bond

When a $Me_3SiCH_2^-$ group is attached to a benzene ring, as in benzyl silanes, the group is quite strongly electron releasing to the aromatic ring. This is shown by the substituent constants σ_m and σ_p values of - 0.165 and - 0.24. The corresponding values for Me_3CCH_2 group are - 0.08 and - 0.1. The difference in the behavior of these two groups is best explained by the hyperconjugative model,[12] as shown in Scheme 9.

Scheme 9

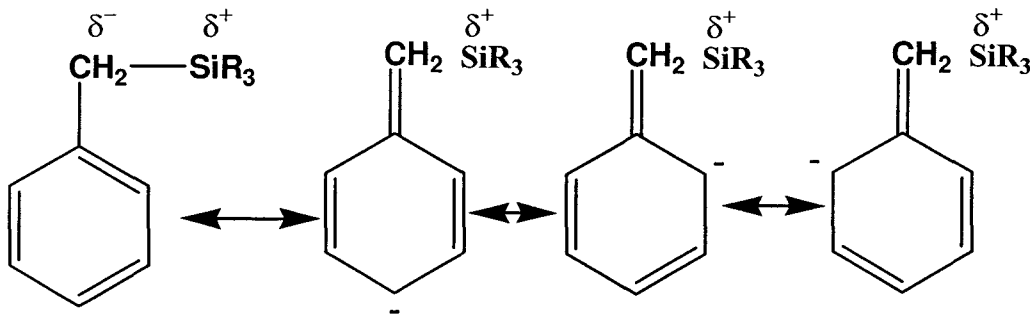

Reynolds[18] *et al.* estimated the inductive σ_I and resonance σ_R components of substituent constants for $-Si(CH_3)_3$ and $-CH_2Si(CH_3)_3$ by using proton and ^{13}C chemical shifts in 4-substituted styrenes. Their results are concisely given in Table 1.2, and are consistent with the conclusions concerning the electronic effects of these groups as the 4-$Si(CH_3)_3$ group in styrene is electron releasing through inductive/field effects and electron withdrawing through resonance effects, whereas the 4-$CH_2Si(CH_3)_3$ group in styrene is electron releasing through both inductive and resonance effects.

Table 1.2 Inductive σ_I and resonance σ_R components of substituent constant σ in 4-substituted styrenes

Substituent	σ_I	σ_R
$CH_2Si(CH_3)_3$	- 0.1	- 0.15
$-Si(CH_3)_3$	- 0.09	+ 0.07
$-CH_2C(CH_3)_3$	- 0.07	- 0.06
$-CH_2Cl$	+ 0.19	- 0.01

Coplanarity: Like all other types of π-conjugation, Si-Cσ-π conjugation requires coplanarity[19] of the Si-C bond with the aromatic p-orbitals forming the π-electron cloud. Any deviation from coplanarity will remove or reduce the effect of σ-π conjugation. This was demonstrated by Hanstein[19] while attempting to quantify the σ-π conjugation (vertical σ-π conjugation) in series of compounds containing Sn-C bonds (Sn also has the capability of σ-π conjugation like Si). He measured the σ-π conjugation in terms of charge-transfer frequencies of the complex between the donor type Sn or Si compounds with well-known acceptors like tetracyanoethylene (TCNE) or dichloromaleic anhydride (DCMA). The frequency lowering is an indication of a higher extent of stabilization through σ-π conjugation. The charge-transfer frequencies of TCNE complexes with various silicon and tin compounds are shown in Figure 1.3[19].

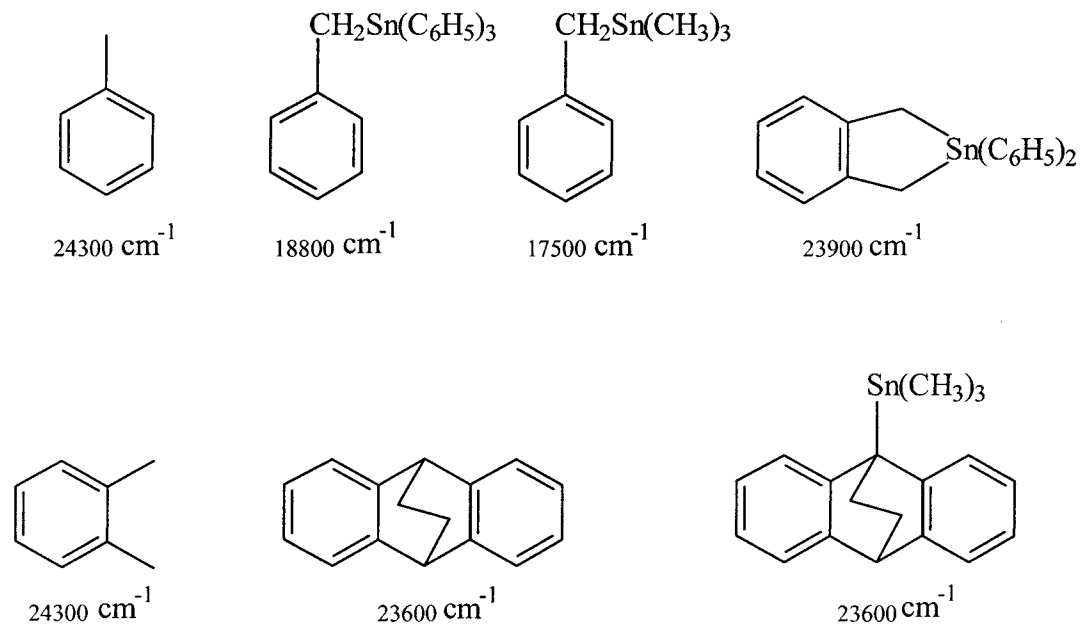

Figure 1.3 Charge-transfer frequencies of TCNE complexes with various tin compounds.[19]

The stereoelectronic requirement for the σ-π conjugation is clearly reflected in the charge transfer complex frequencies. In the two strained tetracyclic compounds, shown in Figure 1.3, the substitution of an α-hydrogen by a trimethyltin [$Sn(CH_3)_3$] group does not change the frequency, indicating the complete absence of σ-π conjugation due to lack of coplanarity. However, substitution of the α-hydrogen of toluene by triphenyl or trimethyltin results in a significant lowering of the charge transfer frequency through Sn-Cσ-π conjugation. Similar data for non-strained compounds reported by the same author[20] are shown in Figure 1.4. The significant amount of electron density release from the Si-C bond to the aromatic ring through σ-π conjugation is indicated by the lowest value (20100 cm^{-1}) for benzyltrimethylsilane among the series.

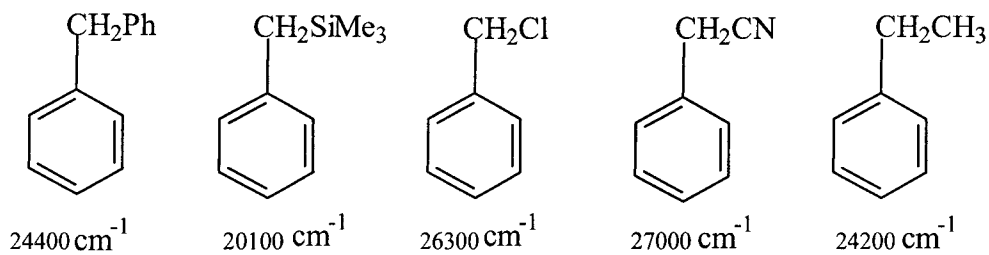

Figure 1.4 Charge-transfer frequencies of TCNE complexes with various organic compounds.[20]

Barrier to rotation about Csp^2-Csp^3 bond: As a consequence of σ-π conjugation between the Si-Cσ bond and the phenyl π-electron system in benzylic-silicon compounds, Rudy Sebastian[21] *et al.* used ^{1}H-NMR to measure an energy barrier of about 7.4 and 8.1 kJ/mol to the rotation about the Csp^2-Csp^3 bond in benzyl silane and benzyltrichlorosilane respectively. These values are higher than that for ethylbenzene. This is attributed mainly to the σ-π hyperconjugative stabilization of the perpendicular

conformer where the C-Si bond is parallel to the aromatic p-orbitals. Also using ^{1}H-NMR, Schaefer[22] isolated the steric and hyperconjugative components of the barrier in benzylic-M(CH_3)$_3$ compounds (M = C, Si, Ge, Sn, Pb). Schaefer got 9.5 kJ/mol for X = Si, Ge, Sn and 12 kJ/mol for X = Pb for the barrier energy, mainly contributed as the hyperconjugative component.

Electron density: As a result of the electron donation through both inductive and resonance effects, the electron density of styrene having -$CH_2Si(CH_3)_3$ group at the *para* position seems to be significantly changed from that of styrene itself, as per the CNDO/2 molecular orbital calculations carried out by Reynolds[18]. Their results are depicted in Table 1.3.

Table 1.3 Excess σ- and π-carbon charge densities for 4-$CH_2Si(CH_3)_3$-styrene, relative to styrene

Carbon	Excess charge density x 10^4c	Carbon	Excess charge density x 10^4c	Carbon	Excess charge density x 10^4c
C-4σ	- 12	C-2, -6σ	- 93	(Cα)σ	- 14
C-4π	+ 533	C-2, -6π	+ 211	(Cα)π	+ 54
C-3, -5σ	+148	C-1σ	+ 122	(Cβ)σ	+ 54
C-3, -5π	- 476	C-1π	- 322	(Cβ)π	- 129
				Σqπ	- 405

1.4 Types of reactions of benzylic-silicon compounds

Benzylic-silicon bond containing compounds are generally sensitive to nucleophilic, electrophilic, and oxidizing type reagents, leading to silicon-carbon bond cleavage in

most cases. The rates of these reactions have been explained in terms of σ-π conjugation from the Si-C bond and an inductive type electron release from silicon.

1.4.1 Nucleophilic reactions

The presence of an α-aryl group in an alkyl group attached to silicon markedly facilitates silicon-carbon bond cleavage by nucleophilic reagents.[23] Nucleophiles prefer to attack on silicon owing to the more electropositive nature of silicon than carbon. The driving force for the silicon-carbon bond cleavage is the resonance stabilization of the resulting carbanion shown in Scheme 10.

Scheme 10

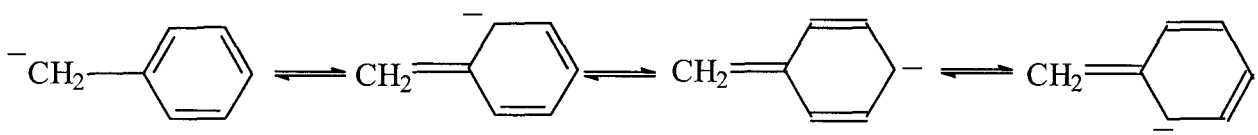

Si-benzyl bonds are in fact readily cleaved by alkali metal hydroxides. Additional α-phenyl groups further facilitate the cleavage so that the ease of removal of the R group from Me_3SiR compounds by sodium ethoxide in ethanol or sodium amide in liquid ammonia is in the order (R=) Ph_3C > Ph_2CH > $PhCH_2$.[24] Gillman[25] *et al.* showed that the alkali metal hydroxide cleavage of the Si-R bonds of various Ph_3SiR compounds in homogeneous solution would be in the order indenyl, 9-fluorenyl > $C_6H_4CF_3$-*m*, C_6H_4Cl-*p*, α-naphthyl > phenyl, β-phenylethyl, hexyl. This sequence corresponds to the order of decreasing acidity of the parent hydrocarbons RH, which is the same order of increasing stability of R as a carbanion. The effects of other groups attached to silicon

on the ease of removal of benzyl group are revealed by the observation that the compound Me_3SiCH_2Ph is less readily cleaved by aqueous-alcoholic alkali metal hydroxide than is the triphenyl analogue, Ph_3SiCH_2Ph, while the latter is more readily cleaved than the tri-*p*-tolyl compound, $(p\text{-}MeC_6H_4)_3SiCH_2Ph$. Additional electron release from tri-*p*-tolyl group towards silicon atom hinders the nucleophilic attack. The steric hindrance renders $Pr^nPr^i_2SiCH_2Ph$ much more resistant than Me_3SiCH_2Ph. Eaborn[26] *et al.* studied the effect of nuclear substituents on the ease of cleavage of benzyltrimethylsilanes by aqueous methanolic alkali. Their reactivity results, shown in Table 1.4, clearly indicate that the electron-withdrawing groups facilitate the cleavage, owing to the enhanced stabilization of the resulting carbanion in the transition state, as shown in Scheme 11

Scheme 11

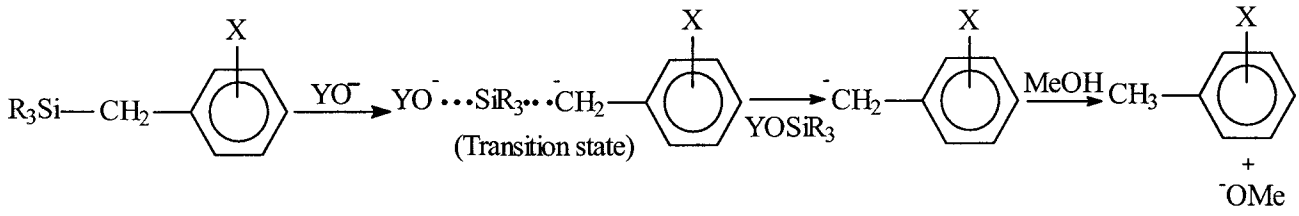

Table 1.4 Relative rates of benzyl-Si bond cleavage of $XC_6H_4CH_2SiMe_3$ by 1N KOH in 39 wt.% water-methanol at 49.7 °C[26]

X	*p*-NO_2	*o*-NO_2	*p*-CONHPh	*p*-$CONH_2$	*o*-$CONH_2$	*p*-$CO2^-$	*o*-Cl	*m*-Cl
Reactivity	$18x10^5$	$50x10^4$	7000	6300	530	320	80	63
X	*m*-CONHPh	*p*-Br	*p*-Me_3Si	*o*-CO_2^-	*m*-CO_2^-	*p*-Me	*p*-MeO	H
Reactivity	31	19	9.6	4.8	2.1	0.2	0.02	1

Our aim is to compare the substituent effect of H-, isopropyl-, vinyl- and corresponding polymeric chain on the nucleophilic reacitvity of benzylic-silicon bonds in styrenic compounds having a 3 or 4-$CH_2Si(CH_3)_3$ group ($XC_6H_5CH_2Si(CH_3)_3$).

1.4.2 Electrophilic reactions

The carbon-silicon bond of benzylsilane is much less reactive towards electrophiles compared to nucleophiles. However, tetrabenzylsilane and tribenzylfluorosilane were completely cleaved in cold concentrated sulfuric acid by Szamant[27] to give phenylmethanesulphonic acid. However, the corresponding trialkylsilicon compound, *n*-Bu_3SiF was found more resistant to acid. Tetrabenzylsilane is decomposed by aluminium chloride, neat or in solution, to give silicon tetrachloride.[23]

The benzylsilanes usually undergo electrophilic substitution reactions on the ring, without the benzyl-carbon bond being cleaved. This is due to the large ortho/*para* activating effect of the $^-CH_2SiMe_3$ group through the σ-π hyperconjugative stabilization of the β-silylcarbonium ion. This makes the benzyl-silicon compounds very reactive in protiodetritiation, protodesilylation, and other electrophilic reactions, compared to benzyl-alkyl compounds of the types shown[28] in Table 1.5. The highest rate factor, among the series in Table 1.5, is shown by benzyltrimethylsilyl groups ($Me_3SiCH_2C_6H_4^-$). As more $^-CH_2^-$ groups are introduced, their inability to provide σ-π hyperconjugative stabilization towards the ring makes the rate factors progressively lower as shown in Table 1.5.

Table 1.5 Rate factors for electrophilic substitution of benzyl-silicon compounds[28]

Ar	Protiodetritiation(Ar^3H)		Protodesilylation($ArSiMe_3$)			Nitration (ArH)	
	o-	*p*-	*o*-	*m*-	*p*-	*o*-	*p*-
C_6H_5-	1	1	1	1	1	1	1
$CH_3C_6H_4$-	220	450	17	2.5	21	47	62
$Me_3SiCH_2C_6H_4$-	9300	82000	31	6.6	270	197	69.5
$Me_3Si(CH_2)_2C_6H_4$-	450	810	17	3.6	28	12	29
$Me_3Si(CH_2)_3C_6H_4$-	270	580	12	3.8	22	16	32

Iron and iodine-catalyzed bromination and chlorination of benzyltrimethylsilanes[12] lead to a mixture of *ortho* and *para* substituted products. When the R in $-CH_2SiR_3$ group was progressively substituted by a more-electronegative atom like chlorine, the overall reactivity and *para* to *ortho* ratio were found to decrease, owing to the progressive reduction in the electron density of the benzylic-silicon bond with subsequent weakening of hyperconjugative donation or stabilization. One example of an intramolecular electrophilic substitution of a benzylsilane with cleavage of the silicon-carbon bond is known,[29] which is shown in Figure 1.5.

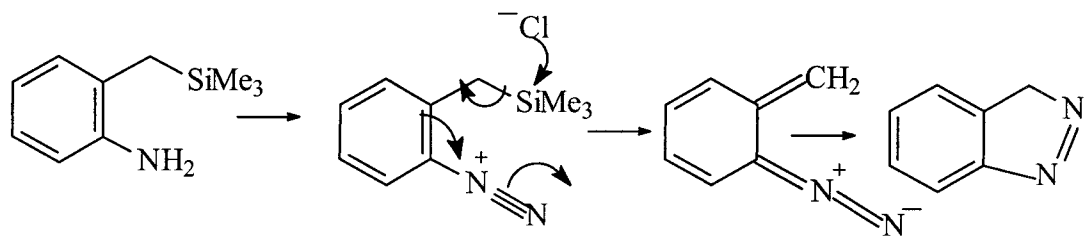

Figure 1.5 Cleavage of benzylic-silicon bond by intramolecular electrophilic substitution.

1.4.3 Oxidative reactions

Most benzylic-silicon compounds are oxidized much more easily than their corresponding carbon compounds due to the lower oxidation potential attributed to significant electron release from Si-Cσ-bond to the aromatic ring through σ-π hyperconjugation. Oxidants including ceric ammonium nitrate[30,31] and Co(III) diacetate bromide complex[32] have been widely used. The benzylic-silicon compounds can be oxidized electrolytically[33] as well.

1.5 An overview of chemical reactivity of macromolecules and small homologs

It is a common assumption in macromolecular chemistry that the reactivity of a functional group does not depend on the size of the molecule to which it is attached. This assumption originates from the fact that a constant rate is postulated for classical polymerization reactions regardless of the gradually increasing polymer size. This assumption is originated from Flory's well-known *Principle of equal reactivity*[34] applicable to polycondensation reactions. However, numerous exceptions to this rule of 'equal reactivity' are known in the literature and these are denoted by the general term the *'polymer effect'*.[35] The reactions of a macromolecular compound and of its low-molecular-weight analog may follow a similar course when the reaction system is homogeneous, with a sufficiently large diffusional mobility of all reactants, intermediates and products. But the reduced diffusional mobility of macromolecules and steric hindrance to the approach of reagents to the functional groups on the macromolecule are the frequent causes of a lower reaction rate in the macromolecular system. The *'polymer effect'* results in either enhanced polymer reaction rate or

reduced reaction rate compared to the low molecular weight analog depending on the specific type of effects that are described in detail below.

1.5.1 Effect of local concentration

The local concentration of functional groups in polymer solutions can be considerably higher than what would be obtained if each reactive group belonged to a small molecule independent from the others[36]. In fact, a polymer molecule with a functional group on every repeating unit represents an extremely high concentration of active species. Thus, the chelating power of poly(methacryloyllysine) is much higher than its low molecular weight analog. Poly(methacrylyllysine)[33] (1) is able to chelate cupric ion at a lower pH than its small homologue (2) where R is a small alkyl group.

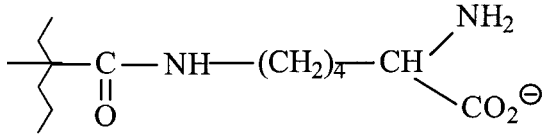

1

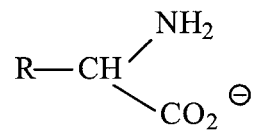

2

Similarly, the bifunctional Cannizzaro reaction of polyacrolein[37] is facilitated by the local high concentration of aldehyde groups along the chain. The reaction is shown in Scheme 12. On the other hand, the reaction conversion is limited by the isolation of single aldehyde group between two pairs of reacted groups. We will study the same kind of effect on a molecular series containing small molecules and polymer analogs for nucleophilic and oxidative reactivity of a particular bonding – benzylic-silicon –.

Scheme 12

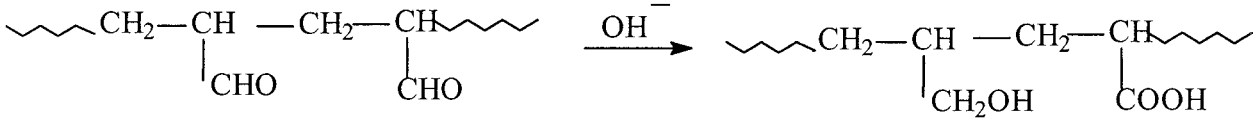

1.5.2 Effect of reaction medium on functional group reactivity

Polymer reactions in solution are greatly influenced by the nature of the solvent[35]. More specifically, these reactions are related to the shape adopted by the macromolecules in solution. Most polymers form a random coil in solution, which represents the set of all conformations with end-to-end distances fitting a Gaussian distribution. However, the coil structure can be altered by changing solvent, pH, temperature etc. The size of the statistical coil and its expansion depends on the polymer-solvent interaction. The coils of a given polymer are expanded more in good solvents and contracted in bad solvents, resulting in higher and lower solution viscosities, respectively. Polymer reaction rates are reduced by an increase in the viscosity of the medium. As well, the effective coil dimension influenced by the solvent medium can affect the reaction rate by varying the reagent accessibility to the polymer domain.

Interactions of a polymer with a reagent of low molecular weight may change the concentration of the small molecule in the polymer domain, which naturally affects the reaction rate. The use of single or mixed solvents having different affinities towards the polymer molecules than to a small reagent, makes the situation even more complex. In case of preferential solvation of the polymer, the solvation sphere of the chain is enriched in one component of the solvent mixture. A reduction of reaction rate is frequently observed in reactions of polyanions and polycations with neutral organic reagents. This is associated with a decrease in charge density from preferential solvation of polyions in the system[35].

When a functional group attached to a polymer chain reacts with a species of low-molecular weight, the reaction site, close to the polymer backbone, may have very different properties from the bulk of medium. Polymer backbones contribute to the effective solvent medium of the functional group or reaction center by changing the polarity of the solvent molecules in the immediate vicinity. Thus, it is expected for any reaction that is sensitive to medium effects to exhibit characteristic differences between the rates observed for polymeric species and their low-molecular weight analogs. We will investigate the effect of polymer backbones of varying polarity on reactivity of a particular functional group attached to the polymer chain.

Havidt and Corett[38] studied hydrogen-deuterium exchange in D_2O solutions of poly(*N*-vinylacetamide), and observed that the rate constants for the exchange of the hydrogen atoms of the polymeric amide groups are lower by a factor of 20 compared with the corresponding exchange rate constants of *N*-methylacetamide. They carried out a complete kinetic analysis and explained that the water in the immediate environment of the macromolecules has a different structure, a lower local concentration and a lower dissociation constant (Kw) than in solutions of low molecular weight compounds. Their interpretation, based on the hydrogen exchange mechanism in protein molecules, is that the macromolecules in solution undergo conformational fluctuations. In some conformations, a given reactive group is freely exposed to the solvent, giving rate constants similar to that of low-molecular weight analogs. In other conformations, the group considered is protected by the other parts of the macromolecule from the exposure to the solvent, and, therefore prevented from the reaction. Thus, the ratio k polymer / k monomer is a measure of the fraction of time spent by the reactive group on

the polymer in free contact with the solvent. Mueller *et al.*[39] also found a 100-fold difference in the deuterium exchange rate for isopropyl propionamide and poly (isopropyl acrylamide) and reasoned the results in the same way.

Sometimes the polymer chain contributes to the properties of the reaction medium by affecting the dependence of the reaction on the nature of the solvent. Thus, the rate of aminolysis[38] of the copolymers of dimethyl acrylamide and of *p*-nitrophenyl acrylate is roughly the same in water at 30 °C and in dioxane at 50 °C. On the other hand, when the aminolysis is carried out on the *p*-nitrophenyl isobutyrate analog, the rate constant is 190 times higher in water than in dioxane. This has been explained by a 'destructuration' of the solvent, some molecules of which are isolated in loops of the chain, changing drastically the dielectric constant in these parts of coil so that solvents of different dielectric constant behave in the same way.

1.5.3 Effect of Morphology

The reactivity of polymers in the solid state is profoundly affected by the regularity[35] in the packing of the chains in the solid state as determined by the degree of crystallinity. The space occupied by the molecules in crystals is characterized by the packing coefficient given as the ratio zV_0 / V, where V_0 is the inherent molecule volume, V is the volume of the unit cell and z is the number of molecules. Depending on the packing coefficient, ideal polymer crystals are almost impenetrable to small reagent molecules and the chemical attack is extremely difficult. The packing coefficient of polymer crystals is enhanced by the strong intermolecular attractions like H-bonding, as in cellulose, and is reduced in polymers with bulky groups.

The complex structure of polymers in the solid state is defined by the intermolecular organization of chains of mainly three types. The ideal *crystalline* state is with extended or folded chains. The *amorphous state* is characterized by the interpenetrating individual coils with some short range ordering. Though the crystalline nature of polymer is unfavorable to chemical reactions, polymer crystals involve numerous defects. Chains of shorter or longer loops and chain folds, together with free chain ends lend an amorphous character to the crystal surface. The *semicrystalline* state is a combination of both amorphous and crystalline states. The degree of crystallinity of semicrystalline materials is very much lower than that of crystalline materials. The two-phase *semicrystalline* polymers exhibit much higher reactivity than perfectly crystallized materials and the reactivity is proportional to the degree of disorder.

Segal[41] *et al.* studied the variations in the rate of oxidation of polyethylene of different morphology including unoriented film, oriented film and powdered crystals, and explained in terms of varying accessibility of functional groups. The surface layers of crystals are oxidized most rapidly since they are most easily penetrated by the oxygen. The higher fraction of crystalline phase in the oriented film exhibits least reactivity towads oxidation.

Rowland[42] reported varying reactivities of cellulose of different morphologies including cotton, wood pulp, mercerized cotton and regenerated cellulose towards a number of reactions including moisture absorption, iodine absorption, acid hydrolysis, alcoholysis, periodate oxidation, formylation and deuteration. These four morphologies

are in the order of increasing disorder in their structure so that the regenerated cellulose exhibits the highest reactivity in all those reactions.

1.5.4 Effect of Neighbouring groups

The influence of neighboring groups on the reactivity of a functional group is well known in organic chemistry and is pronounced in polymer systems. Neighboring group effects on polymer reaction rate can be classified as described below.

1.5.4.1 Electrostatic effect

Electronic interactions of functional groups with reagent molecules may lead to reduction or enhancement in the reaction rate. The rate of nucleophilic reaction between poly(4-vinylpyridine) and α–bromoacetates[36] increases with increasing conversion as the positive charge on ammonium ions in the polymer attract α–bromoacetates into the polymer coils. The ionization constant of poly(acrylic acid)[37] by the action of a base decreases rapidly with conversion. As the reaction progresses, the non-ionized carboxyl groups have carboxylate functions as the neighbors, and the carboxylate negative charge repels the reagent hydroxyl ions. However, this effect is less pronounced when acrylic acid is copolymerized with a non-ionizable monomer, as the electrostatic effect due to neighboring groups is decreased.[36]

Electrostatic interactions retard the alkaline hydrolysis of poly(methacrylamide)[35,37] and even stop it completely at about 70% conversion. The hydroxyl anion is electrostatically repelled from the methacrylamide units by two methacrylate ions, as shown in Structure 3.

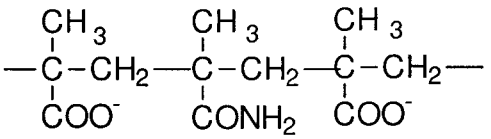

3

In the hydrolysis of copolymers of acrylic acid and 4-nitrophenyl methacrylate,[43] the dissociated carboxyl groups act on the ester group (4), and 4-nitrophenol is eliminated more rapidly than in the corresponding reactions of low-molecular-weight compounds.

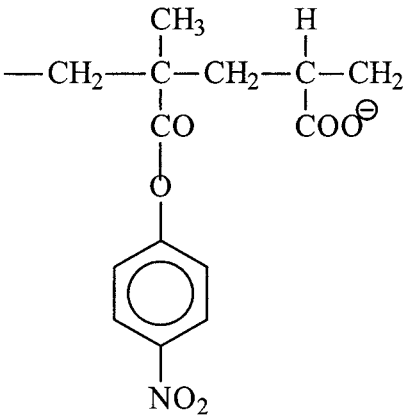

4

Bernard[44] *et al.* studied the electrostatic effect on the second-order rate constant of quaternization of low-molecular weight species such as pyridine, 4-picoline, 4-isopropylpyridine, and poly(4-vinylpyridine) by *n*-butyl bromide. They found the rate constant-time plot to be linear over the entire course of the reaction for all low-molecular weight species, indicating almost identical activation energies of about 16 kcal/mol. However, for poly(4-vinylpyridine), the quarternization started with about the same rate as the other 4-alkylpyridines, but decreased as the reaction progressed. The second order plots were linear up to 50% conversion and became concave afterwards,

showing a decceleration in the rate with an increase in the degree of quarternization. In the initial stages, the reaction would be a random process along the polymer chain, and the probability of quaternization of nearest neighbors is small. As the reaction proceeds, some of the unquaternized nitrogen gains quaternized neighbors, which can retard their reaction for several reasons: a) the positive charge on nitrogen makes the lone pair of electrons on an adjacent pyridine group less available for reaction with alkyl halide. b) the positively charged nitrogen may orient the approaching dipolar molecule of alkyl halide into an unfavorable position for the reaction with the neighbor. c) the quaternized nitrogen may increase the density of the polar solvent at its neighborhood by electrostriction, and thereby making the access of alkyl halide more difficult.

Bernard[44] also reported a similar rate pattern for all samples of poly(4-vinylpyridine) of different molecular weight (between 10^4 and 10^6), without any significant effect from polymer size on the reaction rate. We will study a reaction system containing styrenic type polymers for the same type of effect on a reaction that involves cleavage of benzylic-silicon bonds, but without the formation of charges on the polymer.

1.5.4.2 Steric hindrance

Polymer chains carrying functional groups can cause more steric hindrance to the approaching reagent molecules than is the case with low molecular weight analogs. Sakurada[45] compared initial rate constants, k_0, for the alkaline hydrolysis of poly(methyl acrylate) with those for low molecular weight esters, as given in Table 1.6. They found that both in acid and alkaline hydrolysis, k_0 for poly(methyl acrylate) is much smaller than that for the low-molecular weight esters. Though the apparent activation energy of

hydrolysis for the polymer (12 kcal/mol for poly(methyl acrylate)) and the low molecular weight analogs (11.5 kcal/mol for methyl isobutyrate and dimethyl glutarate) are very much similar, the small k_0 for poly (methyl acrylate) has been interpreted as due to the steric hindrance of neighboring groups. Similar studies were done by the same group[45] on poly(vinyl acetate). They found the rate constant k_0 for alkaline hydrolysis of

Table 1.6 Comparison of rates of alkaline and acid hydrolysis of poly(methyl acrylate) with low molecular weight esters.

Polymer or model	—CH(CO·OCH$_3$)—CH$_2$—	CH$_2$(CO·OCH$_3$)—CH$_3$	CH$_3$—CH$_2$(CO·OCH$_3$)—CH$_3$	CH$_2$(CO·OCH$_3$)—CH$_2$—CH$_2$(CO·OCH$_3$)
Acetone:water				
k_0 5 : 2	0.1	3.8	1.2	4.8
k_0 2 : 5	0.1	8.8	2.8	7.2
k_0 6 : 1	5.2	--	210	--

(k_0 is in 10^{-3} x l/mol/min and the third row of values are of acid hydrolysis)

poly(vinyl acetate), ethyl acetate and isopropyl acetate as 0.37, 3.5 and 0.57 l/mol/min respectively. Our interest is to study the variation in the reactivity of small model molecules containing benzylic-silicon bonding from their polymer analogs.

1.5.4.3 Tacticity

The nearest-neighbor effect on the reactivity of functional groups[35] can be expressed quantitatively by a statistical treatment of the reaction kinetics of polymer-analogous reactions utilizing McQuarrie's kinetic equations. The degree of conversion of a reaction in a polymer chain depends on three rate constants k_0, k_1 and k_2 when groups A

transform to groups B irreversibly by a first-order reaction. The constant k_0 characterizes the transformation of the central group A to B in the sequence triad AAA, k_1 applies to the triads AAB or BAA (with one transformed group B in the neighborhood of A), and k_2 to the triad BAB with two transformed neighboring groups. The magnitude of the neighboring group effect is determined by the ratio of the three rate constants. There is no effect when all three constants are identical, and the groups A and B are randomly distributed in the resulting product. When the constant k_0 is substantially smaller than the other two constants, the neighboring group accelerates the reaction and the blocks of group B are formed in the product. On the other hand, when k_0 is significantly larger than the other two constants, the neighboring group retards the reaction and the isolated groups B predominate in the product. The experimental data on the individual rate constants of chlorination for linear paraffins, cycloparaffins, and polyethylene is shown in Table 1.7[46]. On comparing cycloparaffins with linear polyethylene, only the absolute value of k_0 is changed. However, the ratio of these constants remains practically constant. This means that the conformational peculiarities of various cyclics and linear paraffins do not play any significant role in the reactivity of the CH_2 groups in the chlorination. However, the autoretardation during the course of reaction is due to the inductive influence of chloromethylene groups on the chlorination kinetics. Autoretardation in the reaction rate has also been reported in the case of quarternization of poly(4-vinylpyridine)[44] and the epoxidation of natural rubber.

Table 1.7 Individual rate constants of chlorination of polyethylene and its analogs

Substrate	$k_0 \times 10^3$	$k_0 : k_1 : k_2$
Cyclooctane C_8H_{16}	0.7	1:0.43:0.18
Cyclododecane $C_{12}H_{24}$	0.82	1:0.43:0.17
Cyclooctacosane $C_{28}H_{56}$	1.0	1:0.43:0.18
Cetane $C_{16}H_{34}$	0.7	1:0.35:0.08
Polyethylene $[-CH_2-]_n$	1.85	1:0.38:0.11

The role of stereochemical and conformational factors in autoacceleration and autoretardation of reactions of functional groups on macromolecules has been demonstrated in the hydrolysis of polymethacrylic esters[46]. Table 1.8 shows the effect of tacticity on the polymer reaction rate. The reason for the retardation in the rate of hydrolysis of isotactic PMMA (1:0.4:0.4) and syndiotactic PMMA (1:0.2:0.05) by strong base (KOH) could be the electrostatic repulsion of hydroxide ions governing the alkali hydrolysis by the carboxylate anions. The extent of retardation effect depends on the strength and the concentration of the base, which would influence the ionization of the carboxylic acid functionality formed in the hydrolysis. Thus, the retardation effect is not pronounced in isotactic PMMA (1:0.4:0.4) under 0.2 Molar KOH and in syndiotactic PMMA (1:0.7:0.7) under 0.05 Molar KOH. However, in the weakly basic pyridine-water system, instead of retardation, an acceleration in the hydrolysis rate is exhibited by most polymethacrylic esters. This is attributed to an anchimeric action of carboxylate function neighboring to the ester functions, according to the nucleophilic mechanism.

Table 1.8 Effects of neighbouring groups on the rate constants of polymer–analogous reactions of polymethacrylic esters[46] at 145 °C

Reaction	Tacticity	Medium	$k_0 \times 10^4$ /min	$k_0 : k_1 : k_2$
Hydrolysis of poly(methyl methacrylate)	iso	KOH(0.2M)	90	1:0.4:0.4
	syndio	KOH(0.2M)	5.8	1:0.2:0.05
	syndio	KOH(0.05M)	1.9	1:0.7:0.7
	iso	Pyridine-water (95:5)	5.3	1:8:100
	syndio	Pyridine-water (95:5)	1.1	1:2.5:3.4
Hydrolysis of poly(diphenylmethyl methacrylate)	iso	Pyridine-water (95:5)	0.3	1:20:100
	syndio	Pyridine-water (95:5)	0.5	1:1:1
Hydrolysis of poly(phenyl methacrylate)	iso	Pyridine-water (95:5)	6	1:40:1000
	iso	Dioxan (80 °C).	0.15	1:55:100
	iso	Dioxan (100 °C)	2	1:18:65
	hetero	Dioxan	5	1:2:10
Hydrolysis of poly(methyl methacrylate-*co*-methacrylic acid)	iso	Pyridine-water (95:5)	5.3	1:8:100
	syndio	Pyridine-water (95:5)	--	0:0.5:0.25
Epoxidation of natural rubber (poly(3-methyl 1,3 butadiene)	--	Benzene 25°C	--	1:0.67:0.42
Quarternization poly(4-vinylpyridine) with butyl bromide	--	Tetramethylene sulphone	6.54 l/mol/min	1:1:0.32

It is surprising to note that the constant k_2 is 10 times higher than k_1 for isotactic samples, owing to the bi-functional electrophilic-nucleophilic catalysis when a simultaneous interaction of one dissociated and one undissociated carboxyl groups takes place, which is shown in Scheme 13.

Scheme 13

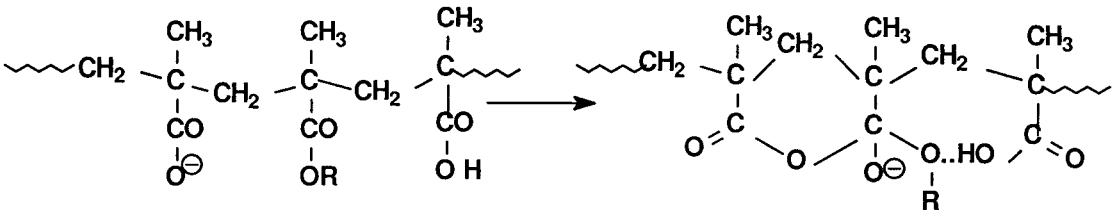

In spite of the acceleration character of the isotactic polymers in pyridine-water medium, the presence of bulky diphenylmethyl groups brings about a decrease in the absolute rate constant (k_0 = $0.3x10^{-4}$min) in comparison with poly(methyl methacrylate). Syndiotactic poly(diphenylmethyl methacrylate) does not show the neighboring group effect at all in weak alkali medium, and the whole reaction can be described in terms of the same reactivity of the ester groups, and of one rate constant.

1.5.5 Reactivity of the polymer gel

The reactivity of functional groups attached to crosslinked polymers is very much different from their reactivity in solution. A system containing reactive functional groups attached to a crosslinked polymer matrix can be roughly classified into two cases such as *gel* and *macro reticular type,*[35] as shown in Figure 1.6. The gel type is formed from a less-densely crosslinked homogeneous gel prepared in good solvent and exhibits a variation in their degree of swelling with diluent type, pore diameter and effective surface area. They allow a good solvent reversibly to be removed and reintroduced. Suspension polymerization of styrene with 2% w/w divinylbenzene yields resin beads, which is a typical example of gel type particle. The macro reticular type involves regions with an aggregated and partially ordered network structure, which is

not perturbed by the action of diluents. During its crosslinking process, a phase separation or desolvation of polymer chains occurs with subsequent irreversible collapse or chain clustering. The crosslinked network with permanent macropores is the result of phase separation during polymerization. This later type of gel is formed in precipitation polymerization of styrene/divinylbenzene with typically higher divinylbenzene content in aliphatic hydrocarbon or alcohol diluents.

Figure 1.6 Gel and macro reticular structure of a cross-linked polymer matrix.

Reactions of functional groups linked to the gel proceed more slowly than the analogous reactions in homogeneous solution. The porosity, crosslink density and reagent size impose restraints on diffusion in the gel to such a degree that the kinetics becomes diffusion controlled. The smaller the size of the gel particle, shorter the path of the reagent from the particle surface to an interior functional group. Thus, there is a reduction in the reaction rate with increase in the particle size and the crosslink density. An important role on the kinetics of a reaction in the gel phase is played by the solvation effect. Perfectly matched polarities of polymer gel and the diluent results in maximum swelling of the particle that makes the reaction easy. Our interest is to study the reactivity of a particular bonding (benzylic-silicon) incorporated into a highly cross-linked microsphere and microgel system.

Aim of Research

The aim of this research is to study the cleavage pattern of benzylic-silicon bonds on different molecular levels, ranging from small model molecules with different substituents over oligomeric analogs, linear polymers and co-polymers to crosslinked polymer materials.

At each level, the aim is to study the structural and conformational effects of the oligomer and polymer backbone, which may be compared loosely with the primary, secondary, tertiary, and quaternary structure in polypeptides.

Three specific cleavage reagents will be studied:

1. Potassium hydroxide (KOH) in ethanol

2. Tetrabutyl ammonium fluoride (TBAF) in THF

3. Ceric ammonium nitrate (CAN) in acetic acid

Cleavage reactions will be carried out on benzyltrimethylsilane, *p*-isopropylbenzyl trimethylsilane, oligomeric and polymeric *m/p*-vinylbenzyltrimethylsilane, and on their copolymers with styrene and MMA. Also, we will attempt the same cleavage reactions on cross-linked microspheres and microgels to see the cleavage feasibility and to explore the effect of their morphologies on the reaction kinetics.

CHAPTER 2. EXPERIMENTAL METHODS

2.1 General experimental procedures

All reactions were carried out in dry glass apparatus under a nitrogen atmosphere, using septa and syringes for the transfer of reagents.

2.2 Materials and purification

Tetrahydrofuran (99.9% anhydrous from Aldrich used without distillation, or reagent grade distilled over potassium with benzophenone), methanol (reagent grade, Caledon), hexanes (reagent grade, Caledon), acetonitrile (reagent grade, Caledon), toluene (reagent grade, Caledon), benzene (Fisher scientific), absolute ethanol (available from Chemical store). AIBN (recrystallized from methanol, Dupont), benzyl chloride (97 % pure, Aldrich), 4-isopropylbenzylchloride (Lancaster, used without purification), vinyl benzylchloride (isomeric mixture containing 55/45 *meta* and *para* isomers, Aldrich, passed through a short silica column to remove the inhibitor before use), potassium hydroxide (BDH Inc), TMSCI (99 % pure, Aldrich), dichlorodimethylsilane (99 % pure, Aldrich, distilled prior to use), tetrabutyl ammonium fluoride (TBAF, 1 Molar solution in THF from Aldrich), ceric ammonium nitrate (CAN, 99 % pure from Sigma, dried at 80 ^{o}C and stored in dessicator), acetic acid (Baker analyzed), magnesium turnings (heated at 100 ^{o}C for 12 hrs).

2.3 Instrumentation and analytical procedures

^{1}H and ^{13}C NMR spectra were obtained on Bruker AC-200 and AC-300 spectrometers using deuterated chloroform and deuterated acetone as solvents. ^{29}Si NMR was

performed on an AC-300 instrument without any deuterated standard. The chemical shifts were recorded with respect to tetramethylsilane as a standard, set at 0 ppm. The abbreviations: s - singlet, d - doublet, t - triplet, q - quartet, dd - doublet of doublets, m - multiplet are used in reporting the spectra.

Molecular weight measurements were carried out on a Waters gel permeation chromatograph using three ultra styragel columns in series with THF as the eluting solvent flowing at 1 ml/min, and a differential refractometer as the detector. Narrow molecular weight polystyrene standards were used for the calibration of the chromatographic system.

Fourier transform infrared spectra were recorded on a BIO RAD FTS-40 spectrometer. Samples were run as neat films on NaCl windows or as KBr pellets. The abbreviations: s - strong, m - medium, w - weak intensities were used in reporting the spectra.

Purity checks of chemicals and quantifications of some reactions were done on a HP-5970 gas chromatograph equipped with a 30 mtr / 0.53 mm HP-5 capillary column and a flame ionization detector, using helium as the carrier gas at a flow rate of 15 ml/min. An oven temperature ramp was programmed from 50 ^{o}C to 250 ^{o}C with a heating rate of 15 ^{o}C/min.

Morphology of the polymer microspheres was studied with an ISI DC-130 scanning electron microscope (SEM). SEM specimens were prepared by redispersing the cleaned particles in acetone and placing a drop of the suspension on a cleaned steel stud using a

piece of glass glued to the stud. The drop was dried in clean air at room temperature and then sputter-coated under vacuum with a 12-15 nm thick layer of gold.

The particle sizes and size distributions were determined using a 256-channel Coulter Multisizer II. An orifice tube with a 30μ aperture was used. A drop of particle suspension in methanol was diluted with isoton II electrolyte and placed in the measurement chamber. A computer interfaced to the Coulter multisizer was used to calculate and plot the size and size distribution of particles. Particle porosity measurements were carried out by nitrogen absorptometry, using the BET method.

2.4 General synthesis of benzyltrimethylsilane (BTMS), *p*-isopropyl benzyltrimethylsilane (ISO-BTMS), *m/p*-vinylbenzyltrimethylsilane (*m/p*VBTMS) and bis(vinylbenzyl)dimethylsilane (BVBDMS) - Grignard Reaction.

All of the model compounds were prepared from their respective benzyl halide through Grignard coupling with halosilane. This method is a modified version of the one described by Li and Stöver[47] for the synthesis of bis(vinylphenyl)ethane (BVPE). The typical reaction was carried out in a 3 necked 250 ml round bottom flask fitted with a dropping funnel and a thermometer under dry nitrogen atmosphere. The reaction flask was placed in an ice bath to maintain a reaction temperature of 0 °C. Mg turnings dried over night at 100 °C were placed in the reaction flask along with 200 ml dry THF. The halosilane was then injected into the flask using a syringe. The mixture was stirred using a magnetic stirrer, and cooled to 0 °C. The required amount of alkyl halide was filled into the dropping funnel. The alkyl halide from the dropping funnel was then added slowly at the rate of 10 drops/min so that reaction temperature was maintained

around 0 °C. An induction period of 3 to 5 min was noticed from the temperature rise in the thermometer. The reaction was stirred for 24 hrs at 0 °C after the addition of the alkyl halide. The reaction mixture was then decanted from unreacted magnesium, the solvent THF removed on a rotary evaporator, and the residue treated with 100 ml of hexanes and 100 ml of water in the separating funnel. The aqueous layer was acidified with 50 ml of 5% HCl and discarded. The organic phase was then washed 3 times with 100 ml of water, separated, and dried with anhydrous magnesium sulfate. The solvent was evaporated on the rotary evaporator to obtain a light yellow oil. The rotary evaporations were carried out by immersing the evaporation flask in cold water in order to avoid any thermal polymerization of vinyl monomers. The final color of the product was improved by passing the product through a short silica column.

Benzyltrimethylsilane (BTMS)

Benzyl chloride (0.15 mol, 19 gm, 17.26 ml), Mg (0.16 mol, 3.96 gm), chlorotrimethylsilane (0.16 mol, 24.4 gm, 22.8 ml). Yield - 16 gm (65 %).

^{1}H-NMR (200MHz, $CDCl_3$) (ppm): 0.00 (s, 9 $C\underline{H}_3$), 2.08 (s, 2 $C\underline{H}_2$), 6.97 - 7.20 (m, 5H aromatic). **^{13}C-NMR** (40MHz, $CDCl_3$) (ppm): -1.91 (3 methyl C), 27.06 (benzylic C), 31.69, 123.95, 128.03 and 128.14 (aromatic), 140.34. **^{29}Si-NMR** (ppm): 0.90. **IR** (NaCl): *v* 3082w, 3062w, 3027 (s, aromatic CH symmetric stretch), 2957 (s, out of plane deformation of 2 H of CH_2) 2896 (s, in plane deformation of 2 H of CH_2), 1601 (s, aromatic C-C double bond stretch), 1494 (s, aromatic C-C double bond stretch), 1452w, 1415w, 1249 (s, Si-CH_3 symmetrical stretch), 1208 (m, benzylic CH_2-Si stretch), 1156m, 1056w, 854 (s, aromatic C-H out of plane bending) 772w, 738w.

***p*-isopropylbenzyltrimethylsilane (ISO-BTMS)**

4-isopropylbenzylchloride (0.05 mol, 8.38 gm), Mg (0.06 mol, 1.5 gm), chlorotrimethylsilane (0.06 mol, 7.6 ml). Yield - 9.13 gm (87 %).

^{1}H-NMR (200MHz, $CDCl_3$) (ppm): 0.04 (s, 9 C$\underline{H}_3$), 1.24 (d, 6 C$\underline{H}_3$), 2.06 (s, benzylic C$\underline{H}_2$), 2.9 (septet, isopropyl C$\underline{H}$), 6.90 - 7.30 (m, aromatic). **^{13}C-NMR** (40MHz, $CDCl_3$) (ppm): -2.02 (3 methyl C), 23.96 (2 methyl C), 26.26 (benzylic C), 33.26 (tertiary C of isopropyl), 125.94 (aromatic), 127.77 (aromatic), 137.29, 144.03. **^{29}Si-NMR** (ppm): 0.78. **IR** (NaCl): *v* 3088w, 3050w, 3020 (s, aromatic CH symmetric stretch), 2959 (s, out of plane deformation of 2 H of CH_2), 2893 (s, in plane deformation of 2 H of CH_2), 1512m, 1464w, 1418w, 1248 (s, Si-CH3 symmetrical stretch), 1209 (m, benzylic CH2-Si stretch), 1157w, 850 (s, aromatic C-H out of plane bending), 762w.

***m/p*-vinylbenzyltrimethylsilane (*m/p*VBTMS)**

m/p-vinylbenzylchloride (0.10 mol, 15.23 gm, 14.23 ml), Mg (0.11 mol, 2.73 gm), chlorotrimethylsilane (0.11 mol, 11.93 gm, 13.94 ml). Yield - 17.10 gm (90 %).

^{1}H-NMR (200MHz, $CDCl_3$) (ppm): 0.04 (s, 9 C$\underline{H}_3$), 2.08 (s, benzylic C$\underline{H}_2$), 6.90 - 7.30 (m, aromatic), 6.67 (dd, vinyl C$\underline{H}$), 5.70(dd, vinyl C$\underline{H}_2$ trans). 5.17 (dd, vinyl C$\underline{H}_2$ cis). A small singlet peak at 2.3 ppm corresponds to a maximum 5% impurity level of 3- or 4-methylstyrene. Residual vinylbenzylchloride showed a small peak at 2.3 ppm in the proton spectrum. Gas chromatogram indicates a doublet peak corresponding to a *meta/para* isomeric mixture of the product. **^{13}C-NMR** (40MHz, $CDCl_3$) (ppm): -1.99 (3 methyl C), 26.84 (benzylic C), 111.8 (Cβ), 126.06 (C-2,-6), 128.04 (C-3,-5), 133.38 (C-

1), 136.79 (Cα), 140.18 (C-4). **^{29}Si-NMR** (ppm): 1.08. **IR** (NaCl): *ν* 3085w, 3047w, 3018w, 2957s, 2894m, 1629m, 1607m, 1509m, 1407s, 1287w, 1248 (s, Si-CH3 symmetrical stretch), 1205(m, benzylic CH_2-Si stretch), 1155m, 1086w, 989 (s, vinyl CH out of plane bending), 901 (s, vinyl CH_2 out of plane bending), 850s, 768w, 738w,

bis(vinylbenzyl)dimethylsilane (BVBDMS)

m/p-vinylbenzylchloride (0.20 mol, 30.46 gm, 28.46 ml), Mg (0.22 mol, 5.46 gm), dichlorodimethylsilane (0.10 mol, 12.91 gm, 12.13 ml). Yield - 25.15 gm (87 %).

^{1}H-NMR (200MHz, $CDCl_3$) (ppm): -0.12 (s, 6 $C\underline{H}_3$), 2.02 (s, 4 benzylic $C\underline{H}_2$), 6.82 - 7.22 (m, aromatic), 6.60 (dd, vinyl $C\underline{H}$), 5.62 (dd, vinyl $C\underline{H}_2$ trans), 5.11 (dd, vinyl $C\underline{H}_2$ cis). This crosslinker appeared in the GC trace as a triplet peak of integral ratio equivalent to a 20/50/30 *p/p, m/m* and *m/p* isomeric mixture. **^{13}C-NMR** (40MHz, $CDCl_3$) (ppm): -3.95 (2 methyl C), 24.93 (2 benzylic C), 112.02 & 113.26 (2 vinyl βC), 121.99, 126.03, 127.64, 128.18 (aromatic), 133.46 (C-1), 137.0 and 137.31 (2 Cα), 139.52 and 139.35 (2 C-4). **^{29}Si-NMR** (ppm): 1.5. **IR (neat)** 3087 (w, C-H aromatic), 3010 (w, C-H of CH_3), 2957 (m, C-H stretch of benzylic CH_2), 1629 (w, vinyl C-C double bond stretch), 1599 (m, ring C-C double bond stretch), 1579 (w, ring C-C double bond stretch), 1484 (w, CC double bond ring stretch), 1407 (w, vinyl CH2 in plane deformation), 1428 (s, Si-CH_3 symmetrical stretch), 1204 (m, benzylic CH_2-Si stretch), 990 (s, vinyl CH out of plane bending).

2.5 Oligomerization of *m/p*-vinylbenzyltrimethylsilane (*m/p*-VBTMS)

Oligomeric poly(*m/p*VBTMS) was prepared using carbon tetrachloride as chain transfer agent with AIBN as initiator in toluene solvent. VBTMS (13.0 gm, 0.068 mol), toluene (10 ml), AIBN (0.91 gm, 7 wt %), and carbon tetrachloride (10 ml) were placed in a three necked round bottom flask fitted with a thermometer under dry nitrogen atmosphere. The contents were stirred using a magnetic stirring bar and heated to 75 °C using an oil bath. After 24 hrs, the reaction mixture was cooled, the solvents evaporated, and the residue dissolved in 15 ml of THF. The oligomer was then precipitated into a 4-fold excess of methanol at -20 °C. The product was reprecipitated from THF into cold methanol and the filtered polymer dried in a vacuum oven for 24 hrs at room temperature. Yield = 5 gm (40%). Mn/PD = 3300/1.88.

^{1}H-NMR (300MHz, $CDCl_3$) (ppm): -0.06 (s, 9 $C\underline{H}_3$), 1.42 (backbone $C\underline{H}_2$), 1.53 (backbone $C\underline{H}$), 1.95 (benzylic $C\underline{H}_2$), 6.3-7.2 (4$\underline{H}$, aromatic), A small shoulder peak at 2.3 corresponds to a maximum impurity of 5% 3 or 4-methyl styrene. **^{13}C-NMR** (40MHz $CDCl_3$) (ppm) and **IR (KBr)** same as in the homopolymer below. **^{29}Si-NMR** (ppm): 0.55.

2.6 Free radical solution polymerization of *m/p-v*inylbenzyltrimethylsilane.

The same procedure used for oligomerization was carried out for the polymerization except for the absence of chain transfer agent. Initiator AIBN (0.114 gm, 0.7 mmol, 1

wt%), toluene (12 ml), isomeric VBTMS (11.4 gm, 0.06 mol), temperature 75 °C. Yield = 6.64 gm (60%). Mn = 13200 Mw/Mn = 1.8.

^{1}H-NMR (200MHz, $CDCl_3$) (ppm): -0.09 (s, 9 $C\underline{H}_3$), 1.33 (backbone $C\underline{H}_2$), 1.53 (backbone $C\underline{H}$), 1.87 (benzylic $C\underline{H}_2$), 6.3-7.2 ($4\underline{H}$, aromatic), A small shoulder peak at 2.3 corresponds to a maximum impurity of 5% as 3 or 4-methyl group. **^{13}C-NMR** (40Hz,$CDCl_3$) (ppm): -1.73 (3 methyl C), 26.49 (benzylic C), 40.17 (methine C), 125.25 (C-2,-6), 127.57 (C-3,-5), 136.44 (C-1), 142.3 (C-4). **^{29}Si-NMR** (ppm): 0.60. **IR (KBr)** *v* 3087 (w, C-H aromatic), 3010 (w, C-H of CH_3), 2957 (m, C-H stretch of benzylic CH_2), 1629 (w, vinyl C-C double bond stretch), 1599 (m, ring C-C double bond stretch), 1579 (w, ring C-C double bond stretch), 1484 (w, CC double bond ring stretch), 1407 (w, vinyl CH_2 in plane deformation), 1428 (s, Si-CH_3 symmetrical stretch), 1204 (m, benzylic CH_2-Si stretch), 990 (s, vinyl CH out of plane bending).

2.7 Copolymerization of *m/p*-vinylbenzyltrimethylsilane with styrene and methyl methacrylate

These copolymerizations were carried out using a procedure similar to that used for the polymerization described above. The copolymerization parameters includes feed ratio, composition, yield and molecular weight are shown in section 3.1.

Poly(VBTMS-*co*-Styrene): ^{1}H-NMR (200MHz, $CDCl_3$) (ppm): -0.09 (s, 9 $C\underline{H}_3$), 1.33 (backbone $C\underline{H}_2$), 1.53 (backbone $C\underline{H}$), 1.87 (benzylic $C\underline{H}_2$), 6.0-7.2 (aromatic), **^{13}C-NMR** (40MHz, $CDCl_3$) (ppm): -1.99 (3 methyl C), 26.49 (benzylic C), 40.14 (methine C), 125.36 (C-2,-6), 127.64 (C-3,-5), 136.44 (C-1), 145.2 (C-4).

Poly(VBTMS-*co*-methyl methacrylate): ^{1}H-NMR (200MHz, $CDCl_3$) (ppm): -0.067 (s, 9 $C\underline{H}_3$), 1.33 (backbone $C\underline{H}_2$), 0.4 - 0.6 (methacrylate protons) 1.53 (backbone $C\underline{H}$), 1.87 (benzylic $C\underline{H}_2$), 2.9-3.5 (methoxy protons), 6.3-7.2 (4$\underline{H}$, aromatic), **^{13}C-NMR** (40MHz, $CDCl_3$) (ppm): -1.81 (3 methyl C), 17.9 and 19.9 (backbone methylene C) 26.49 (benzylic C), 51.40.17 (methine C), 125.7 (C-2,-6), 127.7 (C-3,-5), 136.44 (C-1), 140.2 (C-4), 145.5 (methoxy C), 177.3 (carbonyl C).

2.8 Selective cleavage of benzylic-silicon bonds by KOH/EtOH/THF

The cleavage reactions on small molecules including benzyltrimethylsilane (BTMS), *p*-isopropyl benzyltrimethylsilane (ISO-BTMS), and mono and bifunctional vinyl benzyl type monomers (VBTMS and BVBDMS) were carried out in 10 mm NMR tubes, and the bond cleavage was followed quantitatively by INVERSEGATE ^{29}Si NMR on a AC-300 Bruker NMR spectrometer. In a a typical reaction, the reaction mixture was prepared in 20 ml vials from 2.5 mmol of silane, 10 ml of dry THF, 5 ml of 4N KOH in absolute ethanol and 5 ml of absolute ethanol. This results in 0.125 and 1.0 Molar concentrations for the substrate and the KOH respectively. 4 ml of this reaction mixture was then transferred into a 10 mm NMR tube and sealed using vacuum freeze thaw technique. The reaction was carried out by keeping the NMR tube in an oil bath at 70 +/-2 °C and monitoring the ^{29}Si-NMR spectra at different intervals after arresting the reaction in liquid nitrogen each time.

The same reaction was carried out on benzyltrimethylsilane and *p*-isopropylbenzyl trimethylsilane in a 3 necked round bottom flask fitted with a water condenser, a thermometer, a stirrer bar, nitrogen atmosphere, and an oil bath set to 72 °C. The

reaction mixture was made up as 40 ml volume solution, keeping the same concentrations for substrate and KOH as above. The mixture was then made to reflux at 70 +/-2 °C. Aliquots of 2 ml were taken by syringe at different reaction times and combined with 2 ml of 1N HCl to neutralize the hydroxide. 1 ml of an internal standard (*n*-decane in THF) was added to each aliquot before injection into the GC for the quantitative cleavage measurements.

The same reaction on polymers and copolymers was done in a 3 necked round bottom flask fitted with a water condenser, a thermometer, a stirrer bar, nitrogen atmosphere, and an oil bath for heating. The mixture was then made to reflux at 70 +/- 2 °C. Aliquots of 3 ml were taken by syringe at different reaction times and some of the solvent was evaporated on the rotary evaporator, and then precipitated into cold methanol. It was then filtered, washed thoroughly with methanol, and dried for 24 hrs at 50 °C under vacuum to remove methanol. The bond cleavage was measured by taking ^{1}H-NMR spectra of the polymers or copolymers at different degrees of cleavage.

2.9 Selective cleavage of benzylic-silicon bonds by tetrabutyl ammonium fluoride/THF

Since the reaction of fluoride ion on our small model molecules was found to very rapid at room temperature, only reactions on polymeric species were carried out, specifically at 22 °C (room temperature) and 0 °C. In a typical reaction, 1 mmol of the polymer was dissolved in 32 ml THF and combined with 8 ml of 1 Molar TBAF in THF to give the desired concentrations (0.025 Molar in polymer and 0.2 Molar in fluoride). This reaction mixture was taken in a 3 necked round bottom flask equipped

with a condenser, a thermometer, a stirrer bar and nitrogen bubbler. Aliquots of 2 ml were taken by syringe at different reaction times and precipitated into methanol. The filtered polymer was then washed with methanol three times, and dried under vacuum overnight. The degree of bond cleavage was measured by taking ^{1}H-NMR spectra of the reaction products.

2.10 Selective cleavage of benzylic-silicon bonds by ceric ammonium nitrate/acetic acid/benzene

This cleavage reaction on the small molecules containing benzylic-carbon bond was carried out in a 3 necked round bottom flask fitted with a condenser, a spin bar, the nitrogen access, and a thermometer reaching below the liquid level. 1 mmol of the substrate molecules (benzyltrimethylsilane and 4-isopropylbenzyltrimethylsilane) was dissolved in 30 ml of glacial acetic acid and 30 ml of benzene as a co-solvent. The reaction mixture was maintained at a temperature of 50 +/- 1 °C using an oil bath. Then 3 mmoles of CAN was added rapidly into the stirring reaction mixture. Aliquots of 2 ml were removed after different intervals of times and the reaction was arrested by immersion in liquid nitrogen. After adding 1 ml of (*n*-decane in THF) internal standard solution, about 3 microlitres of this solution was injected into the GC to measure the bond scission quantitatively.

The reactions on polymers and copolymers were carried out under the same experimental conditions. During the reaction, the color of the solid CAN changed from orange to light yellow and that of the solution from yellow to pale yellow or green. Aliquots were taken, cooled, and precipitated into a 4-fold excess of (4:1 v/v)

methanol-water mixture. The precipitates were then washed 2-3 times with methanol/water mixture until the color of the precipitate turned colorless, and dried under vacuum overnight. The bond cleavage was then estimated from the ^{1}H-NMR spectra of the oxidized polymers. Some reactions were carried out as separate runs for individual data.

2.11 Precipitation polymerization of bis(vinyl benzyl)dimethylsilane (BVBDMS)

Polymerization reactor:

All precipitation polymerizations were carried out in a small reactor having a programmable temperature controller capable of maintaining a set temperature to within +/-1 °C. The reactor consists of a series of rollers mounted horizontally. The reactor agitates the sample in vials placed on the rollers, by rolling the vials at roughly 4 revolutions per minute. The temperature profile used for the polymerizations started with a one-hour ramp from room temperature to 60 °C followed by an hour and 40 minute ramp to 70 °C. Once at 70 °C, the reactions were continued for 24 hrs.

Precipitation Polymerization:

Polymerizations were carried out in duplicate in 20 ml screw-capped polypropylene vials. AIBN (0.0077 gm, 2 wt% relative to BVBDMS) was added to a solution of BVBDMS (0.386 gm, 0.4 ml, 2 vol % relative to total volume) in 100% acetonitrile (20 ml) or a binary solvent system of acetonitrile/toluene mixtures of 80/20, 65/35, and 50/50 vol %. The reaction mixtures were found turbid in 100% acetonitrile, and clear in the binary systems used. The vials were rotated in the reactor, using a temperature

profile from room temperature to 60 °C in 60 min, from 60 °C to 70 °C in 100 min, and at 70 °C for another 24 hrs. After the polymerization, a small amount of hydroquinone was added to arrest the polymerization before the particles were separated from the solvent by centrifugation, and then washed with THF once. The THF washings were then combined with the separated solvent and the sol-fraction was precipitated into methanol. The particles were then resuspended twice in ethanol and in acetone, and centrifuged. The cleaned particles were then dried under vacuum for 48 hrs at room temperature. The identification of BVBDMS microspheres formed in 100/0, 80/20, and 65/35 vol % acetonitrile/toluene mixtures are PP01, PP02, PP03 and the microgels formed from 50/50 vol % acetonitrile/toluene mixture is PP04. Mn and PD of the three purified sol-fractions and the purified microgel were measured using GPC.

Microgel (ID-PP04)**:** ^{1}**H-NMR** (200MHz, $CDCl_3$) (ppm) -0.12 (6 $C\underline{H}_3$), 2.02 (s, 2 benzylic $C\underline{H}_2$), 6.82 -7.22 (aromatic protons), 1.1- 1.6 (backbone $C\underline{H}_2$). **IR (KBr):** 3087 (w, C-H aromatic), 3010 (w, C-H of CH_3), 2957 (m, C-H stretch of benzylic CH_2), 1629 (w, vinyl C-C double bond stretch), 1599 (m, ring C-C double bond stretch), 1579 (w, ring C-C double bond stretch), 1484 (w, CC double bond ring stretch), 1407 (w, vinyl CH_2 in plane deformation), 1428 (s, Si-CH_3 symmetrical stretch), 1204 (m, benzylic CH_2-Si stretch), 990 (s, vinyl CH out of plane bending). **Microspheres**: IR(KBr): Same peak positions of microgel, but some peaks of different intensity.

2.11.1 Determination of apparent rate of polymerization

Precipitation polymerizations were carried out in duplicate in 20 ml screw-capped polypropylene vials. AIBN (0.0077 gm, 2 wt% relative to BVBDMS) was added to a

solution of BVBDMS (1.118 gm, 0.4 ml, 2 vol% relative to total volume) in acetonitrile (20 ml). Instead of using any temperature ramp, the reactor was set at 70 °C for 24 hrs reaction time. Aliquots of 1 ml were removed by syringe at different intervals of reaction time. A small amount of hydroquinone was added to each aliquot to arrest the polymerization. A drop from each aliquot was used for the particle size determination using the Coulter multisizer. Another aliquot of internal standard (*n*-decane in THF) was combined with each of the above aliquots before injecting into the GC to measure the monomer conversion.

2.11.2 Cleavage of bis(vinylbenzyl)dimethylsilane (BVBDMS) microspheres / microgel by tetrabutyl ammonium fluoride/THF

In a typical reaction, 146 mg (1 mmol in silicon-carbon functionality) of microspheres was placed in a round bottom flask, containing 8 ml of 1 Molar TBAF in THF and 32 ml of THF, making up the fluoride concentration 0.2 Molar and that of Si-C functionality 0.025 Molar. The flask was fitted with a thermometer, nitrogen access, a condenser and a magnetic stirring bar. Aliquots were removed at different intervals of reaction times, diluted with THF to dissolve completely any soluble polymer, and then centrifuged. The degraded microspheres were resuspended in methanol and then in acetone, and dried. They were analysed by SEM for their morphological change.

Microgel: The reaction on microgel was carried out in the same manner described above. The aliquots were removed from the reaction mixture as a function of time and diluted with a 2-fold excess of THF. They were then precipitated into a large excess of

methanol. The degraded microgel was then dried and analysed for quantitative silicon-carbon bond cleavage by FTIR and ^{1}H NMR spectroscopy.

2.11.3 Cleavage of bis(vinylbenzyl)dimethylsilane (BVBDMS) microspheres by ceric ammonium nitrate/acetic acid/benzene.

In the reaction, 146 mg (1 mmol in Si-C functionality) of the microspheres were placed in a mixture of 30 ml acetic acid and 30 ml benzene in a 100 ml round bottom flask fitted with a thermometer, nitrogen access, a condenser and a magnetic bar. Keeping the temperature of the reaction mixture at 50 +/-1 ^{o}C, 3 mmoles of solid CAN were added into the stirring solution. The progress of the reaction was noticed from the color change of solid CAN and the solution from orange to yellow, and from the morphological change of the particles seen through an optical microscope. Aliquots were removed at different intervals of reaction time and the residual solid CAN was dissolved by adding a 50/50vol mixture of distilled water and THF, and then centrifuged. The microspheres were resuspended thrice in methanol/water mixture and twice in acetone before drying. The centrifugate was then concentrated in rotary evaporator and precipitated into methanol to isolate any soluble polymer separated from the microspheres. The dried soluble polymer fractions and the degraded microspheres were analyzed for quantitative silicon-carbon bond cleavage by FT-IR spectroscopy, and the SEM pictures of degraded microspheres were taken to see their morphological change.

CHAPTER 3. RESULTS AND DISCUSSION

3.1 Synthesis of small molecule and linear polymer model compounds

The first step of this project was to synthesize polymers and low molecular weight analogs containing benzylic-silicon bonds. The low molecular weight analogs including benzyltrimethylsilane (BTMS) and *p*-isopropylbenzyltrimethylsilane (ISO-BTMS), and the required vinyl monomers including vinylbenzyltrimethylsilane (*m/p*-VBTMS) and bis-(vinylbenzyl)dimethylsialne (BVBDMS) were prepared using a Grignard coupling reaction similar to the one described by Li and Stöver[47] for the synthesis of BVPE (bis(*p*-vinylphenyl)ethane). All reactions gave good yields of products with reasonable level of purity.

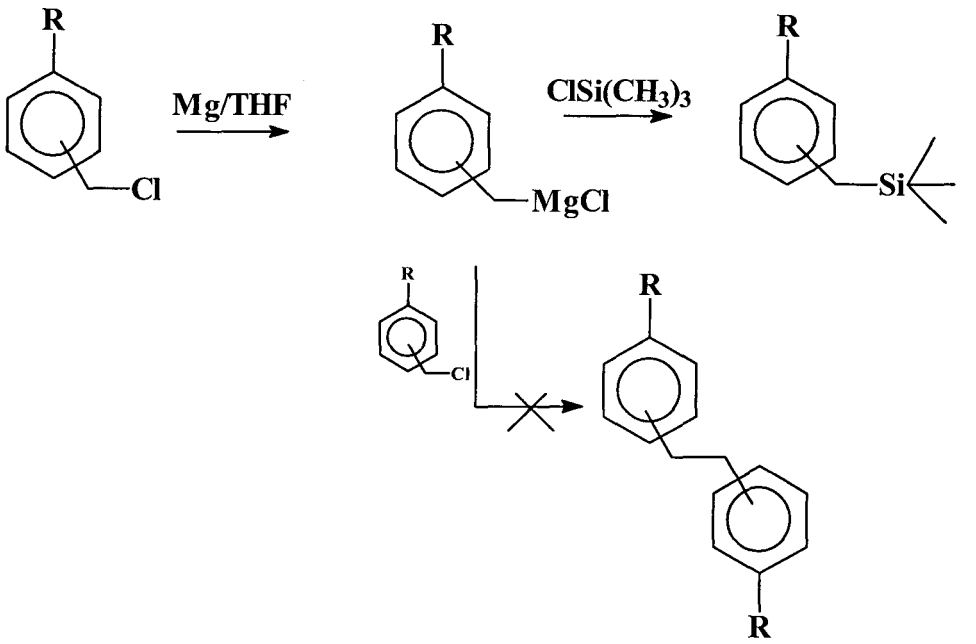

Figure 3.1.1 Typical Grignard synthesis.

The typical synthetic route to the model or substrate molecules is shown in Figure 3.1.1. Traces of methyl-styrene impurities were found very difficult to eliminate from the reaction. The possible side-reaction leading to the coupling of starting materials $RC_6H_4CH_2Cl$ (R = H or isopropyl, vinyl), is completely prevented due to two reasons. One is the much higher reactivity of trimethylsilylchloride (TMSCl) towards Grignard reagents compared to the reactant, $RC_6H_4CH_2Cl$. Secondly, the reaction is carried out in such a way that during the reaction, the concentration of the $RC_6H_4CH_2Cl$ derivative in the reaction mixture is as low as possible. As a consquence, the initially formed benzylic Grignard is immediately captured by reaction with the chlorotrimethylsilane (TMSCl).

Figure 3.1.2 shows the proton NMR spectra of *m/p*VBC (vinylbenzylchloride), *m/p*VBTMS (vinylbenzyltrimethylsilane) and poly(*m/p*VBTMS). The small singlet peak at 2.3 ppm of *m/p*VBC and *m/p*VBTMS corresponds to an impurity level of about 5% of 3- and 4-methylstyrene. This impurity appeared in the spectrum of poly(*m/p*VBTMS) as a small shoulder. This impurity is in part present in VBC, and in part formed during the reaction with traces of water. All peak assignments are given in the experimental section 2.4 and 2.6.

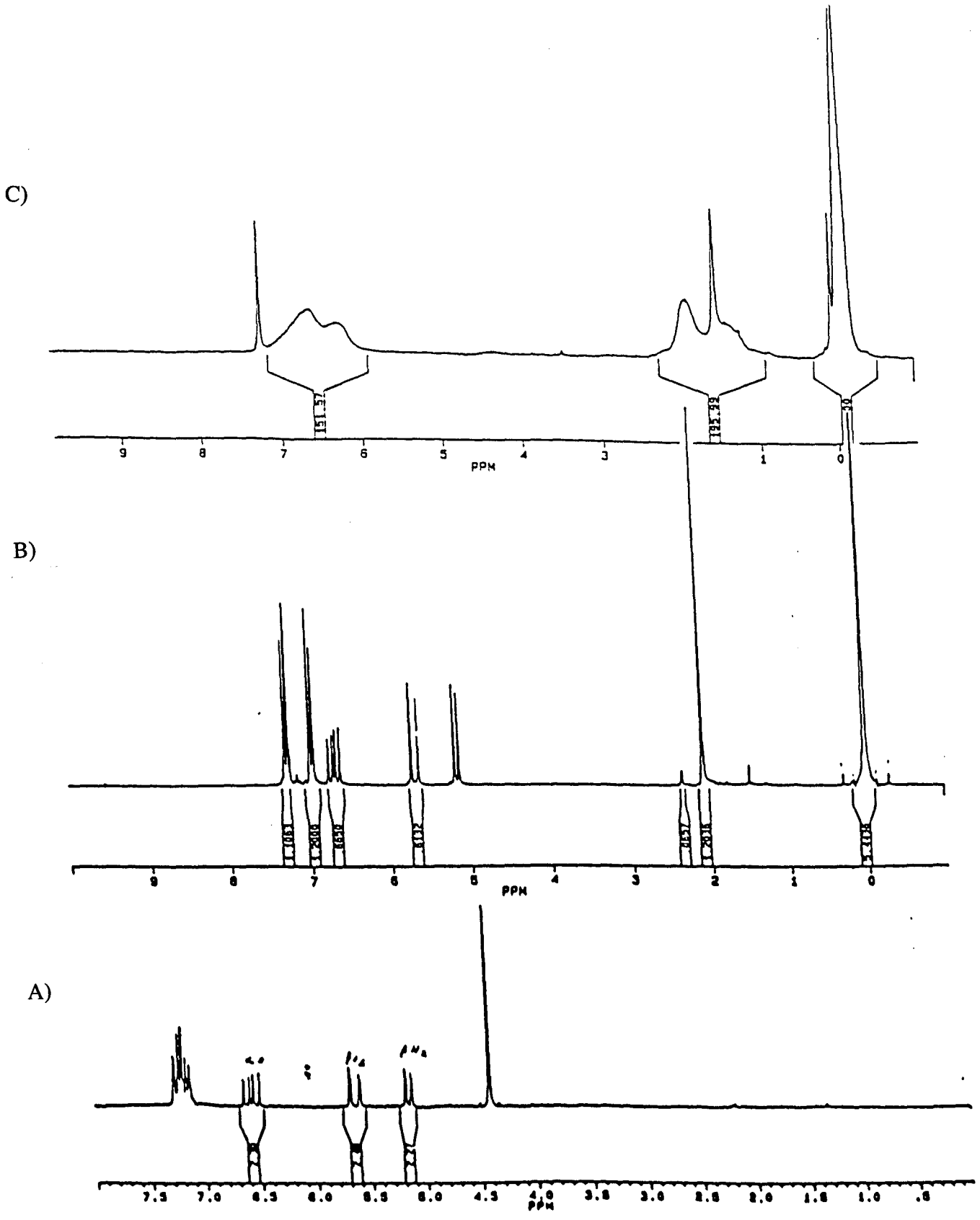

Figure 3.1.2 ^{1}H-NMR spectra of A) *m/p*VBC B) *m/p*VBTMS C) poly (*m/p*VBTMS)

In order to study the effect of copolymer type, composition, chain length, and their chain structure on reactivity of benzylic-silicon functionality, copolymers of VBTMS with styrene and methyl methacrylate (MMA) were synthesized with different compositions. The results of the copolymer preparation are depicted in Table 3.1.1.

Table 3.1.1 Synthetic details of poly(VBTMS-*co*-styrene) and poly(VBTMS-*co*-methyl methacrylate)

	Poly(VBTMS-*co*-styrene)					Poly(VBTMS-*co*-methyl methacrylate)				
Copolymer ID	VS15	VS15'	VS12	VS11	VS11'	VM15	VM15'	VM12	VM12'	VM11
Feed molar ratio vbtms:comonomer	1 : 5	1 : 5	1 : 2	1 : 1	1 : 1	1 : 5	1 : 5	1 : 2	1 : 2	1 : 1
Monomer [mmol]	6	6	15	30	30	6	6	15	15	30
Wt % of AIBN to comonomer	2.0	2.0	2.0	2.0	2.0	0.72	2.0	2.0	0.72	2.0
R.Time hrs	24	13	24	24	13	24	24	24	24	24
Copolymer composition vbtms : comonomer	13.5:86.5	14:86	30:70	48:52	45:55	18:82	19:81	36:64	37:63	52:48
Mn	10000	9600	17200	27900	17100	36700	26700	26600	26650	40800
PD	2.1	1.81	3.8	3.2	3.1	2.0	2.8	2.1	2.99	2.7
Yield %	60	27	73	54	40	60	30	66	42	70

Reaction temperature 75 °C, Solvent benzene added to make comonomer concentration 1 Molar.

The copolymer pairs VS15 and VS15', and VS11 and VS11' were prepared using an identical feed molar ratio and reaction temperature, but with different reaction times (13 & 24 hrs). Since, the polymerization is not of 'living type', both members in either pair are similar in composition and chain length (the Mn of VS11 (27900) and VS11' (17100) are not considered as significantly different as their polydispersities are in the range of 3). Thus, VS15 and VS11 represent copolymers of vinylbenzyltrimethylsilane (V) and styrene (S) of 1:5 and 1:1 composition. VS12 stands for the copolymer of 1:2 composition. Similarly, VM stands for the copolymers of vinylbenzyltrimethylsilane (V) and methyl methacrylate (M). VM15 and VM15' are of 1:5 composition, and VM12 and VM12' are of 1:2. Among the former pair, VM15 showed a higher molecular weight (36700) than VM15' (26700) due to 0.72 wt % of initator used in place of 2% for VM15'. However, VM12 and VM12' of 1:2 composition are identical in Mn.

3.1.1 Structure and composition of styrene and methyl methacrylate copolymers of vinylbenzyltrimethylsilane

^{1}H NMR and ^{13}C NMR were used to study the structure of styrene and MMA copolymers of VBTMS. The composition of MMA copolymers were calculated based on the integral area of the methoxy peak of MMA at 3.5 ppm with respect to that of the trimethylsilyl peak of VBTMS at about 0.0 ppm, and for the styrene copolymers, it was based on the following ratio A : B where:

A = No. of aromatic rings of VBTMS = Total trimethylsilyl integral x 4/9

B = No. of aromatic rings of Styrene = $\frac{\text{Total aromatic integral - A}}{5}$

Yukio Nagasaki[46] reported the reactivity ratios (r_1 and r_2) for the free radical copolymerization of VBTMS (M_1) with styrene and MMA comonomers in benzene at 60 °C with their *Q-e* values (Table 3.1.2).

Table 3.1.2 Free radical copolymerization parameters of vinylbenzyltrimethylsilane (VBTMS)[52]

M_1	M_2	r_1	r_2	Q_1	e_1
VBTMS	Styrene	0.36	1.15	1.85	-1.74
VBTMS	MMA	0.06	0.17	1.83	-1.72

(Sty: Q = 1.00 ; *e* = - 0.80. MMA: *Q* = 0.74 ; *e* = 0.40)

Yukio Nagasaki also reported a small compositional drift from feed ratios in both copolymers in the form of a sigmoid curve. In VBTMS-Sty copolymers, styrene incorporation was always higher than the styrene content in the feed. In contrast, in VBTMS-MMA copolymers, MMA incorporation was slower than VBTMS in the early stages of the polymerization. He mentioned that the alternating tendency of his VBTMS-MMA copolymers was higher than that of the coplymerization of styrene with MMA. Since, the derived r_1 and r_2 values for the monomer pair VBTMS and MMA are less than one and much more closer than those for the pair VBTMS and styrene, the VBTMS-MMA copolymers are expected to have a more alternating tendency than the VBTMS-Sty copolymers. The reactivity ratios[30] of 4-methylstyrene and MMA at 60 °C are 0.44 and 0.405 respectively. The free radical solution copolymers of 4-methylstyrene and MMA synthesized by Quan Sheng[30] were reported to have alternating tendency. Consistent with the results of Yukio Nagasaki[48], all of the VBTMS-Sty copolymers, as depicted in Table 3.1.1, showed a compositional drift with

slightly higher styrene incorporation in the copolymer than the styrene content in the feed. However, in VBTMS-MMA copolymers, the alternating tendency led to a slightly lower or same incorporation of MMA monomer compared to VBTMS. Yukio Nagasaki[48] mentioned that the large negative *e*-value (- 1.74) of VBTMS associated with electron rich vinyl group of this monomer compared to that of styrene (- 0.80) led into the higher incorporation of styrene in the VBTMS-Sty copolymers. However, in VBTMS-MMA copolymers, positve *e*-value of 0.40 shows the electron poor character of MMA, which can show alternating character in the copolymer with VBTMS. So, the probability for an environment where two MMA units surround a VBTMS unit is high, especially with increasing MMA content in the copolymer. However, the r_1 and r_2 values differ more from each other in styrene copolymers so that the alternating tendency in styrene copolymers is lower than in MMA copolymers. A qualitative representation of the probabilities of structural arrangement in VBTMS-MMA copolymer is shown in Table 3.1.3.

Table 3.1.3 Probabilities of environments for methyl methacrylate copolymers of vinylbenzyltrimethylsilane (Poly(VBTMS-*co*-MMA))

VBTMS:MMA Composition	VBTMS-VBTMS-VBTMS	VBTMS-VBTMS-MMA	MMA-VBTMS-MMA
1:1	Low	Low	High
1:2	Low	Low	High
1:5	Very low	Very low	Very high

There are three possible environments around VBTMS units in the copolymer. It can be surrounded by two VBTMS units, two MMA units or one of each. The much more

alternating tendency of our VBTMS-MMA copolymers compared to VBTMS-Sty copolymers is supported by the NMR spectrsal evidences, as shown in Figures 3.1.3, 3.1.4 and 3.15. In both ^{1}H NMR and ^{13}C NMR spectra of the VBTMS-MMA copolymers, the most peaks are getting sharper with increasing MMA content due to the fewer types of environments around the VBTMS units. In contrast, VBTMS-Sty copolymers of different composition, as shown in Figure 3.1.4, do not show any variation in peak broadness as a function of styrene content. This differentiates ^{1}H NMR spectra of all MMA copolymers from styrene copolymers in terms of their difference in alternating tendencies in free radical copolymerization.

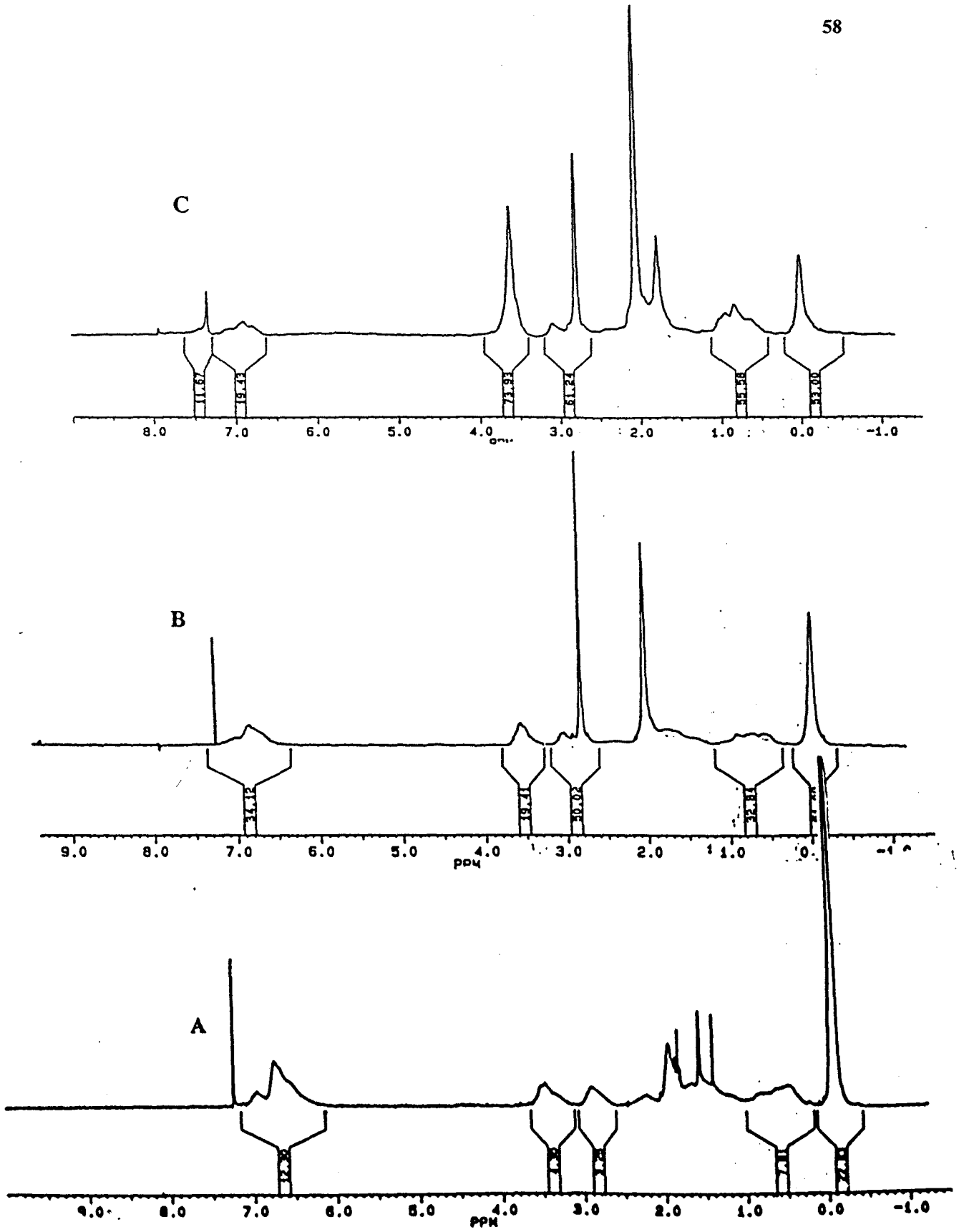

Figure 3.1.3 Comparison of ^{1}H NMR spectra of copolymers of VBTMS and MMA with different feed ratio A) 1:1 VM11 B) 1:2 VM12 C) 1:5 VM15

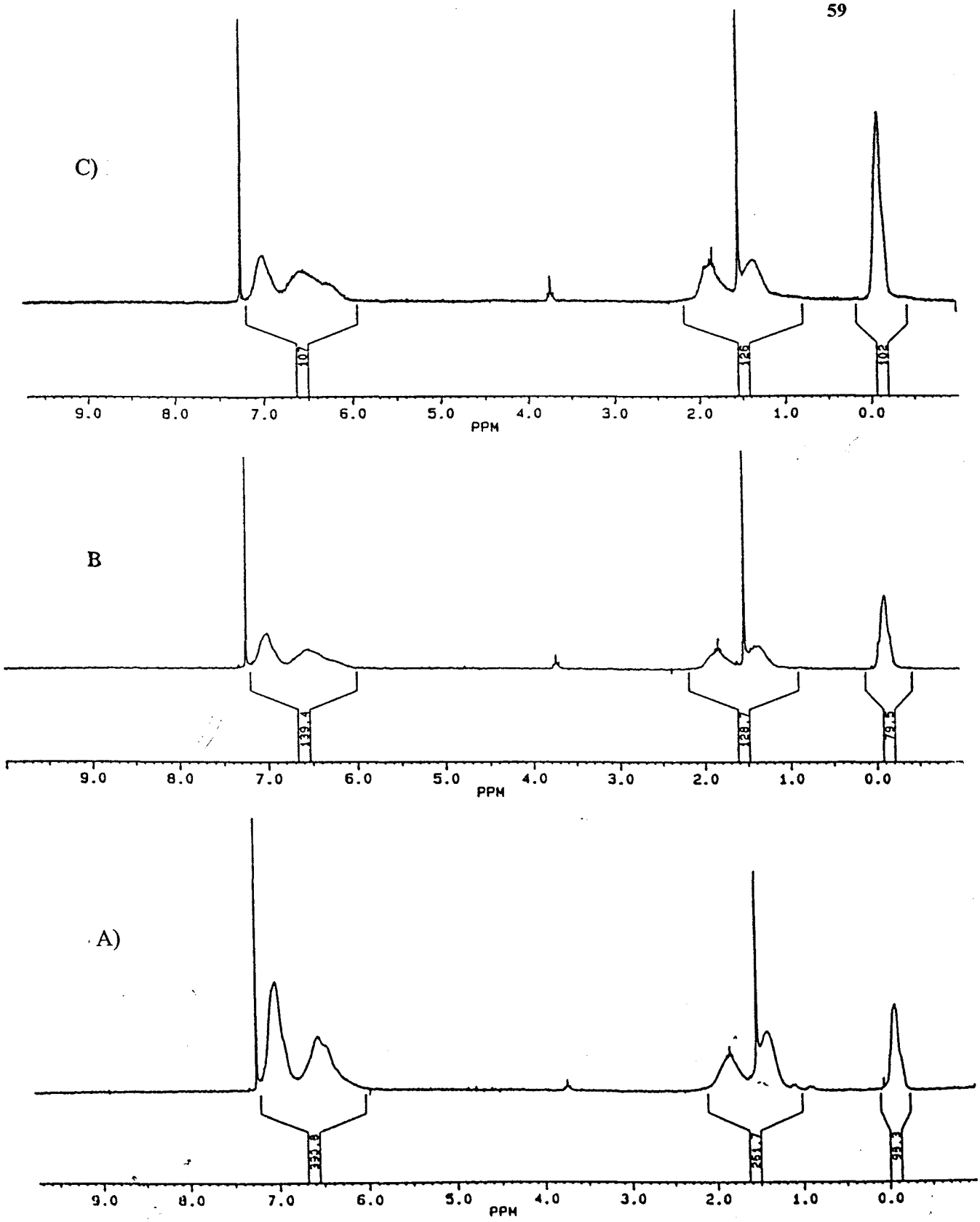

Figure 3.1.4 Comparison of ^{1}H NMR spectra of copolymers of VBTMS and styrene with different feed ratio A) 1:1 VS11 B) 1:2 VS12 C) 1:5 VS15

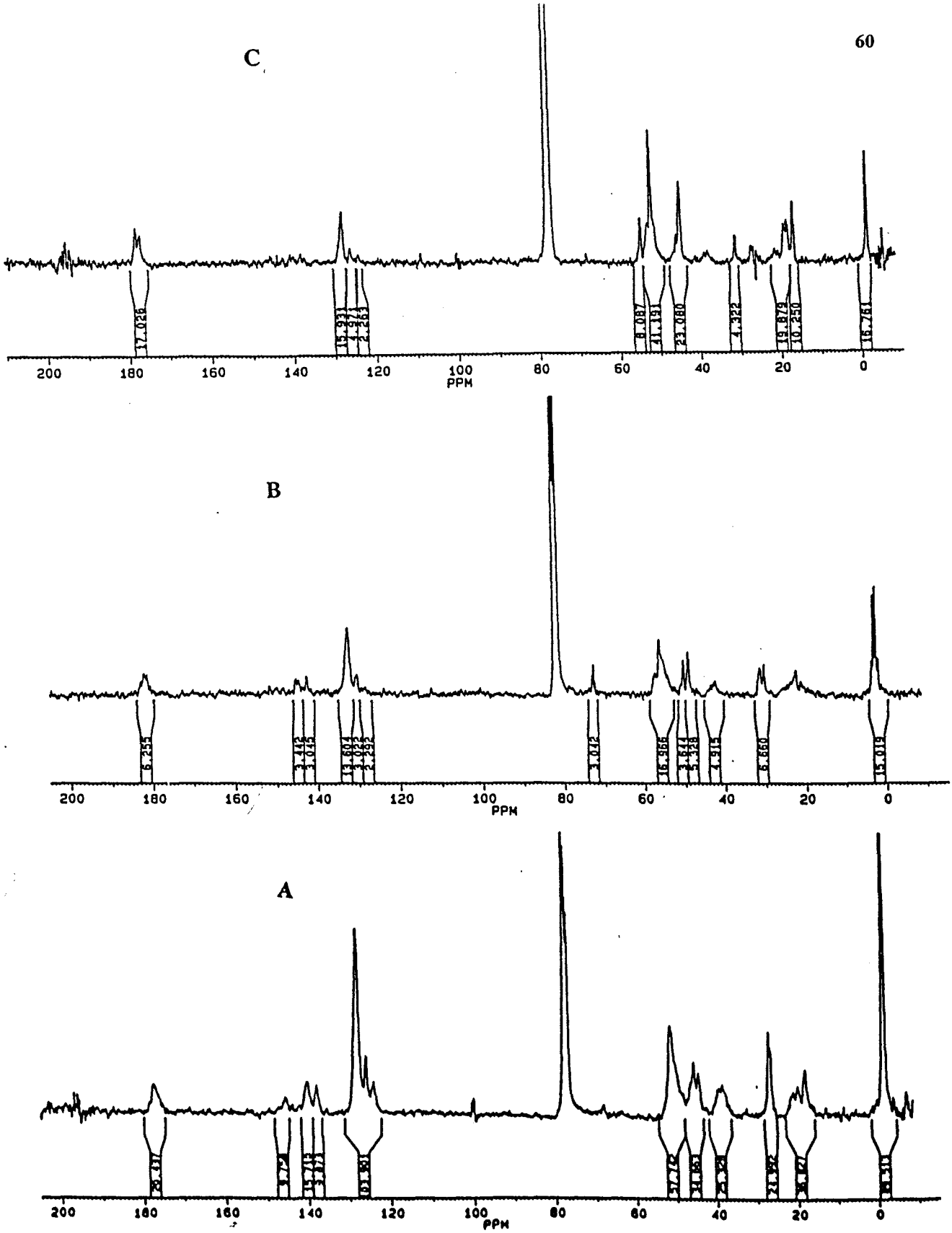

Figure 3.1.5 Comparison of ^{13}C NMR spectra of copolymers of VBTMS and MMA with different feed ratio A) 1:1 VM11 B) 1:2 VM12 C) 1:5 VM15

3.2 Synthesis of crosslinked model compounds

This chapter describes the synthesis of crosslinked polymer models containing labile C-Si bonds. The initial objective in this chapter is to make narrow dispersed particles of bis(vinylbenzyl)dimethylsilane (BVBDMS) by precipitation polymerization and to study the kinetics of polymerization to get information about its reactivity compared to divinylbenzene.

Many studies have been done on precipitation polymerization[49,50,51] including studies on kinetic parameters, particle formation mechanism, and solvency effect on polymer morphologies. These studies included crosslinkers such as DVB and bis(vinylphenyl)ethane and comonomers like styrene, 4-methylstyrene, maleic anhydride, glycidyl methacrylate and vinylbenzyl chloride (VBC). The typical process involves polymerizing a difunctional monomer in a near theta solvent. Normally, the precipitation polymerization starts in homogeneous solution. As the polymer chains grow to exceed a critical chain length, polymer precipitation takes place and leads to various morphologies depending largely on different reaction parameters such as monomer type and loading, and the solvency of the reaction medium for the polymer.

Synthesis of the new crosslinker bis(vinylbenzyl)dimethylsilane (BVBDMS) through Grignard reaction, as shown in Figure 3.2.1, using dichlorodimethylsilane instead of TMSCl did not show any sign of coupling of the starting material, vinylbenzyl chloride (VBC). The traces of methylstyrene impurity, in part already present in the starting material, could not be eliminated. The corresponding small peak at 2.3 ppm is shown in Figure 3.2.2. The gas chromatogram (GC) shown in Figure 3.2.3 confirms the product

as containing three isomers *pp, mm* and *mp* in the ratio 20:50:30, and the ^{1}H-NMR spectrum gives an isomeric ratio of 21:49:31, based on the integral of three resolved peaks appeared for the dimethylsilyl group of the BVBDMS.

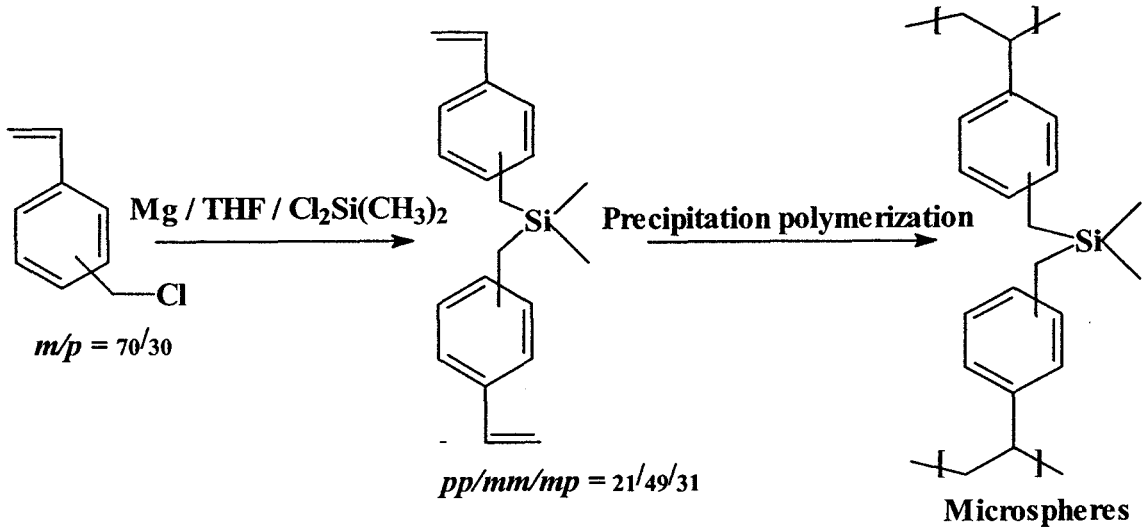

Figure 3.2.1 Synthesis of bis(vinylbenzyl)dimethylsilane (BVBDMS) microspheres.

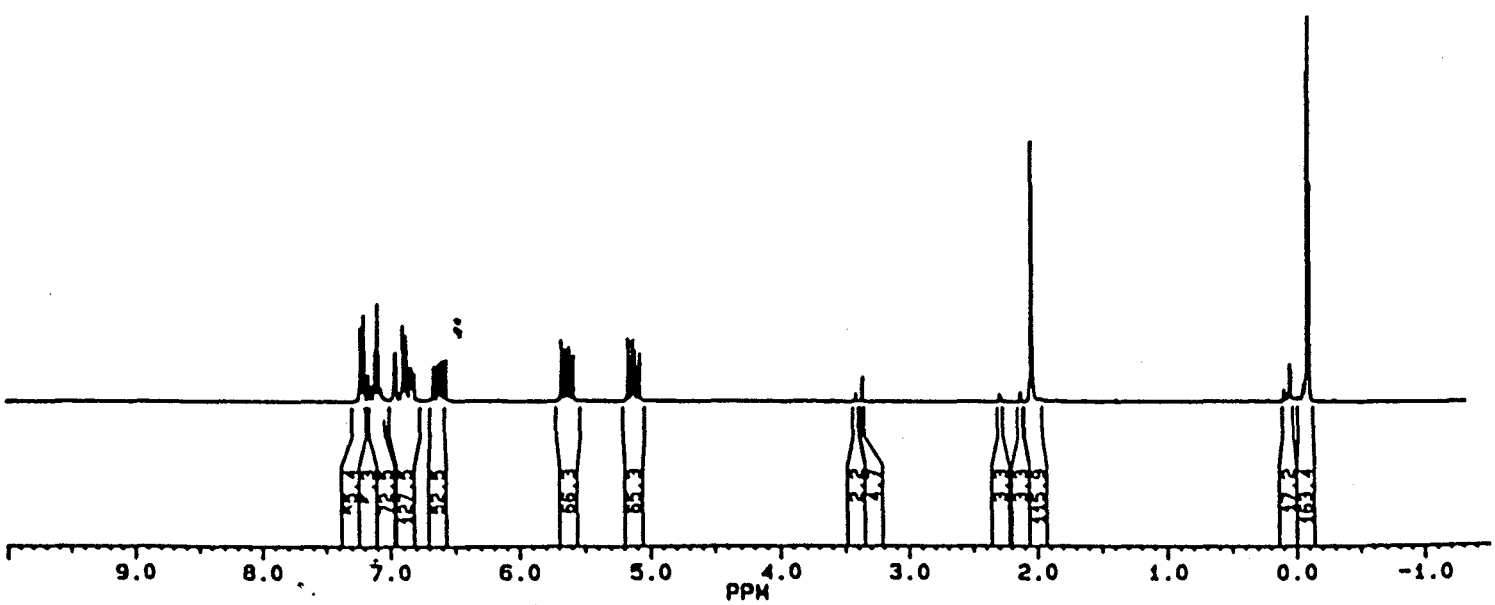

Figure 3.2.2 ^{1}H-NMR spectrum of bis(vinylbenzyl)dimethylsilane (BVBDMS).

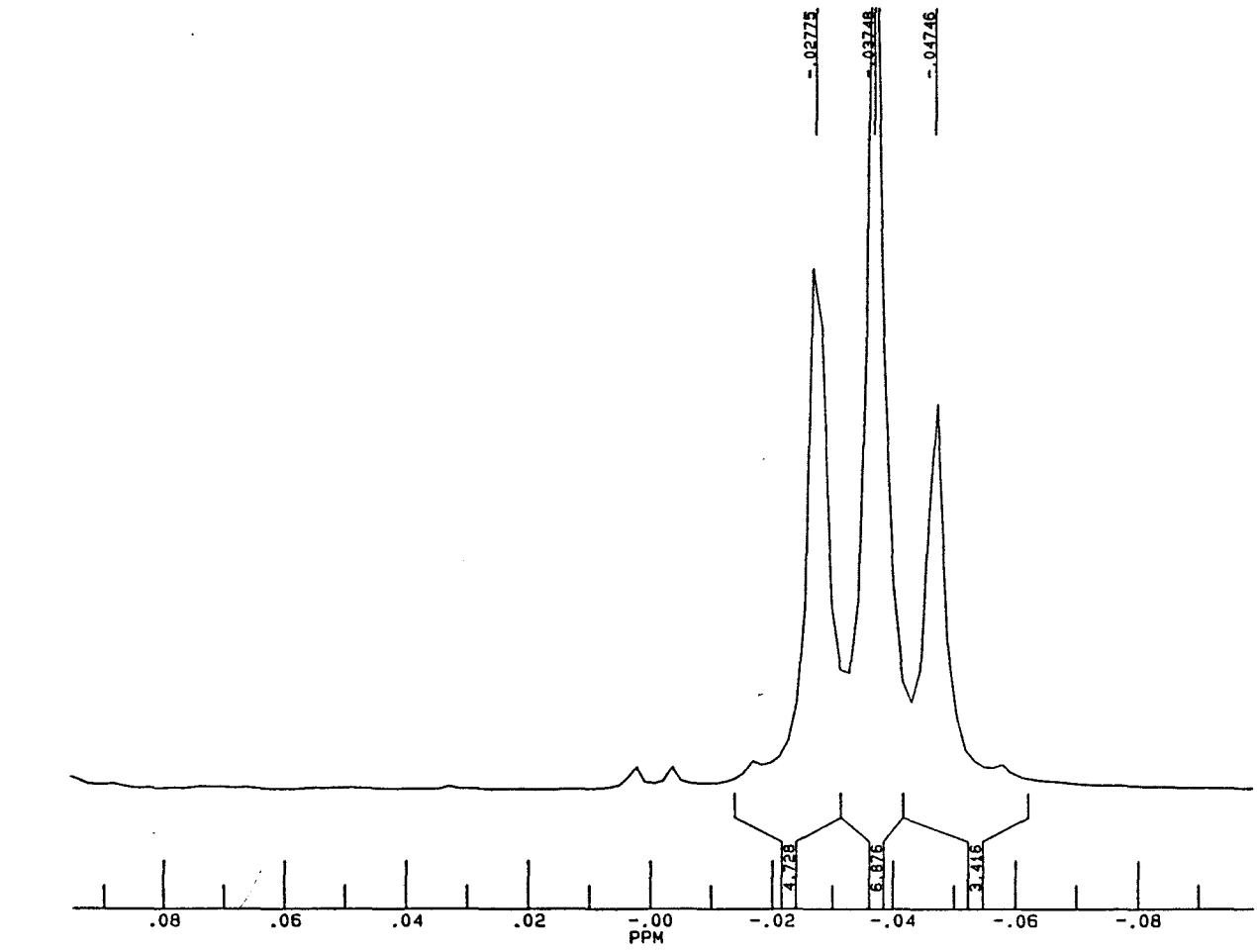

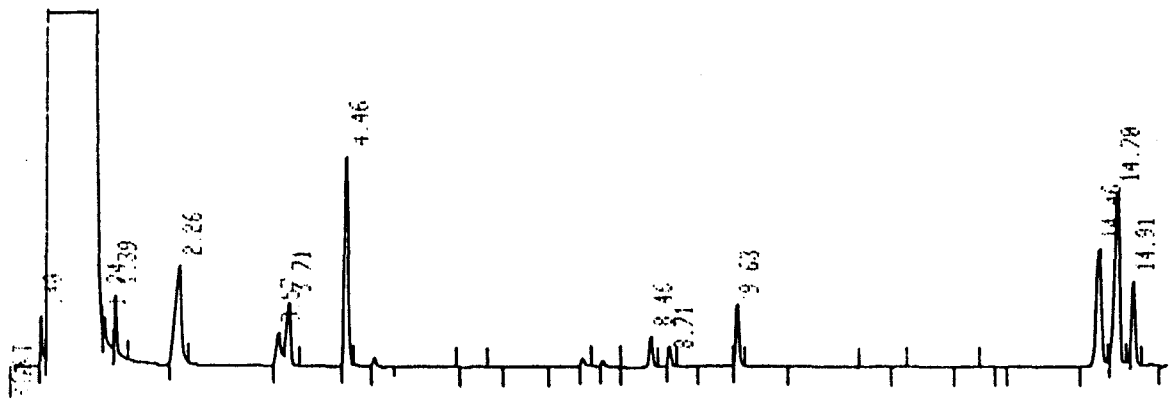

Figure 3.2.3 Gas chromatogram (Bottom) and the resolved ^{1}H-NMR dimethylsilyl peaks (Top) of bis(vinylbenzyl)dimethylsilane (BVBDMS) to show *m/p, m/m & p/p* isomeric ratio.

3.2.1 Mechanism of particle formation

Precipitation polymerization reaction proceeds in three stages; (A) Oligomer formation, (B) Nucleation, and (C) Growth of particle, as shown in Figure 3.2.4.[49] The typical reaction system contains initiator, BVBDMS monomer and the solvent acetonitrile (Figure 3.2.4 A). At the polymerization temperature (70 °C), the initiator decomposes and the initiator radicals react with the monomer to form oligomeric radical networks as in classical solution polymerization (Figure 3.2.4 B). Oligomers can continue their growth through intermolecular reactions, intramolecular crosslinking, and cyclization that leads to their precipitation into primary particle nuclei from which a lot of polymer chains carrying radicals extend into the reaction medium. Precipitation of primary nuclei can be driven by either entropic desolvation of oligomers (cross-linking prevents the polymer and solvent from freely mixing) or for enthalpic reasons (unfavorable polymer-solvent interactions)[50] (Figure 3.2.4 C). The primary particles then continue to grow not through their mutual coagulation, as their concentration is very low, but through the capture of oligomeric radicals from the bulk of solution. The outer layer of the growing particles consist of just captured oligomers that form a steric layer which prevents the particles from coagulation. More and more oligomers are then captured onto the growing particle depending on the oligomeric concentration in the solution (Figure 3.2.4 D).

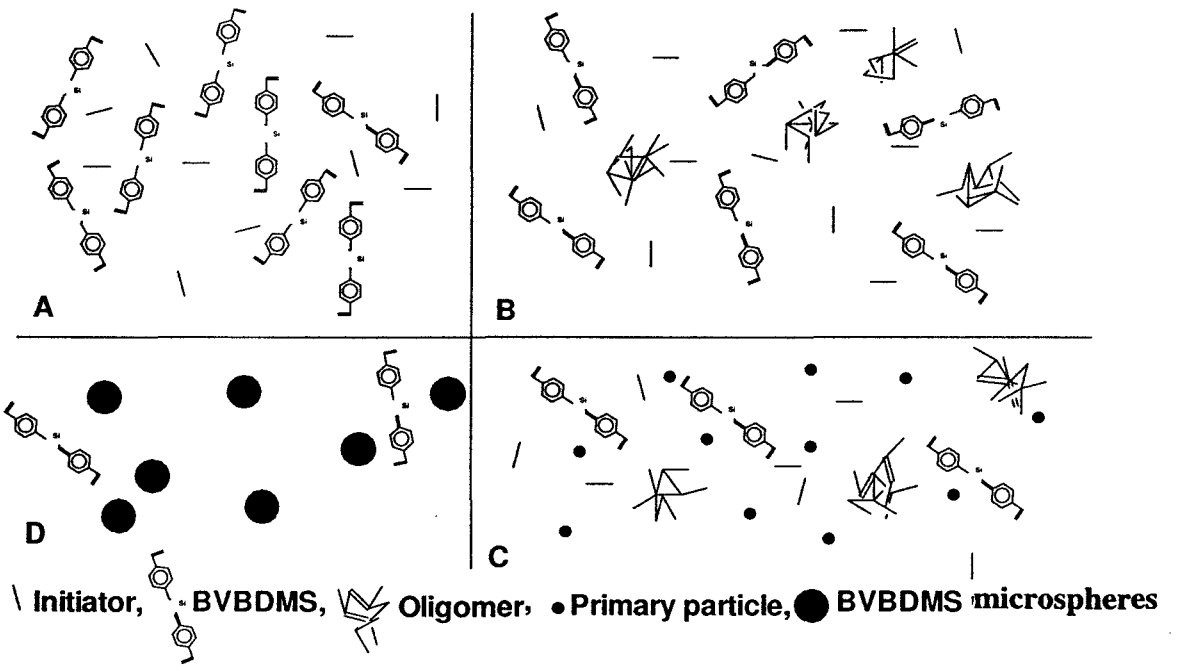

Figure 3.2.4 Schematic representation of microsphere formation in precipitation polymerization.

The results of precipitation polymerization of BVBDMS in a binary solvent system, acetonitrile / toluene, of different volume ratio are depicted in Table 3.2.1. The results are consistent with the above-proposed mechanism of particle formation. Recently,

Table 3.2.1 Effect of co-solvent composition on precipitation polymerization of bis(vinylbenzyl)dimethylsilane (BVBDMS).

Particle I.D	Acetonitrile/Tol vol %	Solubility parameter $\delta mix(cal/ml)^{1/2}$	%Particle fraction	Particle size μm	CV % in size	Mn / PD of sol fraction
PP01	100 / 0	11.85	54	2.29	14.3	2500/1.31
PP02	80 / 20	11.26	49	2.13	16.3	4700/1.49
PP03	65 / 35	10.82	46	3.89	41.42	6800/1.57
PP04	50 / 50	10.38	Microgel	---	---	11550/2.46

Conditions: 2 vol% monomer loading; 2 wt% AIBN; Temp. 70 °C

Frank[51] reported about the effect of reaction-solvency on the precipitation polymerization of DVB (divinylbenzene) and maleic anhydride in the MEK/Heptane system. He found only coagulum formation under the poorest solvency conditions (neat heptane), and reported a solvency window in which spherical particles are formed with decreasing particle size as the solvency (MEK content) is increased within the window. He got a smooth transition in polymer morphology from microsphere to microgel when the solvency exceeds the window until a space filling gel results at the highest solvency conditions. The explanation for this morphological transition is that within the microsphere solvency window, the cross-linking reactions are facilitated, leading to entropy driven phase separation without any significant swelling of the growing particles. Towards the upper end of the solvency window as the oligomeric radicals are more and more solvated, the cross-linking reactions become retarded or inhibited, and many individual microgels or at the extreme upper end of the solvency window, one space filling microgel is formed

In the system of precipitation polymerization of BVBDMS, the microspheres are formed in acetonitrile/toluene mixtures over a range of acetonitrile volume % from 100 to 65, having a solvency range indicated by the solubility parameter δmix of 11.85 to 10.82 $cal/ml^{1/2}$. It is expected that acetonitrile is a poor solvent and toluene is a good solvent for the polymers from BVBDMS. The exact solubility parameters (δ) of BVBDMS polymers are not available in the literature. In 100% aceonitrile, narrow dispersed particles are formed, as shown by the SEM pictures in Figure 3.2.5. Figure 3.2.6 shows the effect of increasing solvency on the microsphere formation.

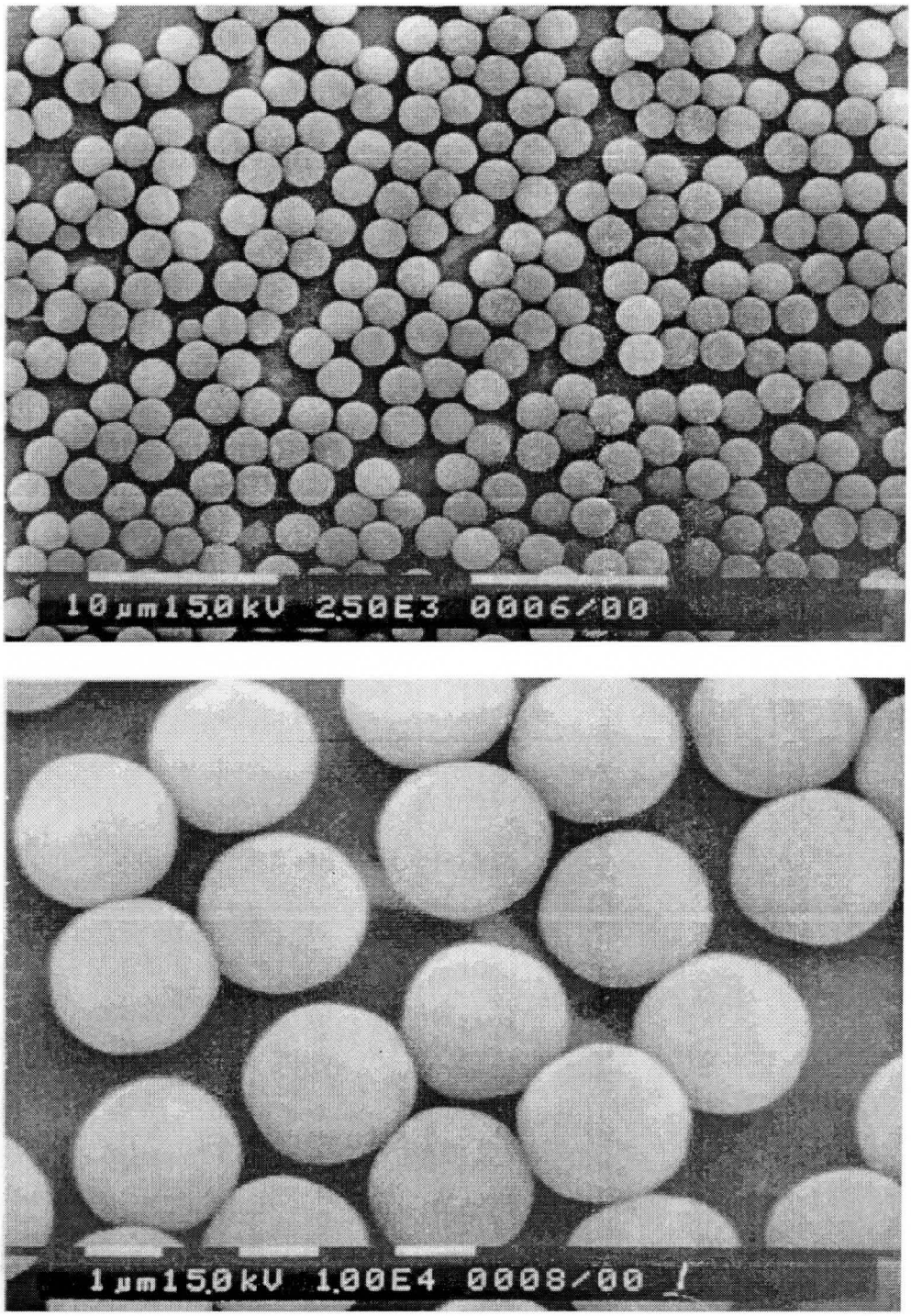

Figure 3.2.5 Narrow dispersed bis(vinylbenzyl)dimethylsilane (BVBDMS) microspheres prepared in neat acetonitrile. Conditions: 2 vol% monomer loading; 100% acetonitrile; 2 wt% AIBN; Temp. 70 ^{o}C.

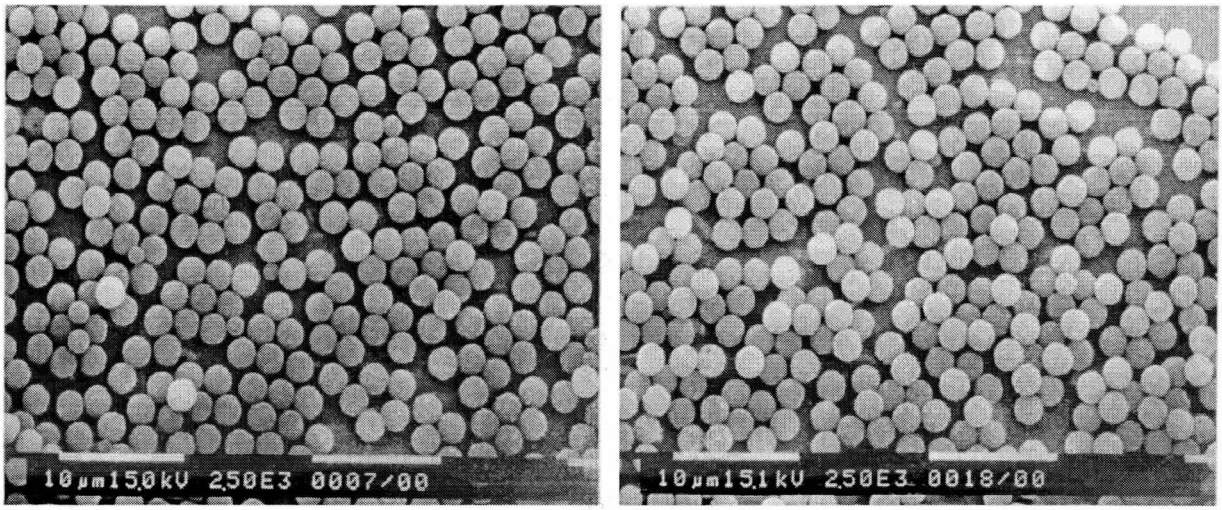

A B

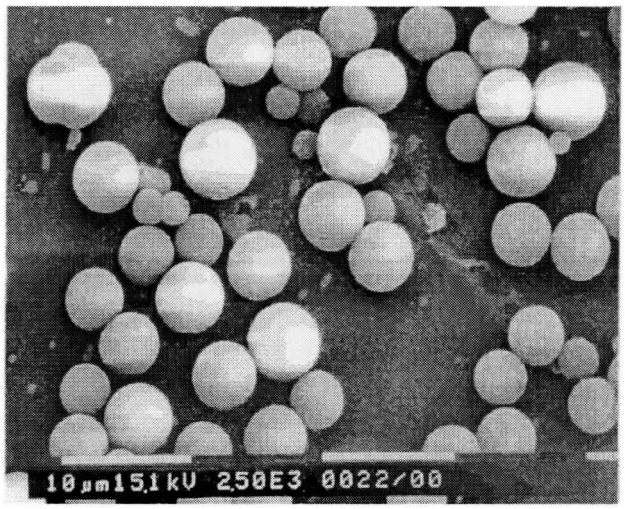

C

Figure 3.2.6 Effect of Acetonitrile/Toluene volume ratio on bis(vinylbenzyl)dimethylsilane (BVBDMS) particle formation. Conditions: 2 vol% monomer loading; 2 wt% AIBN; Temp. 70 °C. A) 100:0 B) 80:20 C) 65:35

At the highest solvency condition (Figure 3.2.3 C), the particles are formed with very high value of CV%. The smooth transition in morphology from the microsphere to microgel towards higher solvency region matches with the increasing molecular weight and the polydispersity of the soluble polymer fraction recovered from the reaction system, as shown in Table 3.2.1. Figure 3.2.7 shows the particle size build up during the polymerization of BVBDMS in 100% acetonitrile. The size build up is relatively smooth with time, and is in agreement with a short initial particle initiation period.

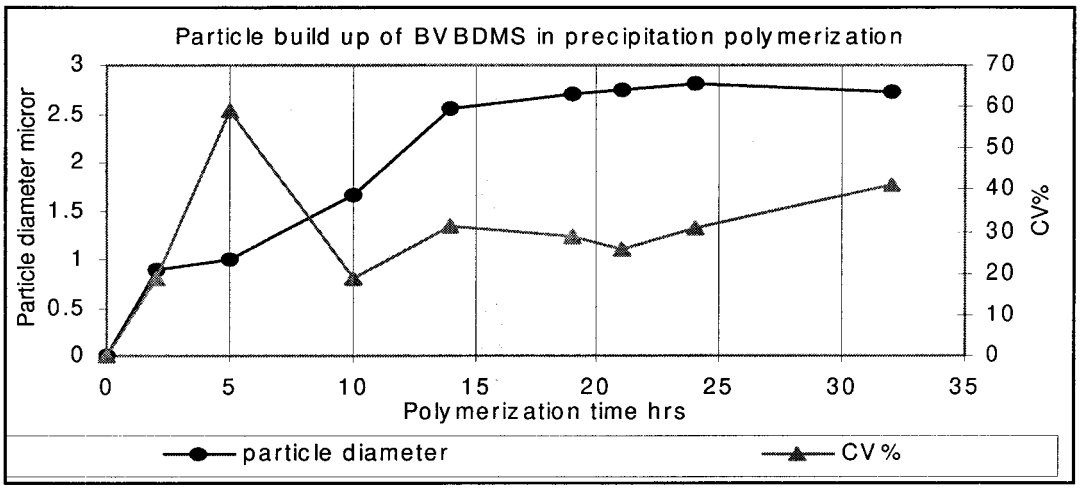

Figure 3.2.7 Particle size build up during precipitation polymerization of bis(vinylbenzyl)dimethylsilane (BVBDMS). Conditions: 2 vol% monomer loading; 100% acetonitrile; 2 wt% AIBN; Temp. 70 °C.

3.2.2 Kinetic considerations

A free radical polymerization can be broken down into three stages[49]: initiation, propagation and termination as shown in Scheme 14.

Scheme 14

Initiation

Initiator I $\xrightarrow{k_d}$ 2 R•

R• + M $\xrightarrow{k_i}$ R-M•

Propagation:

R-M• + nM $\xrightarrow{k_p}$ RM_nM•

Termination:

$R\text{-}M_nM\bullet + R\text{-}M_mM\bullet \xrightarrow{k_{tc}} R\text{-}M_{(m+n+2)}\text{-}R$

$R\text{-}M_nM\bullet + R\text{-}M_mM\bullet \xrightarrow{k_{td}} R\text{-}M_{n+1} + R\text{-}M_{m+1}$

During initiation, the initiator I decomposes to form two radical species (R•) which then react with monomer to produce the radical species R-M•. The rate of initiation is given by the expression $R_i = 2 f k_d [I]$, where f is the initiator-efficiency (fraction effective for forming R-M•). The propagation step involves addition of monomer molecules to the radical species R-M•, forming the growing macromolecular chain. The rate of propagation $R_p = k_p [M][M\bullet]$, which contains concentration terms for monomer M and radical M•. The termination reaction of radicals is the sum of two types: coupling and disproportionation. Coupling involves reaction between two reactive radical chain-ends to form an inactive chain. Disproportionation results in two inactive chains. The rate expression is given as $R_t = 2 k_t [M\bullet]$. Under steady state conditions of equal rate for both initiation and termination, the radical concentration remains constant in the system. The monomer is consumed through initiation and propagation steps. When the rate of propagation is greater than the rate of initiation, high molecular weight polymer is formed. After grouping and substituting different terms in the above expressions, one can arrive at the apparent rate of polymerization as $\ln [M_0] / [M] = k t$

where M_0 is the initial monomer concentration and M is its concentration at reaction time t.

The GC calibration plot for three isomeric BVBDMS cross-linker using decane as internal standard is shown in Figure 3.2.8 where the y-axis corresponds to the area under the peak in the gas chromatogram, and the x-axis to their concentration.

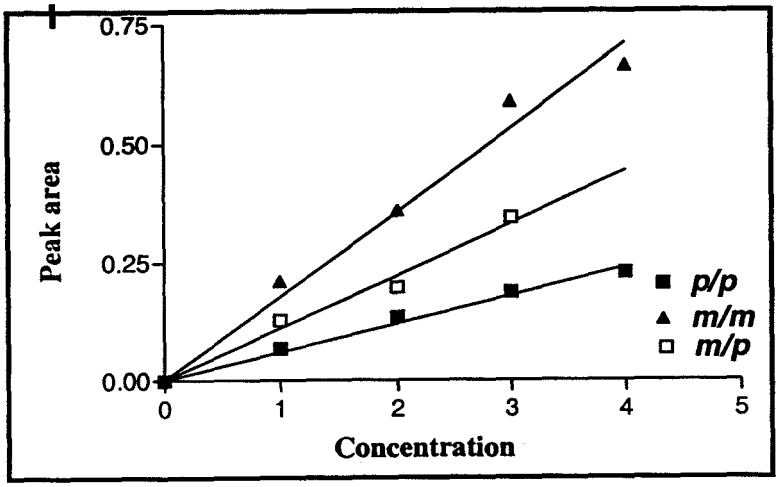

Figure 3.2.8 GC calibration plot for three isomeric BVBDMS.

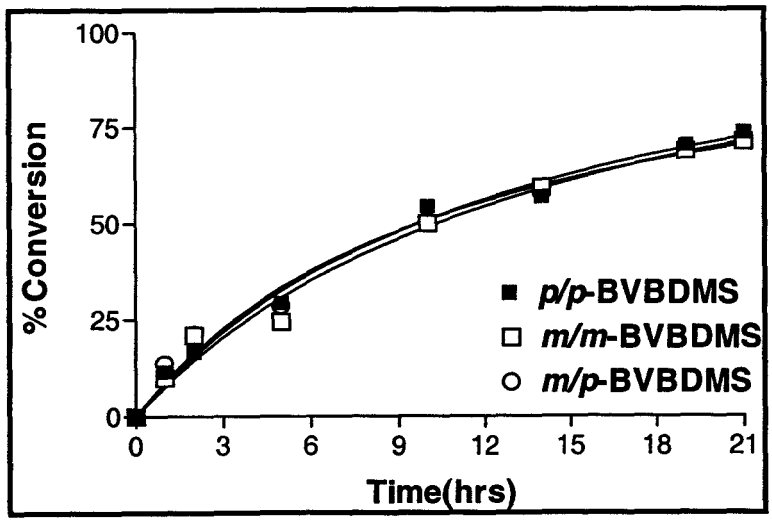

Figure 3.2.9 Conversion-Time plot of precipitation polymerization of BVBDMS(GC). Conditions: 2 vol% monomer loading; 100% acetonitrile; 2 wt% AIBN; Temp. 70 °C.

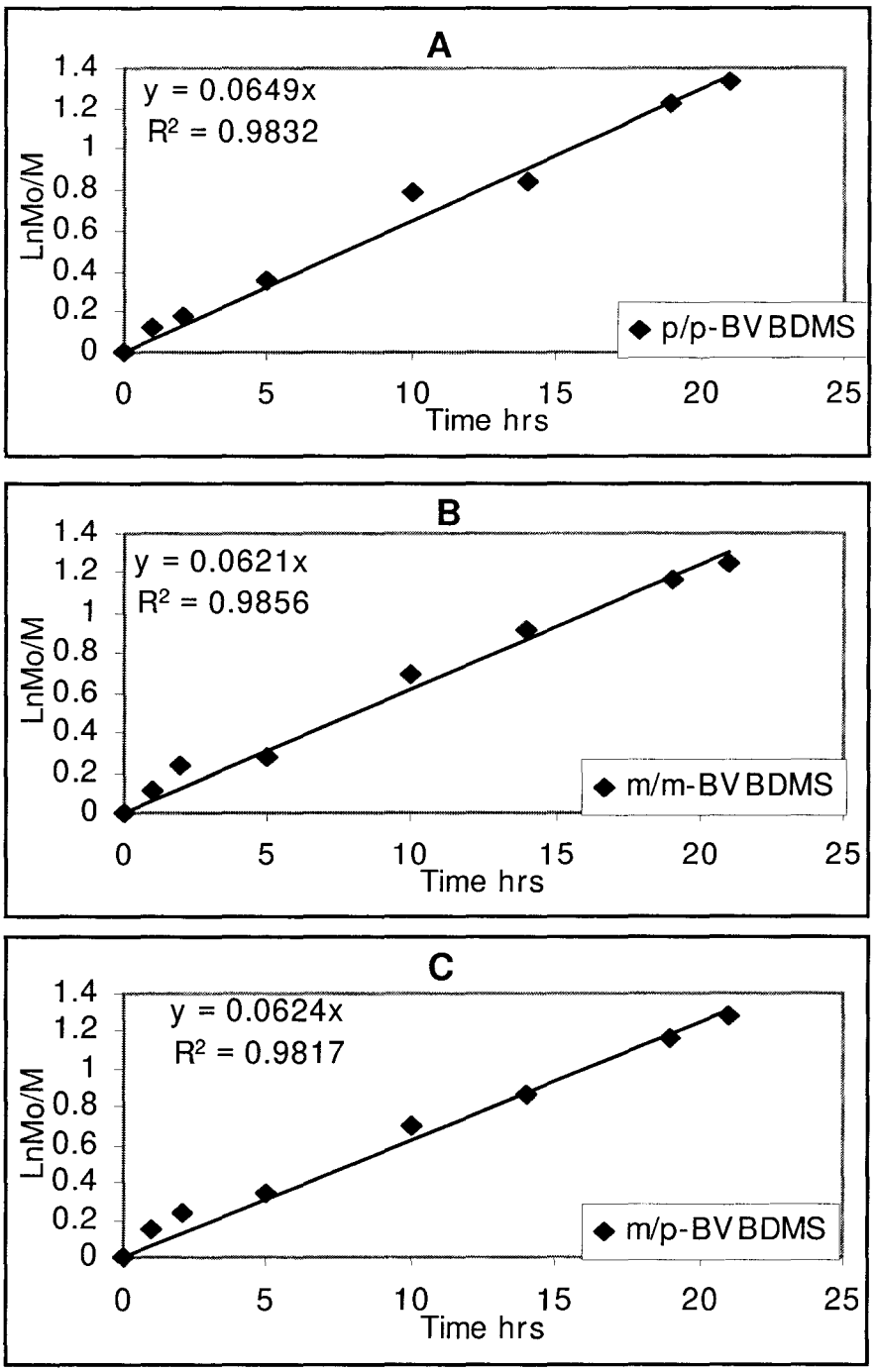

Figure 3.2.10 First-order plot of conversion in precipitation polymerization for A) *p/p*, B) *m/m*, C) *m/p* isomers of bis(vinylbenzyl)dimethylsilane (BVBDMS). Conditions: 2 vol% monomer loading; 100% acetonitrile; 2 wt% AIBN; Temp. 70 °C.

Figure 3.2.9 shows the conversion-time plot of three isomeric BVBDMS cross-linker during precipitation polymerization in neat acetonitrile at 70 °C. Similar reactivity of three isomers in the polymerization can be seen from their similar first-order plots, as shown in Figure 3.2.10, and the first-order rate constant values entered in Table 3.2.2. Also, there is no autoacceleration at any point in the course of polymerization as indicated by the conversion-time curve along which the monomer conversion drops towards the end of polymerization.

Table 3.2.2 Comparison of precipitation polymerization rates of DVB-55[49] and bis(vinylbenzyl)dimethylsilane (BVBDMS). Conditions: 2 vol% monomer loading; 100% acetonitrile; 2 wt% AIBN;Temp. 70 °C

Monomer	First-order rate constant k hr^{-1}	% Monomer conversion at 21st hr of polymerization	Reference
DVB-55			
p-DVB	7.25×10^{-2}	79	49
m-DVB	5.35×10^{-2}	69	49
p-EVB	2.26×10^{-2}	39	49
m-EVB	2.34×10^{-2}	38	49
BVBDMS			
pp-BVBDMS	6.48×10^{-2}	73.7	This work
mm-BVBDMS	6.20×10^{-2}	71.4	This work
mp-BVBDMS	6.24×10^{-2}	72.1	This work

The linearity of the first-order plots indicates that the reaction is first-order in monomer throughout the polymerization time. This is consistent with Li's[49] observation on precipitation polymerization of DVB-55 in acetonitrile under identical conditions. DVB-55 contains *m*- and *p*-isomers of DVB along with *m*- and *p*- isomers of ethyl

styrene. As their reactivities are different, as shown in Table 3.2.2, each isomer incorporates into the polymer at different rates so that a slightly heterogeneous structure results in the microsphere with maximum cross-link density towards the particle core corresponding to a faster incorporation of divinyl isomers than of ethyl styrene isomers. In contrast, the BVBDMS cross-linker is very much different from divinylbenzene (DVB) with respect to their electronic structures. The two vinyl groups are isolated in BVBDMS, as in bis(vinylphenyl)ethane, without any conjugative stabilization between the double bonds. In contrast, in DVB the two double bonds are conjugated through the aromatic ring. Hence, the two double bonds in BVBDMS are expected to have similar reactivity and the incorporation of the first double bond would not affect the reactivity of the second double bond. Thus, the isolated two vinyl groups of BVBDMS could be the reason for all the three isomers to have identical reactivity as shown by their similar polymerization rate constants. Therefore, a homogeneous structure is expected for BVBDMS particles, without any gradient in cross-link density from the particle surface to the particle core.

Evidence for very few pendant or residual double bonds in the particles: The isolated double bonds of the BVBDMS isomers give them identical reactivity in the precipitation polymerization. Therefore, it is expected that incorporation of both double bonds occur more efficiently, leaving fewer residual double bonds in the particles. This expectation is supported by the infrared spectra shown in Figures 3.2.11 and 3.2.12. The three peaks corresponding to vinyl groups shown are: 1) the vinyl carbon double bond stretch at 1630 cm^{-1} 2) the vinyl C-H out of plane deformation at 990 cm^{-1} 3) the vinyl C-H in plane deformation at 1410 cm^{-1}.

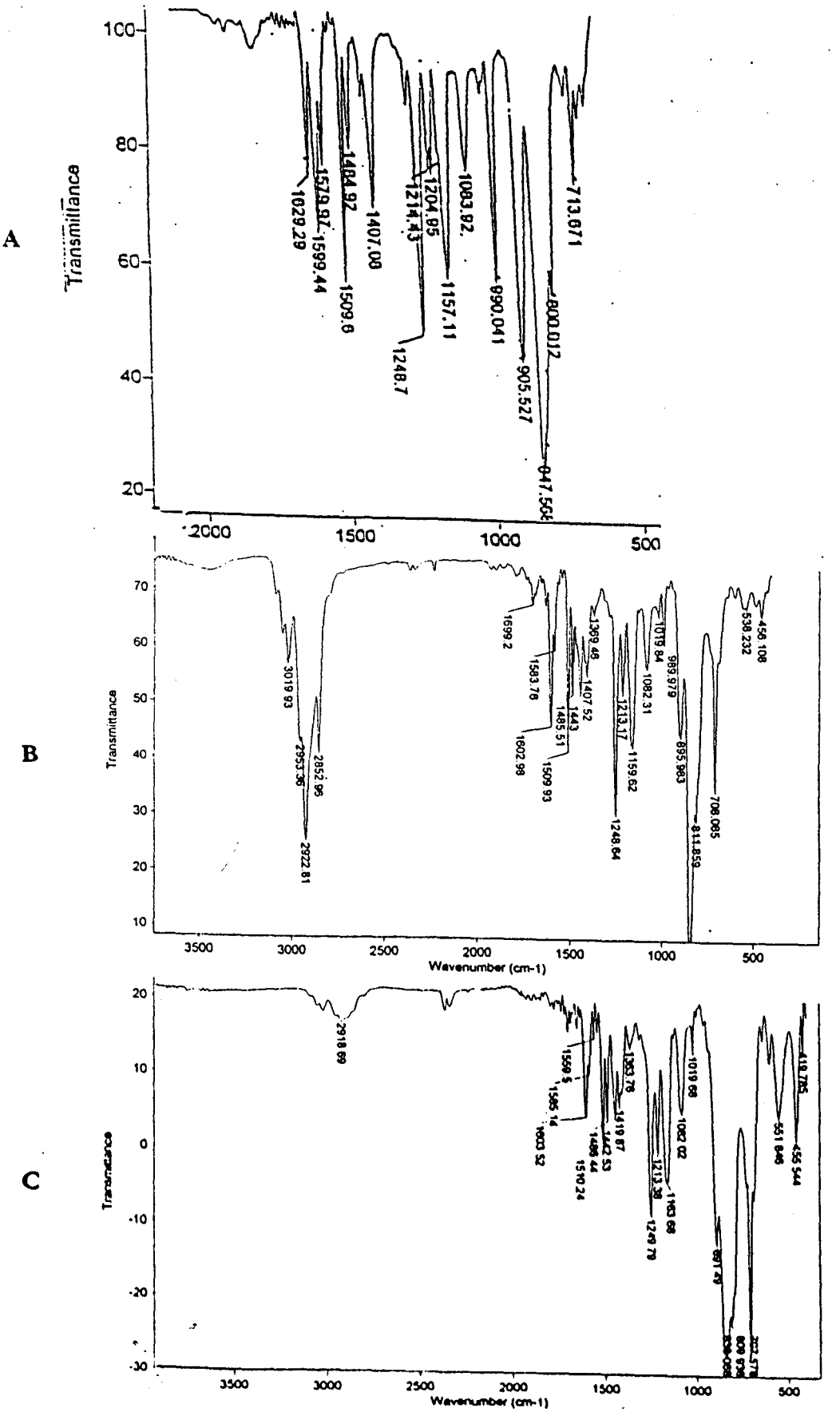

Figure 3.2.11 FT-IR spectra of A) BVBDMS crosslinker B) BVBDMS sol fraction C) BVBDMS microspheres.

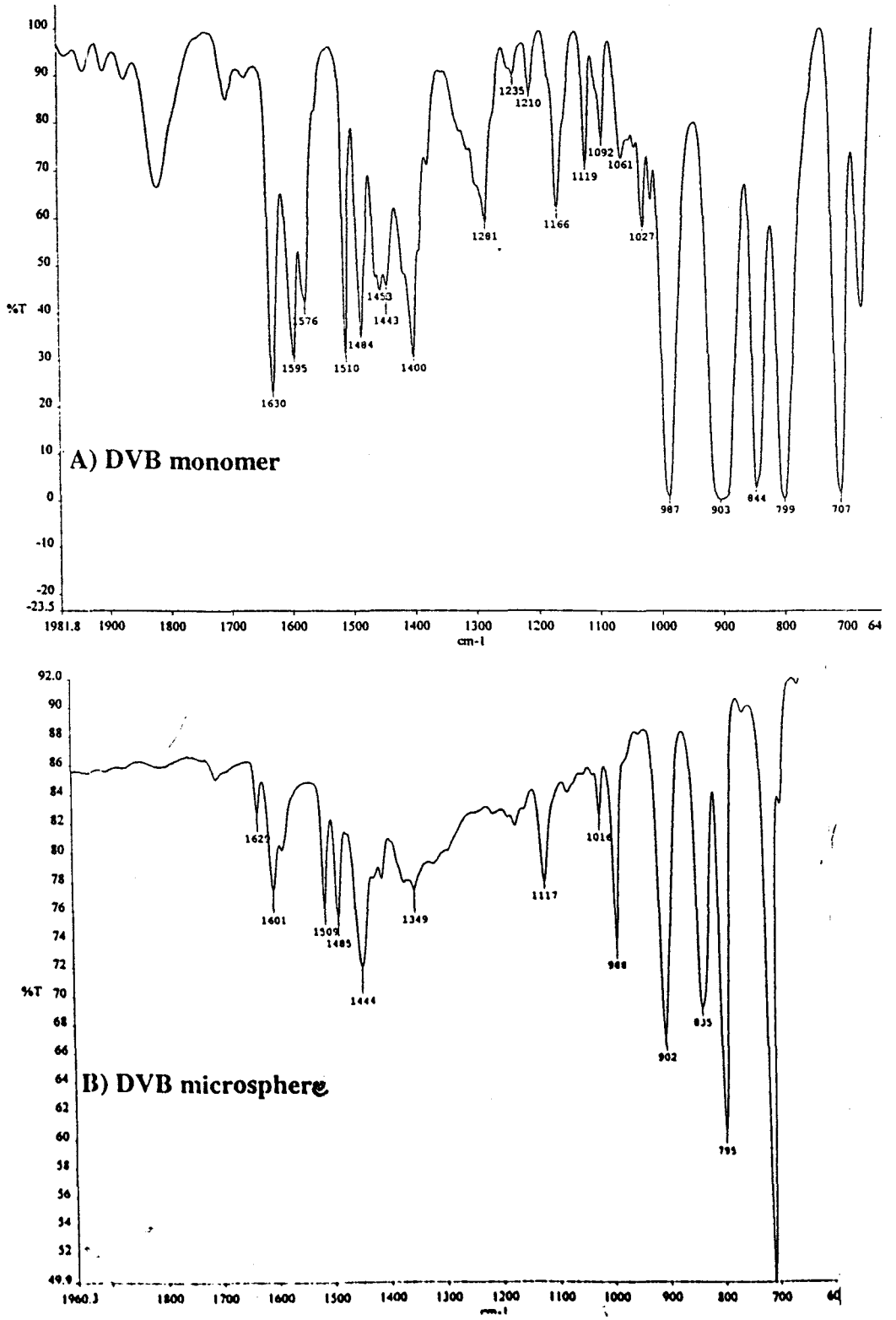

Figure 3.2.12 FT-IR spectra of A) DVB monomer B) DVB microspheres.

On comparing the spectra, the intense peaks in the BVBDMS monomer corresponding to its vinyl groups are getting weaker in the soluble fraction and almost disappeared in the microsphere spectrum, showing that the concentration of pendent double bonds in the particles is minimal. Figure 3.2.12 is intended to compare the level of double bond concentration in the microspheres of DVB-55 with respect to its monomer. Comparatively intense vinyl peaks in the spectrum of DVB microsphere, made under identical precipitation polymerization conditions, with respect to its monomer is an indication of significant amount of double bonds in the DVB particles. This is a typical behavior for DVB beads, where the lower reactivity of second double bond together with the reduced mobility leaves the DVB particle surface and interior with a lot of pendant double bonds. Similar to BVBDMS, microspheres from bis(vinylphenyl)ethane[49], having isolated double bonds, have been made through precipitation polymerization. However, no report on monomer reactivity and evidence for pendant double bonds of this crosslinker is available in the literature.

BVBDMS particles formed in neat acetonitrile are expected to have no porosity in accordance with Li's[49] studies on DVB-55 particles formed in 100% acetonitrile. We could not find any particle porosity from BET absorption measurements done on the particle ID PP01, which is made in 100% acetonitrile.

Reactivity of BVBDMS isomers: The most striking observation is that the reactivity of the three isomers of BVBDMS in free radical polymerization lies between those of *m*- and *p*-DVB. This behavior is further confirmed from their corresponding % conversion data at 21st hour of polymerization, which is shown in Table 3.2.2.

It is known that the reactivity of the vinyl group in styrene derivatives is closely related to the chemical shift of the vinyl β-carbon[48] in ^{13}C-NMR spectra, and that electron-withdrawing substituents enhance the rate of polymerization of styrene derivatives[50]. Imoto[52] reported the propagation rate constants for a series of substituents from a kinetic study to investigate substituent-polar effects on radical polymerization of *p*-substituted styrenes. He found that electron-withdrawing substituents lead to a greater overall rate of polymerization. The rate values are shown in Table 3.2.3.

Table 3.2.3 Effect of *p*-substituents on overall rate of radical polymerization of substituted-styrenes[50]

X-Styrene	*p*-CH_3O	*p*-CH_3	Styrene	*p*-F	*p*-Cl	*p*-Br	*p*-CN
Overall rate R_p (mol/l/sec)	8.43	7.72	9.13	7.72	12.7	19.2	31.4

Reynolds[18] *et al.* used ^{1}H and ^{13}C-NMR chemical shifts of 4-substituted styrenes to estimate inductive and resonance contribution of $M(CH_3)_3$ and $-CH_2M(CH_3)_3$ groups (M = Si, Ge,Sn or Pb). They found that a trimethylsilyl group at the *para* position of styrene exhibits an electron donating inductive effect due to the lower electronegativity of silicon, and an electron withdrawing resonance effect through d_π-p_π conjugation. However, the $-CH_2Si(CH_3)_3$ group at the *para* position of styrene is electron donating through both inductive and resonance effects operating through Si-Cσ-π back donation. These electronic effects contribute significantly to the net electron density on ring carbons and vinyl carbons and, accordingly, to vinyl reactivity in radical and nucleophilic reactions. Therefore, the β-carbon of the vinyl group of these 4-substituted

styrenes assumes a particular position in ^{13}C-NMR spectra, depending on its net electron density. Table 3.2.4 depicts the ^{13}C chemical shift of substrates with some literature data for comparison.

Table 3.2.4 ^{13}C-chemical shifts of β-Carbon of vinyl group of substituted styrenes

Monomer	[a]Rate constant 10^4k	10^4. Net charge density on vinyl β-C	^{13}C-Chemical shift of vinyl β-C (δ ppm)	Δ δ	Reference
Styrene	16.0	0	112.96, 113.2	0.0	54, 18
Chloromethyl styrene	--	--	113.99	1.03	53
4-methylstyrene	3.2	- 20	111.59	-1.37	53
4-tert-butylmethylstyrene	--	--	112.43	-0.53	16
4-trimethylsilylstyrene	34.4	+ 26	113.09	0.13	53
4-trimethylsilylmethylstyrene	--	- 44	111.3, 111.62	-1.66	53, 18
3 or 4-trimethylsilylmethylstyrene	--	--	111.8	-1.16	This work
4-bis(trimethylsilyl)methylstyrene	2.3	- 51	111.3	-1.66	53
2-Vinylpyridine	--	--	118.0	5.04	--
1,4-divinylbenzene	43.5	--	113.55	0.59	54
1,3-divinylbenzene	--	--	113.86	0.90	54
bis(vinylbenzyl)dimethylsilane	--	--	113.26	0.30	This work

([a] Second-order rate constant of an anionic addition reaction with lithium diisopropylamide)

The table shows that the electron releasing groups, 4-methyl and 4-*tert*butylmethyl, increase the electron density of the vinyl β-carbon of styrene as reflected in the shifted chemical shift towards up-field, compared to that of styrene. In trimethylsilylstyrene, the net electron-withdrawing effect results in a reduced electron density that manifests itself in a down-field chemical shift, and in an enhanced reactivity towards nucleophiles. The case with trimethylsilylmethylstyrene is just the reverse, where the electron releasing inductive and resonance contributions from the trimethylsilylmethyl

group combine to reduce the reactivity due to a higher net charge density at the vinyl β-carbon. The literature value of chemical shift for trimethylsilylmethylstyrene (VBTMS) exactly coincides with the value obtained from our work. In order to correlate the trend in the ^{13}C chemical shift of the vinyl β-carbon of polymerizable monomers to their reactivity in free radical polymerization, information on reactivity ratios is necessary. In Table 3.2.4, the highest down field shift from styrene is shown by 2-vinylpyridine whose reactivity ratio[55] in free radical polymerization with styrene in benzene solvent is 0.7 (r_1) and 0.335(r_2). This higher reactivity of 2-vinylpyridine than styrene resulted in a higher incorporation of 2-vinylpyridine in its copolymer with styrene. It is quite surprising to notice that the ^{13}C chemical shift of the β-vinyl carbon of bis(vinylbenzyl)dimethylsilane is identical to that of 1,3 and 1,4 DVB, indicating that they must have identical reactivity in free radical polymerization. Table 3.2.5 shows the comparison of reactivity ratios[46,53,54] of several monomer pairs.

Table 3.2.5 Correlation of ^{13}C chemical shift[46,53,54,55] and reactivity ratio of monomeric pairs in free radical polymerization

Monomer M_1	Monomer M_2	Reactivity ratio r_1	r_2	*Q*-value	*e*-value	^{13}C-Chemical shift of vinyl β-C of M_1
2-Vinylpyridine	Styrene	0.7	0.335	--	--	118.0 (112.96 Sty)
4-trimethysilylmethyl styrene	Styrene	0.36	1.15	1.85	-1.74	111.8
4-trimethysilylmethyl styrene	MMA	0.06	0.17	1.83	-1.72	111.8(121.4 MMA)
4-bis(trimethylsilyl) methylstyrene	Styrene	0.31	1.15	1.93	-1.81	111.3
4-bis(trimethylsilyl) methylstyrene	MMA	0.10	0.20	1.65	-1.58	111.3
1,4 DVB	Styrene	1.0	0.20	---	--	113.55
4-methylstyrene	MMA	0.44	0.405	---	--	111.59

Table 3.2.5 shows that the reactivity of vinyl groups in radical polymerization shows a good correlation with ^{13}C chemical shift of β-vinyl carbon. Among each monomeric pair in Table 3.2.5, the one having larger ^{13}C chemical shift shows higher reactivity than its comonomer so that it should result in a copolymer composition rich in more reactive monomer. 1,4-DVB and 2-vinylpyridine has got the highest values for the ^{13}C chemical shift of vinyl β-carbon than that of styrene among the entries in Table 3.2.5, and consequently their reactivity is higher than that of styrene in radical copolymerizations.

Based on the AM1 method of calculations of geometry optimization, Yukio Nagasaki[48] reported the twist angle for C^3(phenyl)-C^4(phenyl)-C-Si as 90° in trimethylsilylmethylstyrene (5).

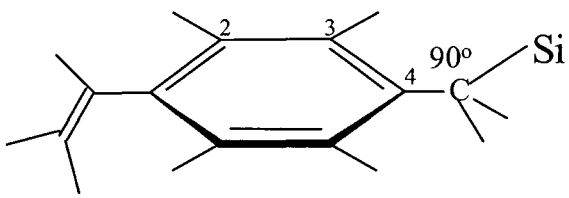

5

It is known that the maximum Si-Cσ-π conjugation is obtained only when the twist angle is 90°. Though there are two bulky vinylbenzyl groups attached to a dimethylsilicon center in the cross-linker, BVBDMS, it is most likely in a 90° torsional angle conformation. This coplanarity of benzylic-silicon bond with aromatic p-orbitals should permit an electron release from silicon to aromatic system. However, the ^{13}C-chemical shift of the vinyl β-carbon of BVBDMS (113.26 ppm) occurs at lower field compared to that of trimethylsilylmethylstyrene (111 ppm), and identical to that of

trimethylsilylstyrene, where the electron donation is balanced by a significant net electron withdrawal through $d\pi$-$p\pi$ conjugation. Apparently, in BVBDMS the basic tendency towards electron donation is diluted by the presence of two styrene units per silicon to a point where it becomes not noticeable through its chemical shift. Accordingly, the observed identical ^{13}C chemical shifts of the vinyl β-carbons in DVB and BVBDMS explains why our cross-linker shows a reactivity identical to that of DVB (*meta* and *para* isomers) in free radical precipitation polymerization.

3.3 Cleavage of Benzylic-Silicon Bonds by KOH/ EtOH / THF

Many compounds, containing benzylic-silicon bonds, have been studied with regards to their base-catalyzed cleavage[24,26,57,58,59]. In most cases, the attacking base is either hydroxide or alkoxide ion in aqueous or organic solvents, specifically alkali metal hydroxides or alkoxides in alcoholic or aqueous-alcoholic mixtures. Eaborn and coworkers are known in this area of kinetic studies. Most of the reactions are carried out under pseudo first-order conditions, *ie* with large excess of the nucleophilic reagent. Accordingly, they follow the kinetic equation, $\ln [M_0 / M] = kt$, where M_0 is the initial substrate molar concentration, M is the concentration at time t, and k the pseudo first-order rate constant with dimension time $^{-1}$. Sometime the specific rate constant k_s is used, which is defined as k / [base] = k_s.

The key objective here is the comparative kinetic study of benzylic-silicon bond cleavage on a series of substrates including small molecules and their polymeric analogs. KOH in 50/50 v/v THF/ethanol has been selected as the cleaving reagent. The solvent mixture was selected as it could dissolve all members of the substrate series including the polymeric substrates. For the cleavage reactions to be in pseudo first-order condition, the KOH concentration was always kept 8 times higher than that of the substrate (1 Molar in KOH and 0.125 Molar in substrate). The reactions were followed by GC and NMR. Below follows the discussion of reaction mechanism of the KOH induced cleavage of benzylic-silicon bonds.

3.3.1 Proposed reaction mechanism

The typical reaction mechanism involves nucleophilic attack of the base on the electropositive silicon to form reversibly an intermediate or a transition state[61] (step 1). This decomposes to carbanion in step 2. In step 3, the carbanion abstracts a proton from the solvent to form the product (Scheme15).

Scheme 15

$$Me_3SiCH_2C_6H_4X + {}^-OR \rightleftharpoons [ROMe_3SiCH_2C_6H_4X]^- \text{ (I)} \quad \text{—— (1)}$$

$$[ROMe_3SiCH_2C_6H_4X]^- \longrightarrow ROSiMe_3 + XC_6H_4CH_2^- \quad \text{—— (2)}$$

$$XC_6H_4CH_2^- + ROH \longrightarrow XC_6H_4CH_3 + RO^- \quad \text{—— (3)}$$

(R = H or alkyl)

There is controversy in the literature[60,61,62] about whether a free carbanion is formed in the rate-determining step. There remains a wide choice of mechanism as given below.

A) Ionization mechanism: The intermediate (I) could be formed reversibly in a fast process with separation of free carbanion in a slow step followed by its rapid proton abstraction step. (1) & (3) fast, (2) slow.

B) S_N2 type mechanism: The attack of the base could be concerted with separation of free carbanion. (1) & (2) slow, (3) fast.

C) Electrophilically-assisted mechanism: (2) & (3) could be synchronous and slow so that the carbanion is never being free. (1) fast, (2) & (3) slow.

Many studies[60,61,62] based on solvent-isotope effect have been reported on series of similar compounds in the literature to answer these questions. In the ionization mechanism, a free carbanion is formed in the rate-determining step. If the products are determined in a fast reaction of the carbanion with the solvent (ionization mechanism), the carbanion can not discriminate the isotopes when the reaction is carried out in an isotopic solvent mixture, ROH/ROD. As a consequence, the ionization mechanism leads to a H/D ratio in the products identical with that in the solvent mixture in which the reaction takes place. In other words, the product isotope effect (P.I.E.) will be unity when either the ionization or the S_N2 type mechanism take place in an equimolar ROH/ROD solvent mixture. Thus, a P.I.E. higher than unity is an indication of electophilically-assisted mechanism where there is a substantial degree of proton transfer to the carbanion in the rate-determining step (C mechanism). The P.I.E. values reported by Alexander[60,61] for the cleavage of substituted benzyltrimethylsilane are shown in Table 3.3.1 below.

Table 3.3.1 Product isotope effect of base cleavage of substituted BTMS[60,61]

$XC_6H_4CH_2SiMe_3$ / MeOH-MeOD(1:1)		X=	H	*p*-Me	*m*-Cl	*m*-OMe	*p*-Cl	$-F_5$	*m*-CF_3	Ref
P.I.E.	1 M NaOH		1.4	1.5	1.6	--	--	--	1.6	60
P.I.E.	2 M NaOMe		1.17	--	--	1.25	1.07	1.16	1.19	61

In all cases among the compound series in Table 3.3.1, the P.I.E. is greater than unity, supporting the electophilically-assisted mechanism. Eaborn[62] carried out similar type of study on the base cleavage of substrates whose carbanions are not stabilized by

conjugative delocalization as in $Me_3SiCH_{(3-x)}X_x$. He reported P.I.E. value 1.0-1.2 for all compounds of the series in NaOMe/MeOH/MeOD system. In an another type of compound series, as in substituted benzyltrimethylsilanes, trimethylsilyl derivatives of di- and tri-phenylmethane, fluorene, and indene, where the carbanion is stabilized by conjugation, the reported P.I.E values vary from 1.1 to 10. Thus, as the silane reactivity towards the base cleavage is increased with the acidity of parent carbon acid formed, the degree of proton transfer from the solvent to the separating carbanion is also increased, as evidenced from the higher and higher P.I.E. values. This is in consistent with the P.I.E. values reported by Jenkins[63] for methoxide cleavage of triethyl and tribenzyl silicon hydrides, and triaryl silicon hydrides with H, *p*-Me, OMe, *p*-Cl and *m*-CF_3 substituted to the aryl group as 2.14, 2.55, 3.0, 3.4, 3.95, 4.32, and 5.03 respectively. He suggested an electrophilically assisted mechanism for all these hydride ion cleavages. Across the compound series, there is a progressive increase in the degree of proton transfer to the separating hydride ion in the rate-determining step. He also reported a linear Hammett plot ($\log k_s$ v/s σ) with very high ρ (Hammett reaction constant) factor, indicating a substantial degree of charge (0.7unit) on silicon in the transition state. This is an indication of the fact that Si-H bond breaking is not synchronous with H-H bond making. He calculated and assigned a bond order of 0.7 for Si--H, 0.3 for H--H and 0.7 for CH_3O--H in the transition state. Also, as the electron withdrawal from silicon by the substituents is increased (as in $(m\text{-}CF_3C_6H_4)_3SiH$), the H--H bond order was found to be increased. Thus, he got maximum P.I.E. value for (m-$CF_3C_6H_4)_3SiH$ with maximum degree of proton transfer in the transition state. Eaborn[29a] also reported the same situation in the cleavage of substituted

benzyltrimethylsilane (BTMS) by aqueous-methanolic NaOH, and $XC_6H_4[CC]_nSiEt_3$ by aqueous-methanolic NaOH[64]. He reported linear Hammett plots for both reactions. The reaction constant ρ obtained for the former reaction for three substituents H, *m*-Cl, and *p*-Cl was 4.7 with strong recommendation for electrophilically-assisted mechanism.

Our reaction system mimics the series of compounds and the experimental conditions used in the determination of P.I.E. by Alexander[60]. However, the solvent system used is ethanol/THF instead of methanol and the substituent is *p*-isopropyl group in place of *p*-methyl group. Based on the above literature survey we propose an electophilically-assisted mechanism for our comparatively less reactive system.

Figure 3.3.1 and Table 3.3.2 show that the specific rate constant of *p*-isopropylbenzyltrimethylsilane for the KOH cleavage is almost independent of KOH concentration or showing a small tendency to lower the rate as the KOH concentration is increased from 1 to 2 Molar. Independence of the specific rate constant on NaOH concentration was reported by Eaborn[26] for the cleavage reaction of *p*-(trimethylsilylmethyl)benzanilide by NaOH in 39 wt% aqueous methanol. However, in 1981 Eaborn[66] reported a slow progressive increase in specific rate (2.7 times) in going from 1 to 3 Molar methoxide in MeOH for $3\text{-}ClC_6H_4CH_2SiMe_3$, and an initial decrease followed by a moderate increase for $3\text{-}ClC_6H_4CH_2SnMe_3$. Eaborn rationalized these results in terms of a balance between the effects of increasing the H_ acidity function of the medium and the decreasing proton availability as more and more solvent (MeOH) molecules engage in solvating the base (NaOMe) through H-bonding so that the proton is less available for electrophilically-assisted process. This may reflect as a lowering of

the specific rate constant with increase in the base concentration as significantly observed in the base cleavage of substituted benzyl trimethylstannanes[66].

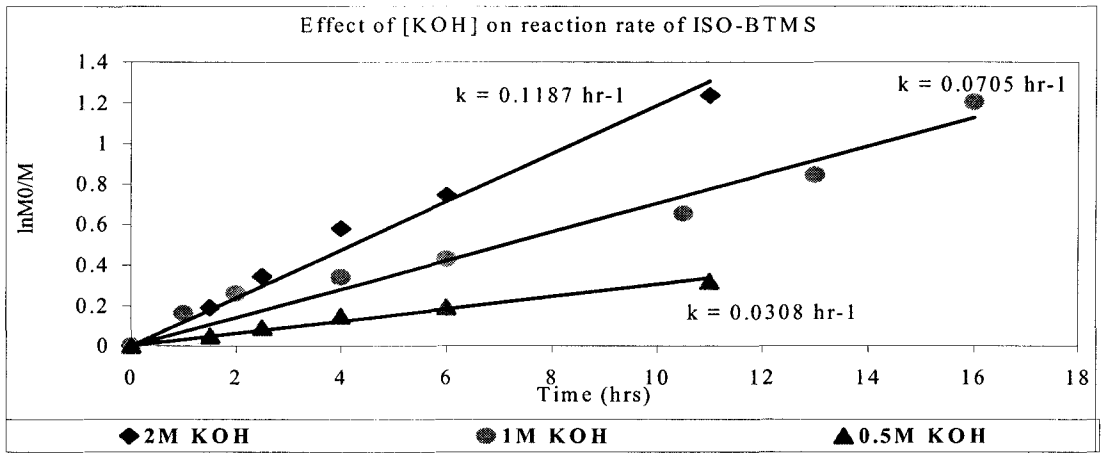

Figure 3.3.1 Effect of [KOH] on cleavage rate of ISO-BTMS (^{29}Si): Conditions: ISO-BTMS 0.125 Molar; THF/EtOH 50/50 vol; Temp. 90 °C.

Table 3.3.2 Effect of [KOH] on first-order specific rate constant of ISO-BTMS

[KOH]	2 Molar	1 Molar	0.5 Molar
Pseudo first-order rate constant k hr^{-1}	198 x 10^{-5}	117.5 x 10^{-5}	51.3 x 10^{-5}
Specific rate constant k_s = k/[KOH] $min^{-1}mol^{-1}.l$	99 x 10^{-5}	117.5 x 10^{-5}	103 x 10^{-5}

Hence, the specific rate constant of ISO-BTMS as a function of KOH concentration are in accordance with the electrophilically assisted mechanism as a principal operating mechanism in the KOH promoted cleavages of our substrates.

3.3.2 Cleavage of small model molecules by KOH/EtOH/THF

The KOH promoted cleavages on the small molecules including BTMS, ISO-BTMS, VBTMS, and BVBDMS were studied for kinetic parameters by GC and ^{29}Si-NMR.

GC results: Typical GC calibration plots for BTMS (benzyltrimethylsilane) and ISO-

BTMS (*p*-isopropylbenzyltrimethylsilane) using decane as an internal standard are shown in Figure 3.3.2, where the y-axis corresponds to the area under the peak in the GC spectrum and the x-axis to their concentration. The conversion-time plots and the first-order plots obtained for the reaction of BTMS and ISO-BTMS with KOH/EtOH/THF at 72 °C are shown in Figures 3.3.3 and 3.3.4.

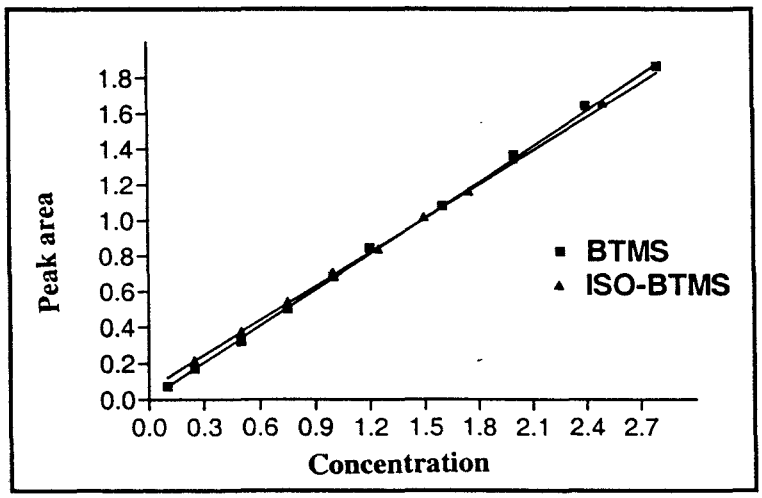

Figure 3.3.2 Typical GC calibration graph for BTMS and ISO-BTMS with decane as an internal standard.

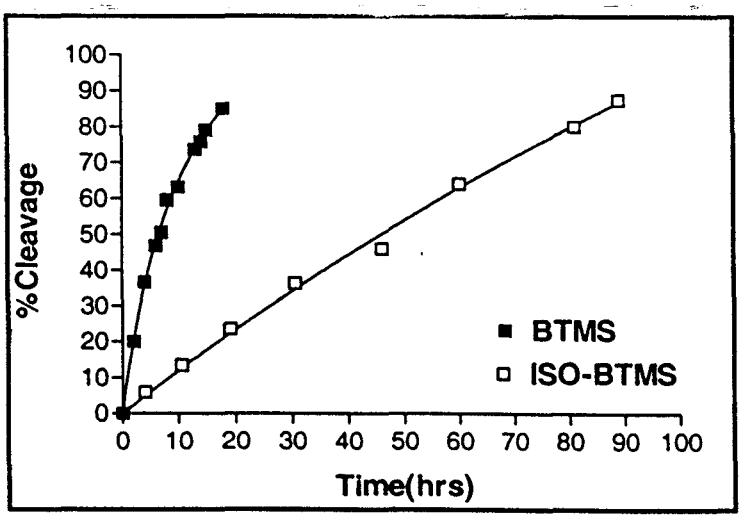

Figure 3.3.3 Conversion-Time plot of alkali cleavage of BTMS and ISO-BTMS (GC): Conditions: BTMS or ISO-BTMS 0.125 Molar; Potassium hydroxide 1 Molar; THF/EtOH 50/50 vol; Temp 72 °C.

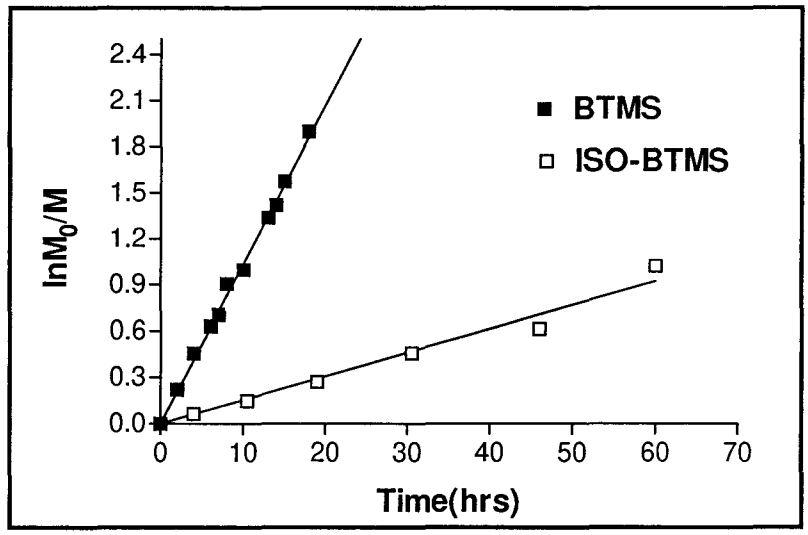

Figure 3.3.4 First-order plot of KOH cleavage of BTMS and ISO-BTMS (GC)-Conditions: BTMS or ISO-BTMS 0.125 Molar; Hydroxide 1 Molar; THF/EtOH 50/50 v; Temp. 72 °C.

The first-order specific rate constant value (k_s), as the slope of the first-order plot, for BTMS and ISO-BTMS obtained by GC method at 72 °C are 174×10^{-5} and $26 \times 10^{-5} min^{-1}$ x $mole^{-1}$ x l respectively. Our rate values are slightly larger than the range of values reported by C. Eaborn and Parker[26] for the cleavage reaction of benzyltrimethylsilanes with NaOH in 39 wt-% aqueous methanol at 49.7 °C. They reported $2.9 \times 10^{-5} min^{-1}$ x $mole^{-1}$ x l and $0.56 \times 10^{-5} min^{-1}$ x $mole^{-1}$ x l as the specific rate constant for BTMS and *p*-methyl benzyltrimethylsilane. Similarly, Hauser[24] *et al.* got 61% conversion in 7 hrs when they refluxed (70-75 °C) 0.9 Molar BTMS with 2 Molar KOH in absolute ethanol. Their reaction is slower than ours, as we obtain 60 % cleavage in 8 hrs when 0.125 Molar BTMS is heated to 72 °C with 1 Molar KOH in a 50/50 THF/EtOH mixture. The enhanced rate observed in our system could be due to the cosolvent THF used. THF may reduce the formation of ethoxide as a nucleophile from

KOH/EtOH/THF system and the ethoxide[26] or methoxide is less nucleophilic on silicon than a hydroxide ion.

Electronic effect: The lower rate of cleavage of ISO-BTMS compared to BTMS can be explained in terms of electron releasing inductive effect of isopropyl group that destabilizes the carbanion intermediate. A related cleavage study[65] showed that the plot of log*k* *v/s* Hammett substituent constant σ is linear with a slope (Hammett reaction constant ρ) of higher positive value, showing that the electron releasing groups in substituted benzyltrimethylsilane can slow down the cleavage rate.

^{29}Si-NMR results: In parallel with GC as a method to follow the benzylic-silicon bond cleavage by KOH, ^{29}Si-NMR was used as a tool to measure conversion of small model molecules. The detailed method of kinetic study of cleavage reactions by ^{29}Si-NMR is described in the experimental section 2.8. The % cleavage of benzylic-silicon bond is estimated as the ratio of reaction product peak integral area to that of reactant in the ^{29}Si-NMR spectra taken on the reaction solutions as a function of reaction time. Figures 3.3.5 and 3.3.6 show the ^{29}Si spectra of BTMS and ISO-BTMS at different % cleavages by KOH/EtOH/THF system.

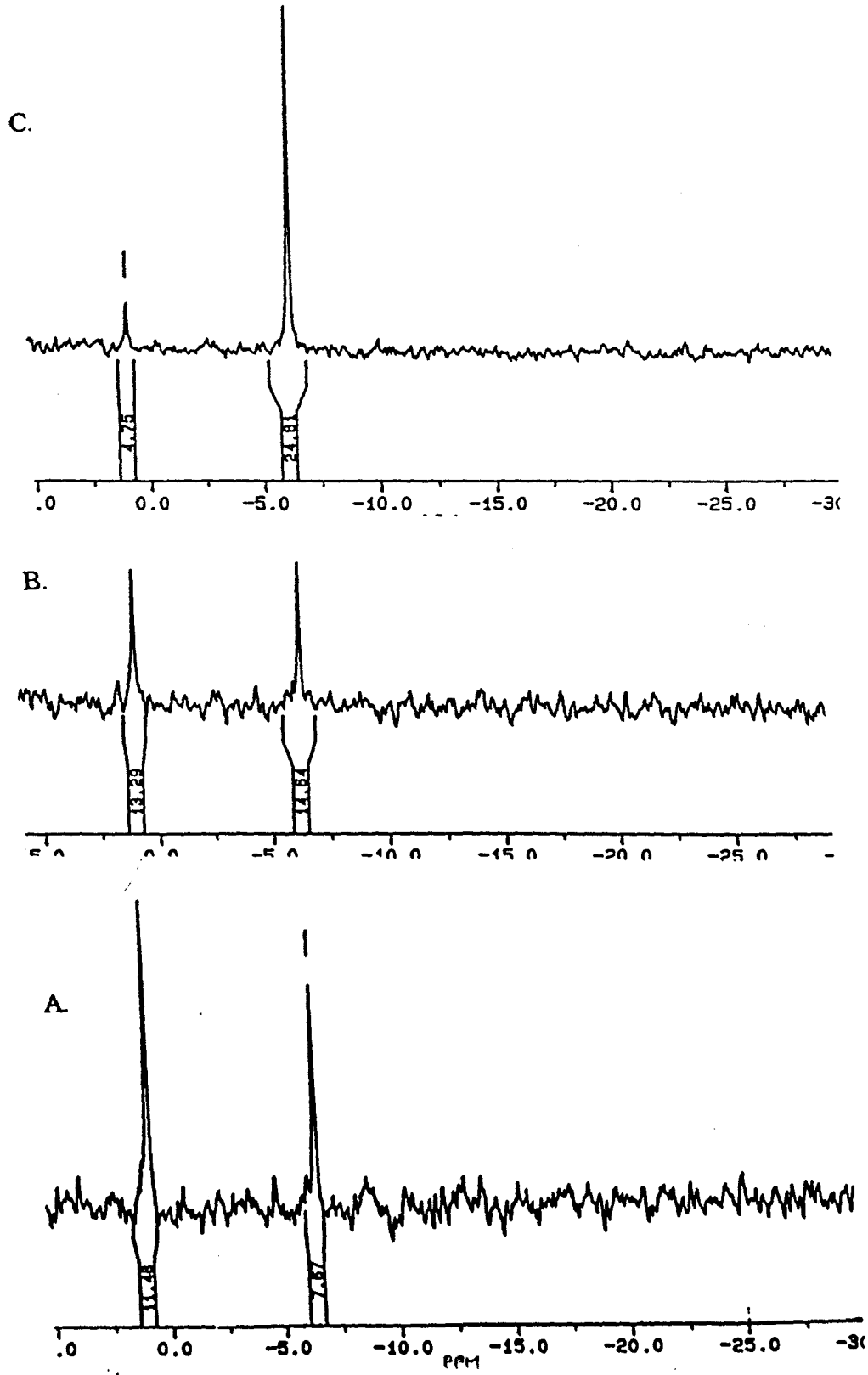

Figure 3.3.5 ^{29}Si INVERSEGATE spectra of BTMS after A. 40% B. 52.5% C. 84% of cleavage by KOH. Conditions: BTMS 0.125 Molar, KOH 1 Molar, EtOH/THF 50/50 v/v, Temp. 72 °C

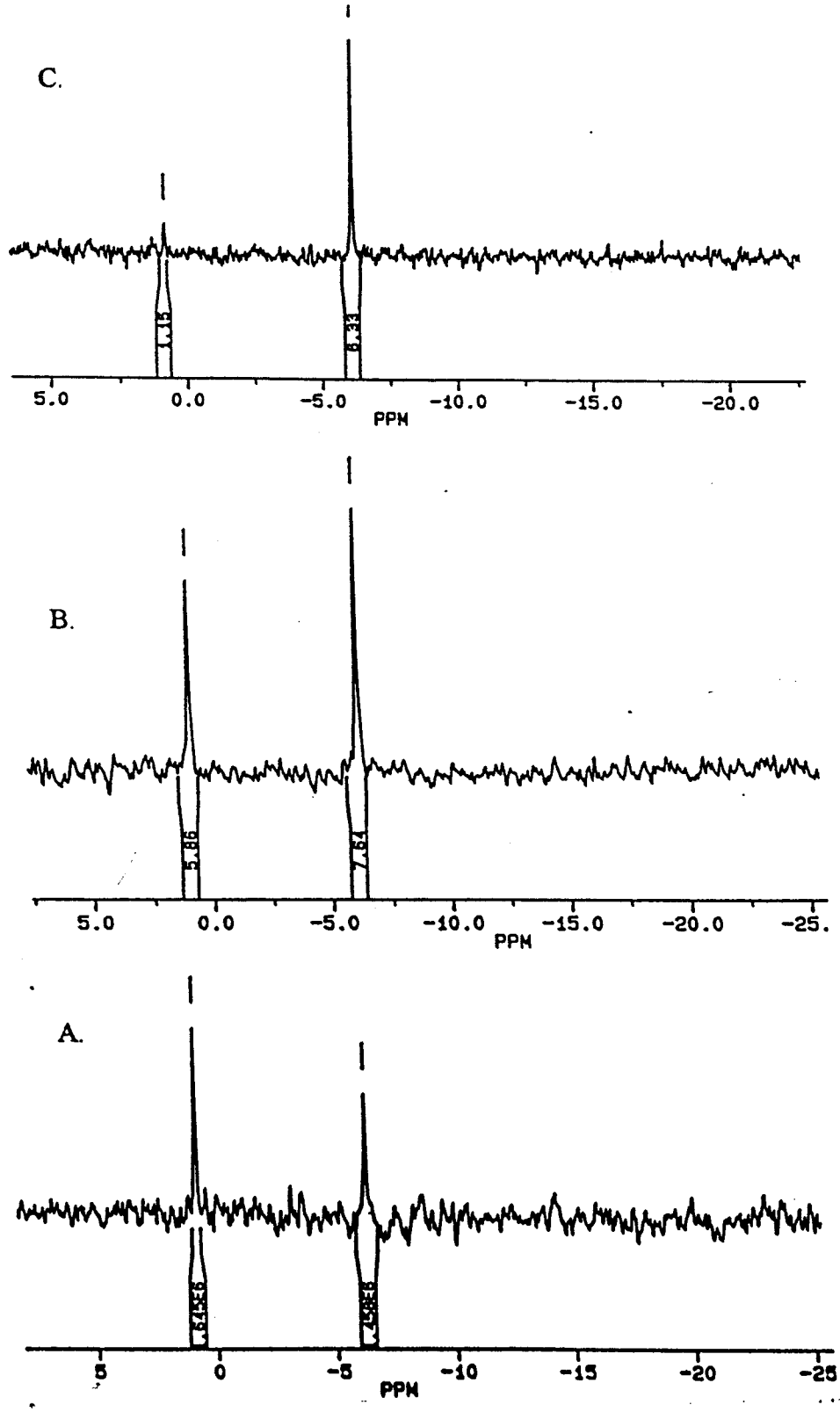

Figure 3.3.6 ^{29}Si INVERSEGATE spectra of ISO-BTMS after A. 46% B. 57% C. 85% of cleavage by KOH. Conditions: ISO-BTMS 0.125 Molar, KOH 1 Molar, EtOH/THF 50/50 v/v, Temp. 90 °C

Comparison of the pseudo first-order rate constants of KOH cleavage derived from both GC and ^{29}Si-NMR data for small model molecules are shown in Table 3.3.3. The difference in reactivity of the monofunctional monomer (VBTMS) and the bifunctional crosslinker (BVBDMS) is shown in Figure 3.3.7. These kinetic curves are drawn based on the ^{29}Si-NMR data. The crosslinker BVBDMS appeared to be less reactive than VBTMS. A lower rate of KOH cleavage is expected for BVBDMS than VBTMS since the benzylic-silicon bond in the former is more sterically hindered from the attack of hydroxide ion due to two vinylbenzyl groups attached to the silicon. The VBTMS is found much more reactive than ISO-BTMS. This can be explained in terms of an additional stabilization of the carbanion intermediate through conjugative delocalization in VBTMS, as shown in Scheme 16.

Scheme 16

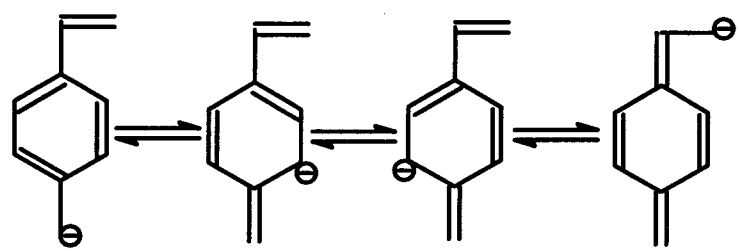

However, the quinoid type of resonance form is absent in ISO-BTMS, where instead there is an inductive electron donation from isopropyl group to the reaction center that destabilizes the carbanion.

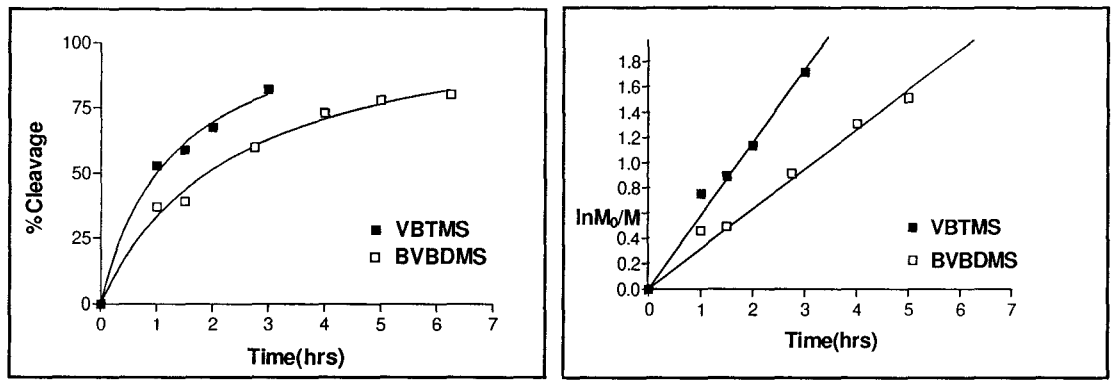

Figure 3.3.7 Conversion-Time plot and first-order plot(^{29}Si) of linear monomer and crosslinker: Conditions: VBTMS or BVBDMS 0.125 Molar; KOH 1 Molar; THF/EtOH 50/50 vol; Temp 50 °C.

Table 3.3.3 Comparison of pseudo first-order rate constants of KOH cleavages

Species	BTMS				ISO-BTMS				VBTMS	BVBDMS
Data source	GC	^{29}Si	^{29}Si	^{29}Si	GC	^{29}Si	^{29}Si	^{29}Si	^{29}Si	^{29}Si
First-order constant k x10^{-5} min^{-1}	174	53.8[a]	278	855	26	9.4[a]	41.6[b]	117.5	977	532
Reaction temp. °C +/- 2	72	50	72	90	72	50	72	90	50	50

Conditions: Substrate 0.125 Molar; Hydroxide 1 Molar; THF/EtOH 50/50 vol. ([a] extrapolated value from Arrhenius plot. ([b] corrected value from GC results.

Table 3.3.3 indicates that for the same reaction temperature, the first-order rate constants derived from ^{29}Si-NMR are greater by a factor of 1.6 than those derived from GC. We attribute some of this difference to the low variability of both methods in their sensitivity, signal/noise ratio of ^{29}Si-NMR. We believe that the rate constants derived from GC results are more accurate compared to those from ^{29}Si-NMR results since here the reaction was arrested by neutralizing the KOH by an acid so that no reaction is expected to occur during the analysis of the reaction mixture by GC. Hence, all reaction

parameters derived from ^{29}Si-NMR data are divided by a factor of 1.6, nullifying the variation in the reaction results obtained by both GC and ^{29}Si-NMR methods.

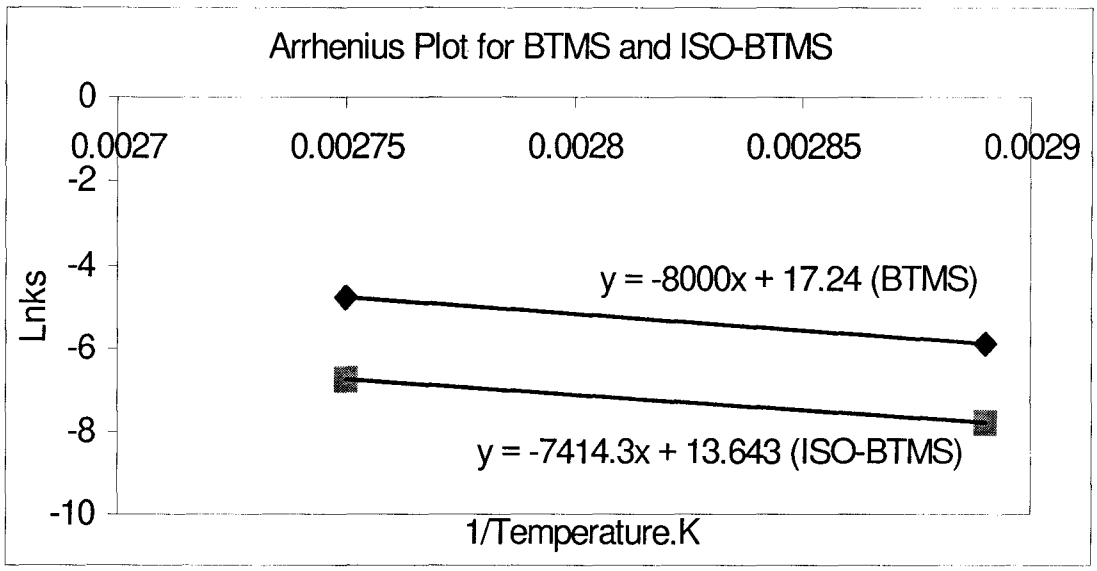

Figure 3.3.8 Arrhenius plot for KOH cleavage of BTMS and ISO-BTMS(^{29}Si).

The Arrhenius plots, as shown in Figure 3.3.8, for both BTMS and ISO-BTMS at 72 °C and 90 °C are based on the rate constants derived from ^{29}Si-NMR results and corrected by a factor of 1.6. The parallel nature of the plots indicates an identical type of mechanism operating in the cleavage reactions of both. Our rate results entered in Table 3.3.3 and 3.3.4 are corrected by a factor of 1.6 for the variation in the results obtained from GC and ^{29}Si-NMR methods. The literature k_s value shown in Table 3.3.4 for the cleavage reaction of BTMS increases with increase in the percentage of water in the reagent. Eaborn[26,57,58] explained that in aqueous-alcoholic solutions of alkali, with increase in water content the equilibrium $OH^- + ROH \leftrightarrow RO^- + H_2O$ would shift more towards hydroxide ion, which is more nucleophilic on silicon. An about 2.6 times increase in rate of cleavage of *m*-Cl-BTMS in NaOH/39wt%water-MeOH/50.4°C

compared to the same in NaOMe/MeOH/50°C is an indication of the fact that hydroxide ion is more nucleophilic than methoxide ion on silicon.

Table 3.3.4 Activation parameters for KOH cleavage of benzylic-silicon bond

Reaction	$k_s x10^{-5}$ min^{-1}	E kcal/mol	LogA /min	Reference
BTMS/NaOMe/MeOH /50°C	2.0	26.1	11.2	58
m-Cl-BTMS/NaOMe/MeOH /50°C	72	--	--	66
m-Cl-BTMS/NaOH/39wt% water-MeOH/50.4 °C	186	--	--	65
BTMS/NaOH/39wt% water-MeOH/49.7 °C	2.9	29.5	15.43	26
BTMS/NaOH/20wt% water-MeOH/50 °C	2.12	---	---	57
BTMS/NaOH/5wt% water-MeOH/49.7 °C	1.76	---	---	26
BTMS/KOH/ETOH/THF/ 50°C(^{29}Si)[b]	33.6[b,a]	---	---	This work
ISO-BTMS/KOH/ETOH/THF/50°C(^{29}Si)[b]	5.9[b,a]	---	---	This work
BTMS/KOH/ETOH/THF/ 72°C(^{29}Si)	174[a]	25.3[a]	11.9[a]	This work
ISO-BTMS/KOH/ETOH/THF/ 72°C(^{29}Si)	26[a]	23.5[a]	9.5[a]	This work

([a] corrected ^{29}Si results from GC results.([b] extrapolated ^{29}Si results to lower temperature)

As shown in Table 3.3.4, the activation parameters derived from our work for BTMS matches closely with the literature value. This is a good indication of the absence of significant error in our rate constant values. The lower rate value for ISO-BTMS is justified from the lower Log*A* factor compared to BTMS, in addition to the rate lowering effect of the electron releasing *p*-isopropyl substituent.

3.3.3 Cleavage of polymer analogs by KOH/EtOH/THF

The KOH initiated cleavage reactions on our polymeric substrates were characterized by ^{1}H-NMR. The extent of cleavage for the oligomer and the homopolymer of *m/p*-VBTMS was obtained from the relative change in the integral ratio of the trimethylsilyl (TMS) peak with respect to the aromatic peak, or between 4-methyl and aromatic

peaks. For styrene copolymers of molar composition 1:Y (VBTMS:Styrene), % cleavage can be calculated from the following equation.

$$\%\text{Cleavage based on Trimethylsilyl group} = \frac{\text{TMS peak integral x 100}}{\text{Aromatic integral x 9/ (4+5 x Y).}}$$

$$\%\text{Cleavage based on 4-Methyl group} = \frac{\text{4-Methyl peak integral x 100}}{\text{Aromatic integral x 3/ (4+5 x Y).}}$$

For methyl methacrylate copolymers, the percentage of cleavage of reaction was calculated based on the change in the integral ratio of trimethylsilyl peak at about 0.0 ppm to aromatic peak at about 6.7-7.8 ppm.

Figure 3.3.9 shows ^{1}H-NMR spectra of the homopolymer poly(*m/p*-VBTMS) at different amount of benzylic-silicon bond cleavage by KOH/EtOH/THF. In the spectra, the integral of trimethylsilyl (TMS) peak at 0.0 ppm with respect to that of the aromatic peak at 6.7-7.8 ppm is lowered as the percentage cleavage is increased, showing the progress of the cleavage reaction. The reaction progress can also be detected from the growing broad peak at 2.3 ppm corresponding to 3- or 4-methyl group of the reaction product, methylstyrene.

Figures 3.3.10 and 3.3.11 show the conversion-time plot and the corresponding first-order plots of KOH/EtOH/THF reaction of ISO-BTMS, oligomer and homopolymer of VBTMS, and its styrene copolymer (VS11'). Their pseudo first-order rate constant values derived as the slope of their first-order plots are shown in Table 3.3.5.

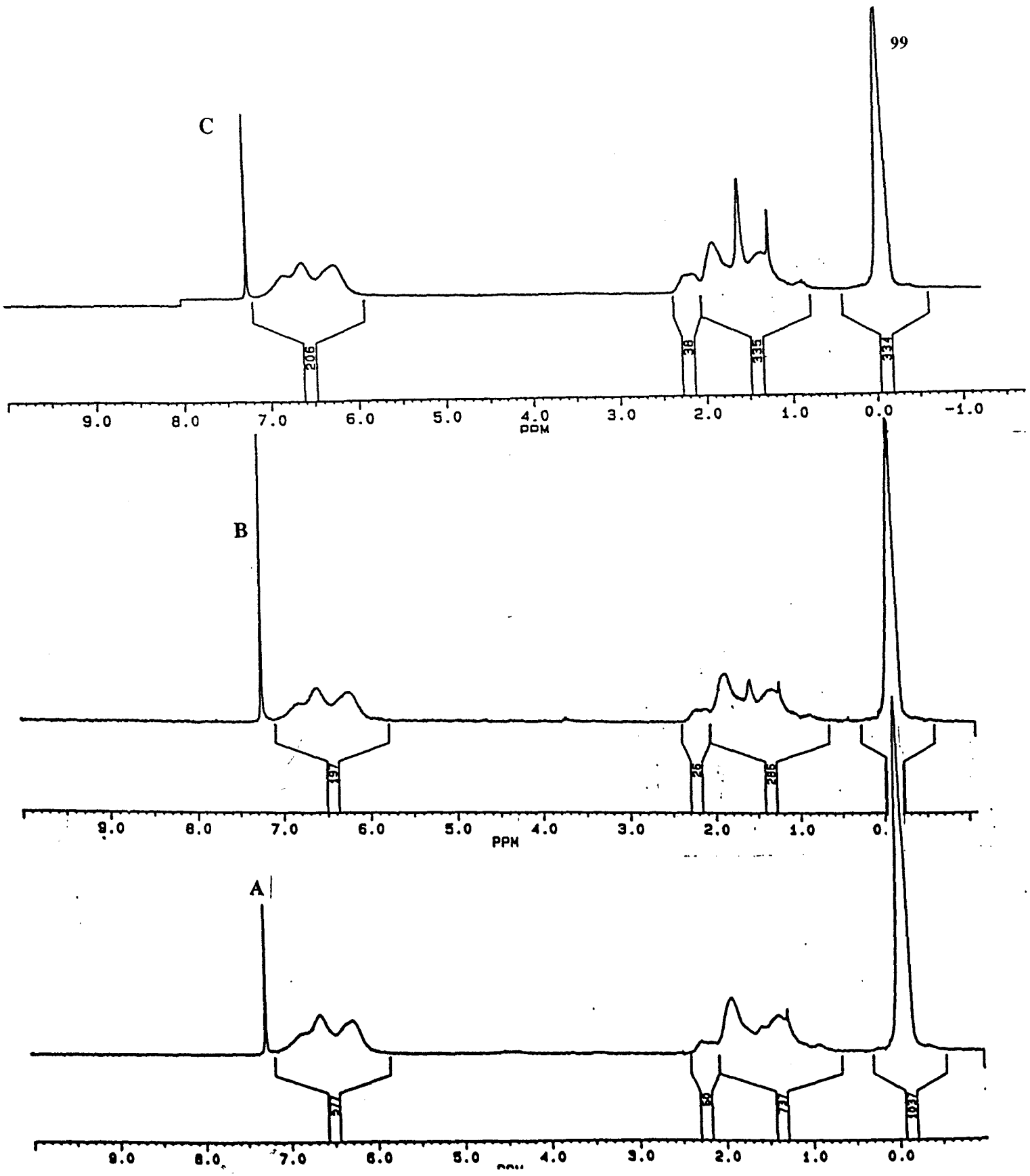

Figure 3.3.9 ^{1}H-NMR spectra of homopolymer poly(*m/p*-VBTMS) at A) 13.8% B) 17.6 % C) 28% of cleavage by KOH/EtOH/THF. Conditions: Homopolymer 0.125 Molar, KOH 1 Molar EtOH/THF 50/50 v/v, Temp. 72 °C.

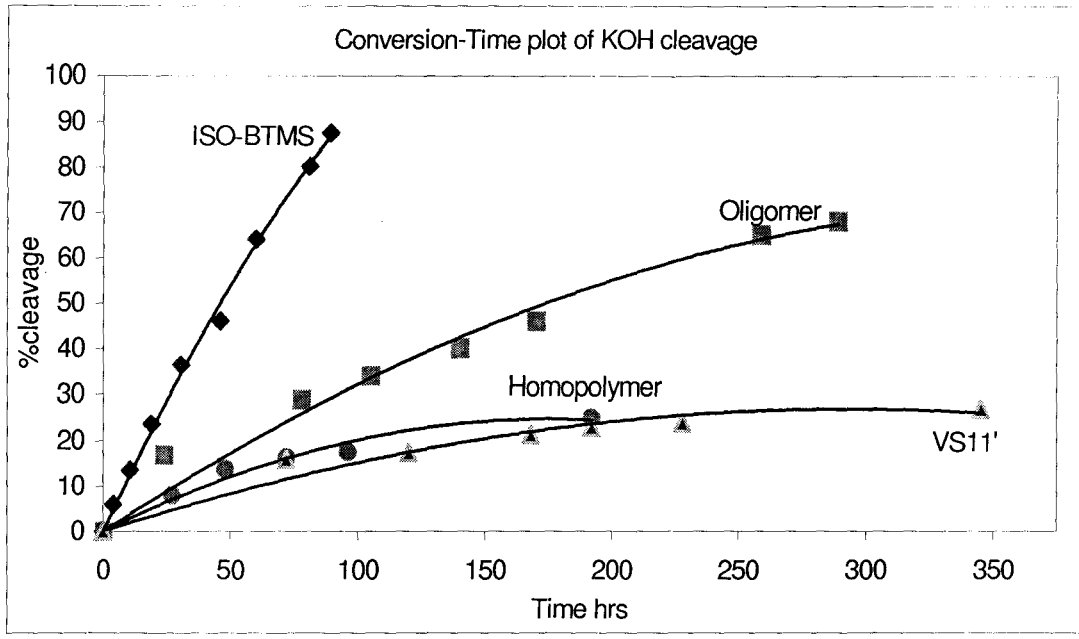

Figure 3.3.10 Conversion-Time plot of KOH cleavage of ISO-BTMS(GC), Oligomer(^{1}H-NMR), Homopolymer(^{1}H-NMR), and Styrene copolymer VS11'(^{1}H-NMR). Substrate 0.125 Molar; Hydroxide 1 Molar; THF/EtOH 50/50 v; Temp. 72 °C.

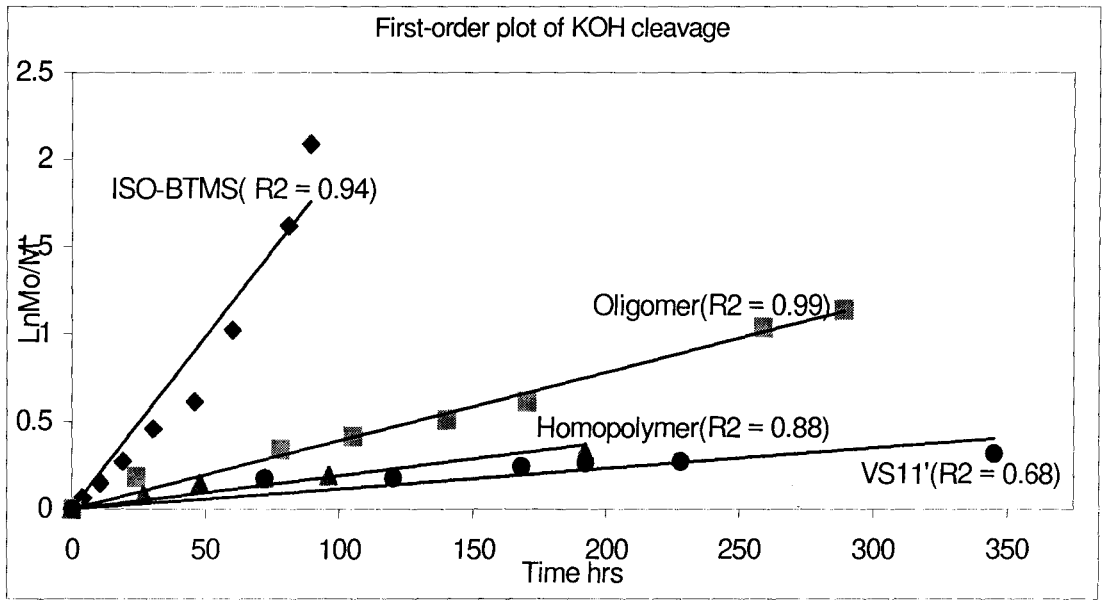

Figure 3.3.11 First-order plot of KOH cleavage of ISO-BTMS(GC), Oligomer(^{1}H-NMR), Homopolymer(^{1}H-NMR) and Styrene copolymer VS11'(^{1}H-NMR). Substrate 0.125 Molar; Hydroxide 1 Molar; THF/EtOH 50/50 v; Temp. 72 °C.

Table 3.3.5 Kinetic data of styrene and methyl methacrylate copolymers towards KOH cleavage. Conditions:

Substrate	Mn	Polynomial fit R^2	Linear fit R^2	k x 10^{-5}min^{-1}
ISO-BTMS	206	0.99	0.94	33.0[#]
VBTMS-oligomer	3076	0.99	0.99	6.5[#]
VBTMS-homopolymer	13250	0.98	0.88	3.16[#], 4.5 (R^2=0.96)*
VS11'	17100	0.99	0.68	2.0[#] , 2.5 (R^2=0.88)*
VS12	17200	0.98	0.79	4.0 (R^2=0.97)*
VS11	27900	0.89	0.43	4.16 (R^2=0.98)*
VS.11'	17100	0.99	0.36	4.16 (R^2=0.95)*
VM12	26600	0.98	0.976	11.20
VM11	40800	0.985	0.98	8.20
VM15	36700	0.98	0.985	16.60
VM12'	26650	0.98	0.98	15.30

Substrate 0.025 Molar, KOH 0.2 Molar THF/EtOH 50/50 v/v; Temp. 72 °C.(* Rate constant based on the slope of initial straight line part of first-order plots and their R^2 value is given in parenthesis), ([#] Rate constant at 0.125 Molar substrate and 1 Molar of hydroxide)

Polymer effect: The behavior of VBTMS-oligomer in comparison with ISO-BTMS towards the hydroxide ion indicates a change in properties of the reaction center, known as 'polymer effect'. A degree of polymerization of 50 in VBTMS-oligomer resulted in a rate reduction by a factor of 4 compared to ISO-BTMS. Sakurada[45] reported the rate constant for the alkaline hydrolysis (NaOH) of poly(vinyl acetate) in acetone-water (75/25 v/v) as one tenth of that for low-molecular-weight analogs. Also, the rate constant for hydrolysis of polymethyl acrylate is much smaller than that for low-molecular-weight analogs, for both alkaline and acid hydrolysis. Sakurada[45] reported similar results for the apparent activation energy of hydrolysis and the collision

frequency, polymethyl acrylate and their low-molecular-weight analogs. He attributed the rate reduction in the hydrolysis of polymers to the steric hindrance of the neighboring groups in the polymeric molecules. Accordingly, we would suggest the same sort of steric factors for the significantly lower rate observed in the VBTMS-oligomer compared to ISO-BTMS.

Effect of molecular weight: As seen from Table 3.3.5, the VBTMS-oligomer reacted about two times faster than the homopolymer with KOH/EtOH/THF. Sakurada[45] observed no noticeable difference in the rate constant of alkaline hydrolysis of polyvinyl acetate as a function of degree of polymerization in dioxane-water mixture (80/20). He did report a decreasing rate constant k_0 (rate constant extrapolated to 0% hydrolysis) as a function of degree of polymerization for poly(allyl acetate), while its k_{50} (rate constant at 50% hydrolysis) was independent of the degree of polymerization. The solvent mixture being a poor solvent for poly(allyl acetate), and the polymer molecules would be in a state of tighter coiling, which hinders the reaction. With increasing hydrolysis, the solvent mixture becomes a better solvent and the coiling is loosened so that the apparent rate constant increases and is independent of the degree of polymerization at 50% conversion. Accordingly, with increase in molecular weight, as in VBTMS-oligomer to poly(VBTMS), poor solubility or tighter polymer coiling is possible so as to have a lower rate of KOH cleavage for the latter than the former.

Anomalous deviation from first-order behavior: The most interesting results regarding the behavior of our polymer analogs in hydroxide ion promoted cleavage of benzylic-silicon bonding is the unexpected deviation from linearity of their first-order

plots. As shown in Figure 3.3.12, the oligomer seems to be perfectly obeying the first-order condition whereas a mild deviation is seen in homopolymer, and a stronger deviation in styrene copolymer VS11'. The cleavage data for VBTMS-oligomer show a 99% fit to the both linear and polynomial regression lines, which are straight lines. This is a characteristic of first-order reactions. However, for the homopolymer and the styrene copolymer, the deviation from the linearity is indicated by the decrease of R^2 value of their linear regression lines to 0.88 and 0.68.

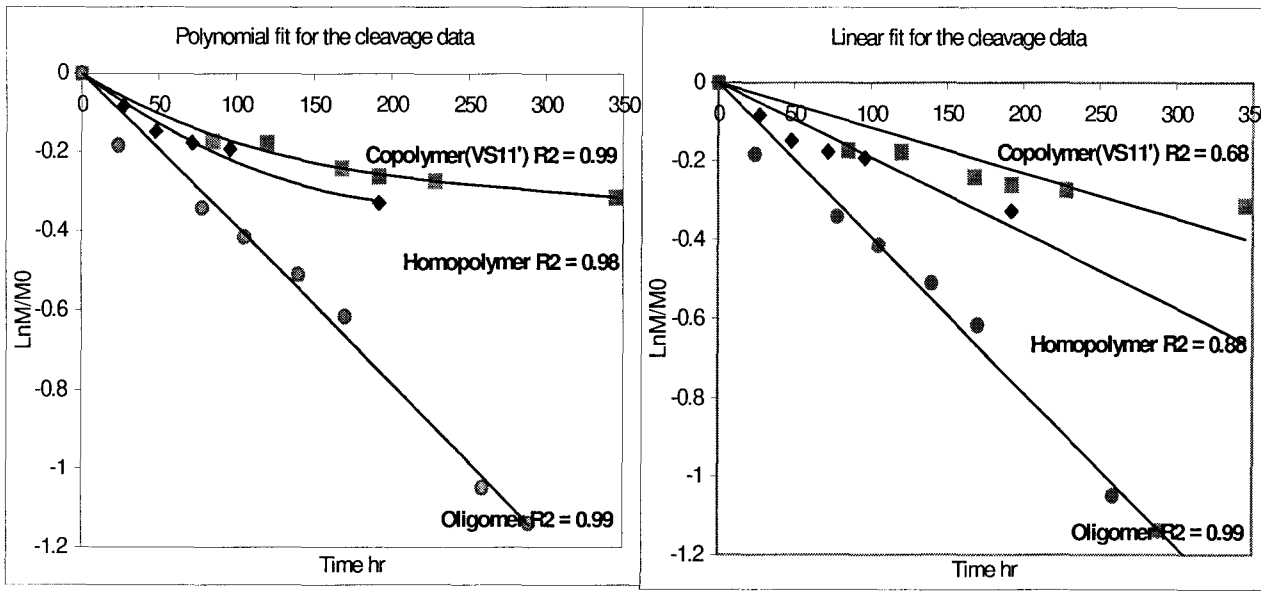

Figure 3.3.12 Deviation from first-order behavior towards hydroxide ion cleavage Conditions: Substrate 0.125 Molar; Hydroxide 1 Molar; THF/EtOH 50/50 v; Temp. 72 °C.

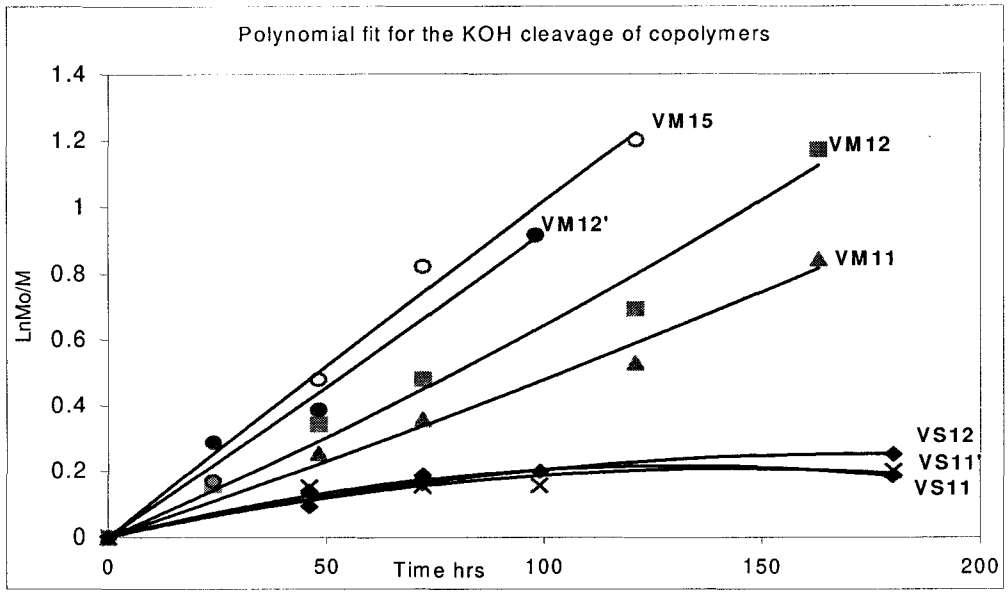

Figure 3.3.13 Kinetic behavior of styrene and methyl methacrylate copolymers towards KOH cleavage. Conditions: Substrate 0.025 Molar, KOH 0.2 Molar, EtOH/THF 50/50 v; Temp. 72 °C.

Their cleavage behavior best fits into the polynomial regression lines, which are curved, an indication of deviation from first-order characteristics. This anomalous behavior is seen in all of our styrene-based copolymers, but surprisingly not in MMA copolymers of VBTMS. We deliberately changed the concentration of the substrate to the reagent KOH for all copolymer-reactions from 0.125 / 1.0 Molar to 0.025 / 0.2 Molar for solubility reasons. Since, in some of our styrene and MMA copolymers including VS12 and VM15, the styrene composition reaches up to 70 mol% and MMA up to 82 mol%. So, these copolymers in silane functionality of 0.125 Molar would be highly thick solutions or a phase separated reaction mixtures in 1 Molar KOH/EtOH/THF system.

The rate constants of KOH induced cleavage of polymers including poly(VBTMS) homopolymer and its styrene copolymers are likely to have some error as they deviate

from first-order behavior. Hence, their rate constants extracted as the slope of initial straight line portion of their first-order plots with higher R^2 value of fit are only entered in Table 3.3.5. It can be seen from Table 3.3.5 that across the substrate series of small molecule, oligomer, homopolymer and styrene copolymers of VBTMS, there is a progressive lowering of the reaction rate. It might be due to the progressive increase in the hydrophobic character of the substrate along the series so that polar reagent, hydroxide ion, is likely to be repelled from the substrate matrix to have a lowering reaction rate.

Across the styrene copolymer series (VS12, VS11, and VS11'), the deviation from first-order kinetics is exhibited by all individual copolymers. However, their rate constants, derived from the initial straight-line part of their first-order plots, seem to be the same irrespective of the variation in their composition or molecular weight. The interpretation here is complicated as their behavior of deviation from first-order kinetics started quite early part of the reaction so that it is hard to extract the rate constant as the slope of a small straight line part of their first-order plots. However, a small tendency to have a lower rate is for VS12 of highest styrene content. Figure 3.3.14 shows the ^{1}H-NMR spectra of the styrene copolymer VS11' at different % cleavage of benzylic-silicon bond by KOH. The progress of reaction can be seen from the relative lowering in the TMS peak integral as a function of reaction time.

In contrast to the styrene copolymer series, MMA series is much more reactive and obeys strictly first-order kinetics. Figure 3.3.15 shows the KOH reaction progress in the ^{1}H-NMR spectra of methyl methacrylate copolymer VM12 with different % of

cleavage, where the relative intensity of TMS peak is progressively lowered. Among the MMA series, the rate constant shows a small increase as the MMA content is increased, and the most reactive one is VM15 with highest MMA content. This can be explained in terms of higher polarity of MMA residue that makes the copolymer hydrophilic so that the hydroxide ion would be effectively attracted to the copolymer domains to facilitate the reaction. The lower rate values of styrene copolymers in comparison with MMA-copolymers are attributed to the hydrophobic repulsion that makes the access of hydroxide ion into the copolymer matrix much more difficult.

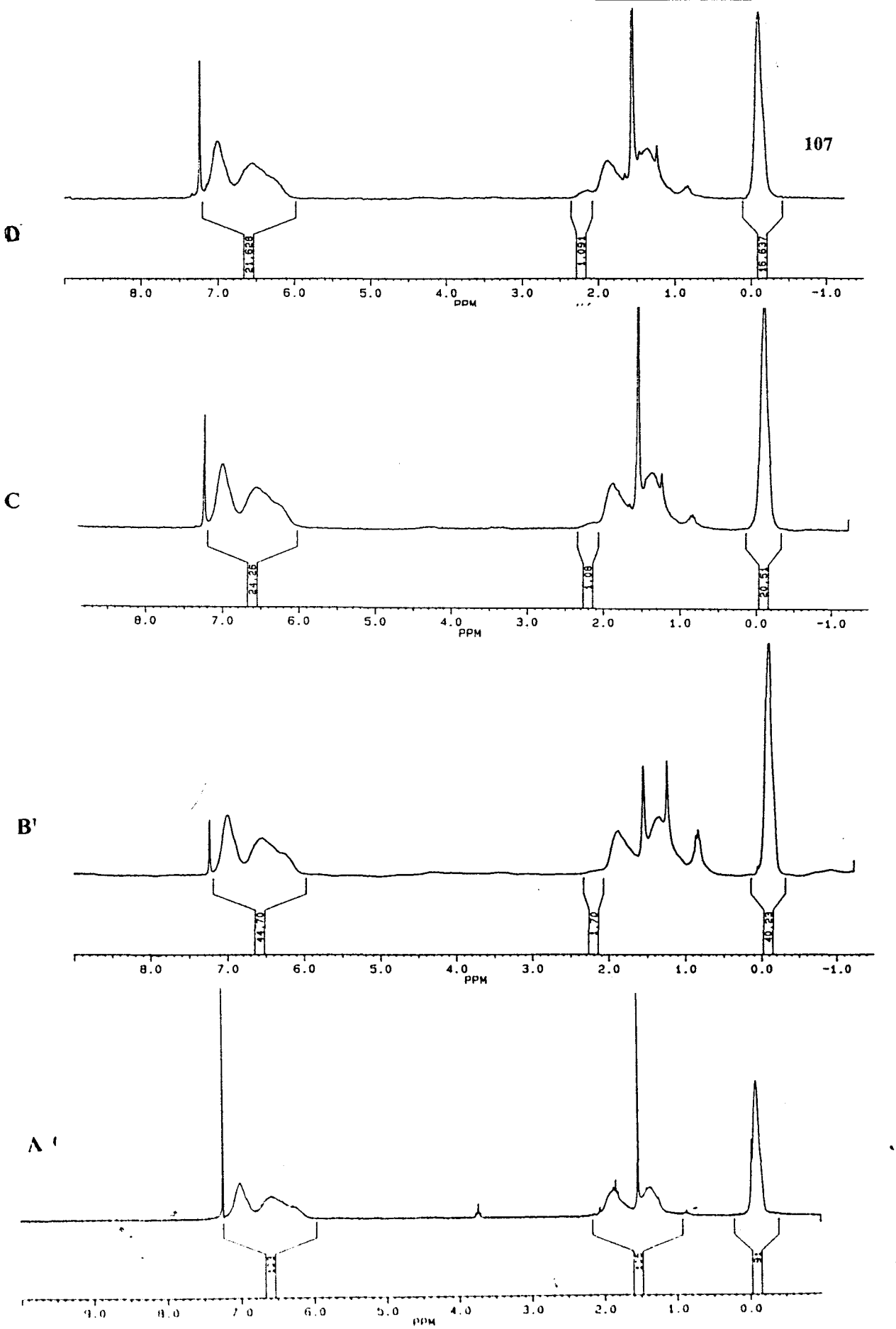

Figure 3.3.14 ^{1}H-NMR spectra of poly(VBTMS-*co*-styrene) VS11' after A) 0% B) 13% C) 15% D) 17% cleavage by KOH. Conditions: VS11' 0.025 Molar, KOH 0.2 Molar, EtOH/THF 50/50 v; Temp. 72 °C.

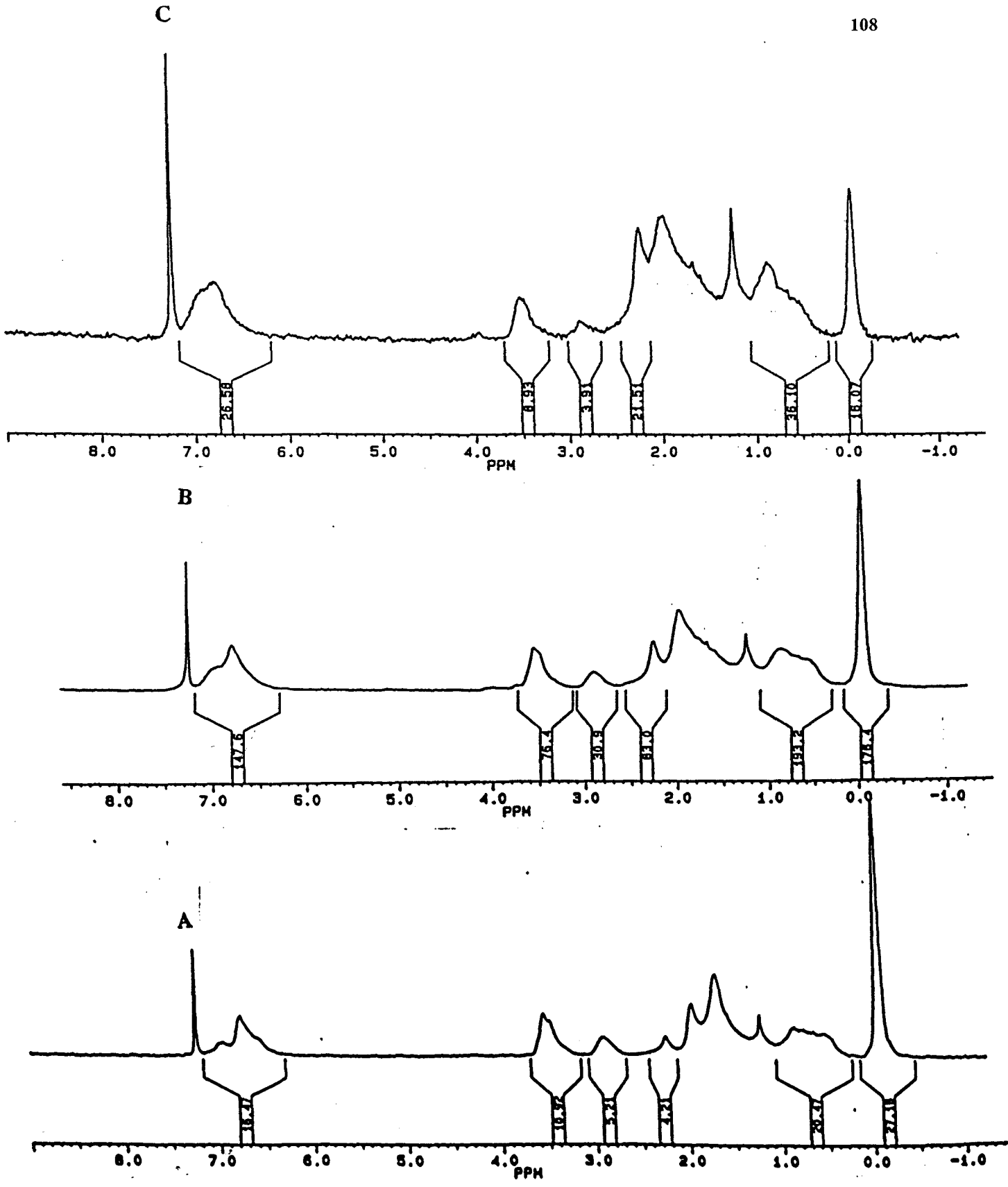

Figure 3.3.15 ^{1}H-NMR spectra of poly(VBTMS-*co*-MMA) VM12 at A) 14.5% B) 38% C) 69% cleavage by KOH. Conditions: VM12 0.025 Molar, KOH 0.2 Molar, EtOH/THF 50/50 v; Temp. 72 °C.

Morawetz[67] reported a similar deviation from first-order behavior exhibited by copolymers of *p*-nitrophenyl acrylates during their aminolysis with various amines. He found a pronounced reduction in the aminolysis rate with styrene copolymers compared to their low molecular weight analog (*p*-nitrophenyl ester of isobutyric acid) due to steric hindrance and the nonpolar nature of the styrene ring where as *N,N* dimethylacrylamide copolymers exhibited a correspondingly higher rate than the analog due to the neighboring group effect of amide groups in the polymer chain. The deviation from first-order behavior was significant only with styrene copolymers, not with methyl acrylate and *N,N*-dimethyl acrylamide copolymers. Morawetz[67] explained this behavior, observed even in completely alternating copolymers, in terms of stereochemical nonequivalence of the isotactic, heterotactic, or syndiotactic triads that can form from the reactive monomer residue (*p*-nitrophenyl acrylate) with its two styrene neighbors. Consistent with his explanation, the significant reduction in rate (about 10 times) observed with our poly(VBTMS-*co*-Sty) compared to ISO-BTMS analog is attributed to the steric hindrance and the non polar nature of styrene units that reduces the accessibility and the solubility of hydroxide ion into the copolymer matrix. This, together with the stereochemical nonequivalence, can result in dispersion in the cleavage rate of our styrene copolymers. The steric factors are of no significance in the case of the much more polar poly(VBTMS-*co*-MMA), which must have behaved like Morawetz's copolymer of methyl acrylate with *N,N*-dimethyl acrylamide, without any deviation from first-order charactistics.

Talu[68] reported a two-step kinetic behavior for the methanolic-KOH hydrolysis of poly(ethyl acrylate) and its styrene copolymer of composition 31:68. The pseudo first-

order plot for poly(ethyl acrylate) was linear up to 40% conversion, and thereafter curved. The styrene copolymer showed a significantly lower rate with early deviation from first-order characteristics. Talu's[68] explanation for this deviation is that as the reaction proceeds, more and more carboxylate anions formed in the polymer chain can progressively hinder the attack of hydroxyl ion through electrostatic repulsion. The lower rate for his styrene copolymer and an early curving of the first-order plot are explained in terms of the steric hindrance arising from the ester groups being blocked by neighbouring phenyl groups, so making the approach of hydrolytic agent difficult. His studies also show an enhancement in rate as a function of KOH concentration is due to an increase in ionic strength of the medium that facilitates functional interaction of the ester groups. It is also mentioned no noticeable effect of polymer molecular weight on the hydrolysis rate constant. Bohmer[69] also observed the same sort of behavior in the aminolysis of *ortho* and *para*-nitrophenyl esters of lower carboxylic acids, and of copolymers of styrene and acrylic acid with butyl amine in dioxane solvent. His oligomeric esters were found to obey first-order kinetics like small model esters when the aminolysis was done in pseudo first-order condition. In addition, the rate of aminolysis on his copolymers was much smaller and exhibited a deviation in first-order kinetics though their activation energies were identical to low molecular weight model esters.

We could not determine the rate constant values for the microsphere particles due to the extremely high cross-link density, which gave no noticeable change in the particle morphology even after several days of reaction.

3.3.4 Equilibrium behavior of trimethylsilanol

In order to investigate the attacking nucleophile on silicon centers in our reaction system containing KOH/EtOH/THF, a series of reactions were carried out using ^{29}Si NMR as a tool to record the chemical shifts of all the possible by-products of reaction. The results are shown in Table 3.3.6.

Table 3.3.6 Cleavage reaction-product analysis.

Reactant	Reaction condition	^{29}Si Chemical shift ppm	Peak integral ratio
Hexamethyldisiloxane	a) ------	6.48	------
$(CH_3)_3SiOSi(CH_3)_3$	b) KOH / ETOH / THF / 0.5hr/ 75°C	6.87 , - 5.6	1 : 1.30
	c) KOH / ETOH / THF / 1.0hr / 100°C	6.7 , - 5.8	1 : 1.34
	d) KOH / ETOH / THF / 1.5hr / 100°C	6.7 , - 5.8	1 : 1.69
	e) KOH / ETOH / THF / 2.5hr / 100°C	6.7 , - 5.85	1 : 1.35
	f) KOH / H_2O / THF / 0.5hr / 75°C	6.7	-----
Trimethylsilanolate $(CH_3)_3SiO^-K^+$	a) Acetonitrile / room temp.	- 14.5	----
	b) THF / room temp.	- 16.1	---
	c) 50/50 ETOH / THF / room temp.	15.1 , 7.0	---
Trimethylethoxysilane $(CH_3)_3SiOCH_2CH_3$	a) -------	14.6	-----
	b) KOH / ETOH / THF / 0.0hr/ 100°C	15.1 , 6.72 , - 5.7	1 : 3.2 : 0.2
	c) KOH / ETOH / THF / 0.5hr/ 100°C	6.72 , - 5.7	1 : 1.13
	d) KOH / ETOH / THF / 0.75hr/ 75°C	15.1 , 6.7 , - 5.8	1 : 9.5 : 2.8
	e) d) was neutralized by acetic acid	15.2 , 7.0	------
Benzyltrimethylsilane BTMS	KOH / ETOH / THF /72°C	0.98 , - 6.42	
Isopropylbenzyltrimet-hylsilane ISO-BTMS	KOH / ETOH / THF / 72°C	0.8 , - 6.31	

([KOH] = 1 Molar)

The reactions b), c), d) and e) on $(CH_3)_3SiOSi(CH_3)_3$ show that it is under dynamic equilibrium with another species at - 5.8 ppm, which may be trimethylsilanol. Though trimethylsilanol is more acidic than alcohols due to the donation of an unshared pair of electrons on oxygen to silicon through (d_π-p_π) bonding, 12N NaOH is needed to convert trimethylsilanol[3] into its sodium salt. Hence, 1 Molar potassium hydroxide can not convert both ethanol and trimethylsilanol into ethoxide ion and trimethylsilanolate in our system. Since our cleavage reactions on BTMS and ISO-BTMS did not show any peak at - 14.5 ppm, $(CH_3)_3SiO^-K^+$ is not expected to form in our reaction system either through salt formation of trimethylsilanol or any possible hydrolysis. The reactions b), c), and d) on trimethylethoxysilane produce hexamethyldisiloxane as a major product at 6.7 ppm and a species at - 5.7 - - 5.8 ppm. Since, our reaction system did not show any peak in the range 14-15 ppm, the formation of trimethylethoxysilane by the action of ethoxide ion as a nucleophile can be ruled out. In the reaction d), the trimethylethoxysilane is completely converted into hexamethyldisiloxane, and a species at - 5.7 ppm (trimethylsilanol) is formed in 0.5 hrs by KOH/EtOH/THF at 100 °C. However, the absence of a peak at 6.7 ppm corresponding to hexamethyldisiloxane eliminates the possibility of ethoxide ion as a nucleophile attacking on silicon.

Recently, Rankin[70] *et al.* investigated the esterification, condensation and deprotonation equilibrium behavior of trimethylsilanol (hexamethyldisiloxane and ethoxytrimethylsilane as substrates) both in acidic and alkaline ethanol/water solutions by ^{29}Si-NMR. They found that at relatively low concentrations of strong acid or strong base and high concentrations of their substrates, trimethylsilanol in equilibrium with its deprotonated form would predominate. However, as the NaOH base concentration is

increased up to 0.5 Molar, the concentration of deprotonated trimethylsilanol outweighs trimethylsilanol as shown by the downfield movement of ^{29}Si-NMR chemical shift of silanol species up to -7.12 ppm. Rankin[70] got a very sharp singlet peak for trimethysilanol, which is in equilibrium with its deprotonated form. The estimated deprotonation exchange rate of trimethylsilanol is 0.3 ms, which is well below the time scale with which the ^{29}Si-NMR spectrum is collected. Consistent with their observation, our reaction system containing 1 Molar KOH also gave singlet sharp product peak at -6.5 ppm. Their esterification equilibrium constant of trimethylsilanol with ethanol has very small value of 0.05 for the whole range of acid or base concentrations. This rules out the formation of ethoxytrimethylsilane in our KOH/EtOH/THF system through esterification of trimethylsilanol. Thus, all the observations are in support of the fact that the only silicon by-product formed in the KOH induced cleavage reactions corresponding to - 6.5 ppm is trimethylsilanol, which might be in a rapid equilibrium with its deprotonated form so as to give a singet peak in ^{29}Si-NMR spectra.

Bunnett,[59] while comparing the nucleophilicity of different bases in nucleophilic substitution reaction of an aryl halide in 60% aqueous dioxane, got ether as a major reaction product along with a small percentage of phenol when NaOH used as the base. Richardson[59] also found that *p*-chloronitrobenzene and KOH in 60% ethanol-water formed 71% *p*-nitrophenetole and only 13% *p*-nitrophenol. He reported that in his solution the hydroxide ions outnumbered the ethoxide ion by about 3:1. The formation of ethers was explained with the argument that the nucleophilic substitution reaction of hydroxide ion would produce phenoxide ion which would be more nucleophilic on

carbon than a hydroxide ion so that further nucleophilic attack of phenoxide ion on the aromatic substrate results in the ether products. In support with Richardson's[59] findings, Caldin[71] reported 0.7 +/- 0.2 as the equilibrium constant *K* for the reaction, OH^- + EtOH = EtO^- + H_2O, observed in a solution of KOH or NaOH in pure ethanol. Caldin's[71] observation is in support of the fact that methanol is a stronger acid than water and ethanol is nearly as acidic as water.

Thus, our reaction system of KOH/EtOH/THF is likely to have ethoxide ions in addition to hydroxide ions as the nucleophile. However, Eaborn[31] suggested that the equilibrium would move more towards hydroxide ion in aqueous-alcoholic alkoxide solutions, and the hydroxide ion would be much more nucleophilic than ethoxide and methoxide on silicon centers (unlike on carbon centers). Hence, the preferred attacking nucleophile on silicon-carbon bonds, even in the presence of ethoxide ion in our KOH/EtOH/THF reaction system, is the hydroxide ion for the following supporting reasons in addition to the ^{29}Si-NMR evidences. A) THF may be able to reduce the acidity of ethanol through donor type H-bonding operating through oxygen atom that 1 Molar KOH may not form ethoxide ion from ethanol. B) 12 N NaOH[3] is needed to convert trimethyl silanol, which is more acidic than ethanol, to its salt. C) Hydroxide ion is much more nucleophilic than ethoxide and methoxide on silicon centers.

Thus, we propose that the only attacking nucleophile on silicon in our KOH/EtOH/THF reaction system is the hydroxide ion, forming trimethylsilanol as a major by-product, which is in a rapid equilibrium with its deprotonated form.

3.4 Cleavage of Benzylic-Silicon Bond by Tetrabutyl Ammonium Fluoride / THF (TBAF/THF)

Our objective here is to use a nucleophile that is more nucleophilic than the hydroxide ion, to cleave the benzylic-carbon bonds in our series of substrates. Tetrabutyl-ammonium fluoride (TBAF) was selected for this purpose since the fluoride ion is about 100 times more nucleophilic on silicon (strong bonding of Si-F[1]) than the hydroxide ion. The F^- ion in TBAF is expected to be much more naked than the F^- ion in KF/ethanol. As the reagent, KF/ethanol was found ineffective with negligible reaction rate on our substrates, TBAF in THF (a good solvent for styrenic polymers) was selected as the reagent for the study.

Reaction mechanism[23]: The typical mode of reaction involves attack of fluoride ion on silicon to form a pentacoordinated silicon intermediate followed by the breaking of benzylic-silicon bond to form a carbanion. Abstraction of a proton from the solvent leads to the products as shown in the sheme 15.

Scheme 15

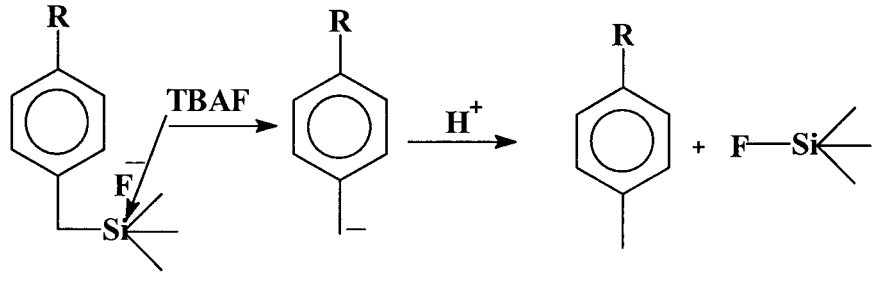

3.4.1 Cleavage on linear polymer models by TBAF/THF

The initial experiments on small model molecules such as BTMS and ISO-BTMS were so rapid at room temperature that the reaction rate could not be estimated either by ^{29}Si-NMR or by ^{1}H-NMR. So, all of the reactions using TBAF as a nucleophile were carried out on the polymeric substrates only. All reactions were carried out in pseudo first-order conditions, keeping a molar ratio 1:8 for silicon functionality to fluoride ion. The extend of cleavage of silicon functionality in all cases was estimated based on the change in the ^{1}H-NMR peak integral ratio of trimethylsilyl (TMS) group to aromatic.

Figures 3.4.1 and 3.4.2 show the cleavage reaction pattern of benzylic-silicon bonds of different substrates under TBAF/THF. Figure 3.4.3 shows the proton NMR spectra of VBTMS-oligomer at different % of cleavage by TBAF/THF. Compared to the hydroxide ion cleavage, the reaction of fluoride ion was found to be extremely clean and rapid so that the work up of the reaction was much easier. Table 3.4.1 depicts the rate constant values of the cleavage reactions.

The most interesting observation is that all reactions were found to follow first-order kinetics irrespective of the substrate type. It was observed that the lowest rate is exhibited by the species of lowest chain length (oligomer). As the molecular weight is increased through the homopolymer to still larger copolymers, the rate is progressively enhanced. As the molecular size increases, the polymer matrix of increasing hydrophobicity may either facilitate the solubility of TBAF in the matrix, or else by hydrophobic interaction between the polymer chain and the counter ion makes the fluoride ion much more 'naked' so as to have an enhanced reactivity.

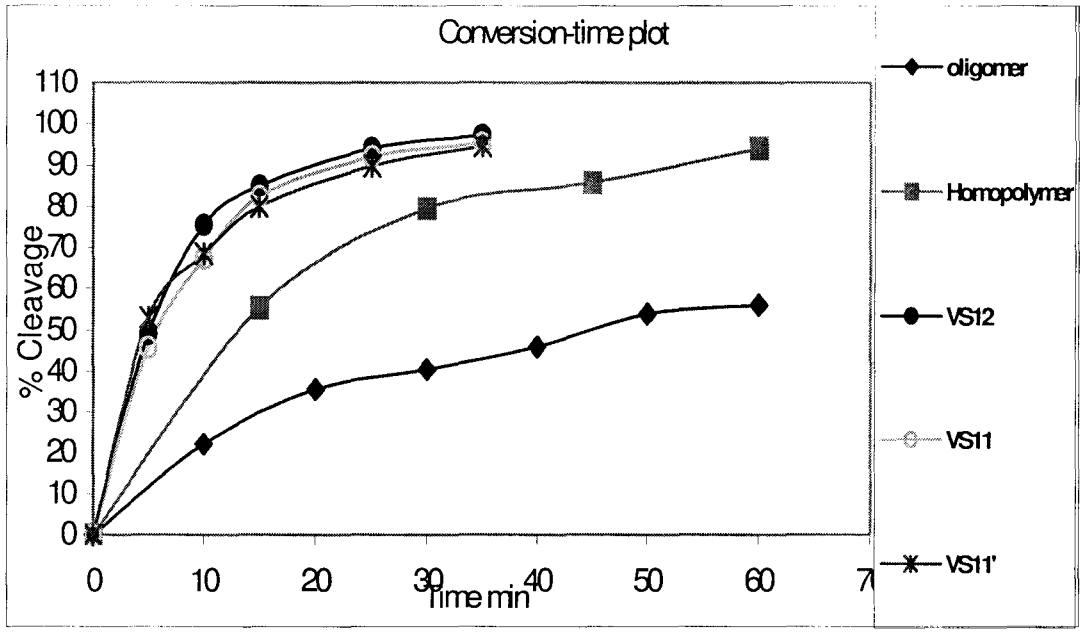

Figure 3.4.1 Conversion-Time plot of TBAF cleavage reaction. Conditions: Substrate 0.025 Molar; TBAF 0.20 Molar; Solvent THF; Temp 22 °C.

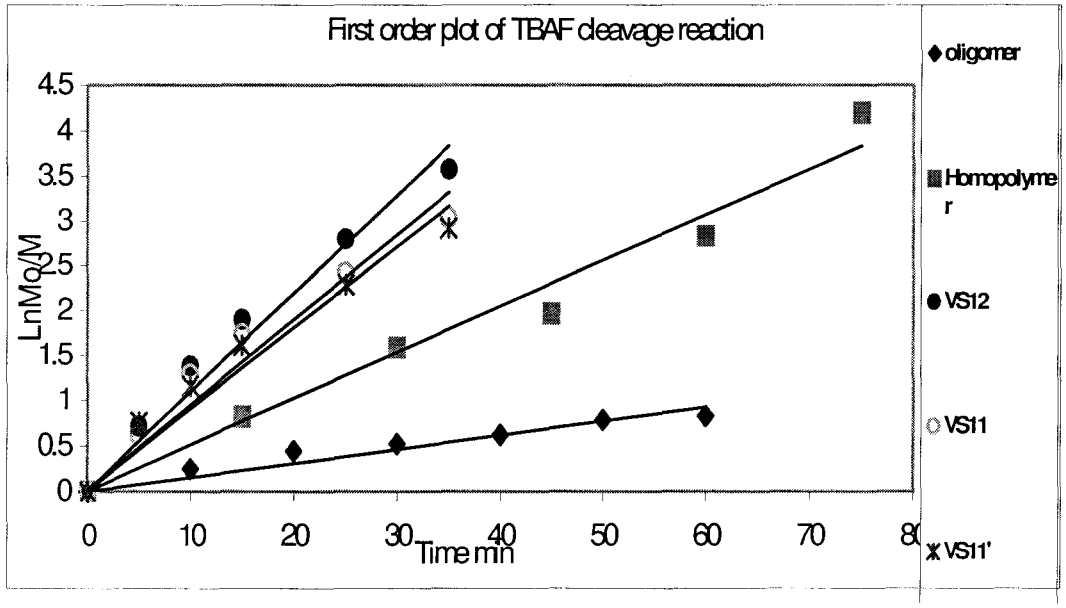

Figure 3.4.2 First-order plot of TBAF cleavage reaction. Conditions: Substrate 0.025 Molar, TBAF 0.2 Molar; Solvent THF; Temp 22 °C.

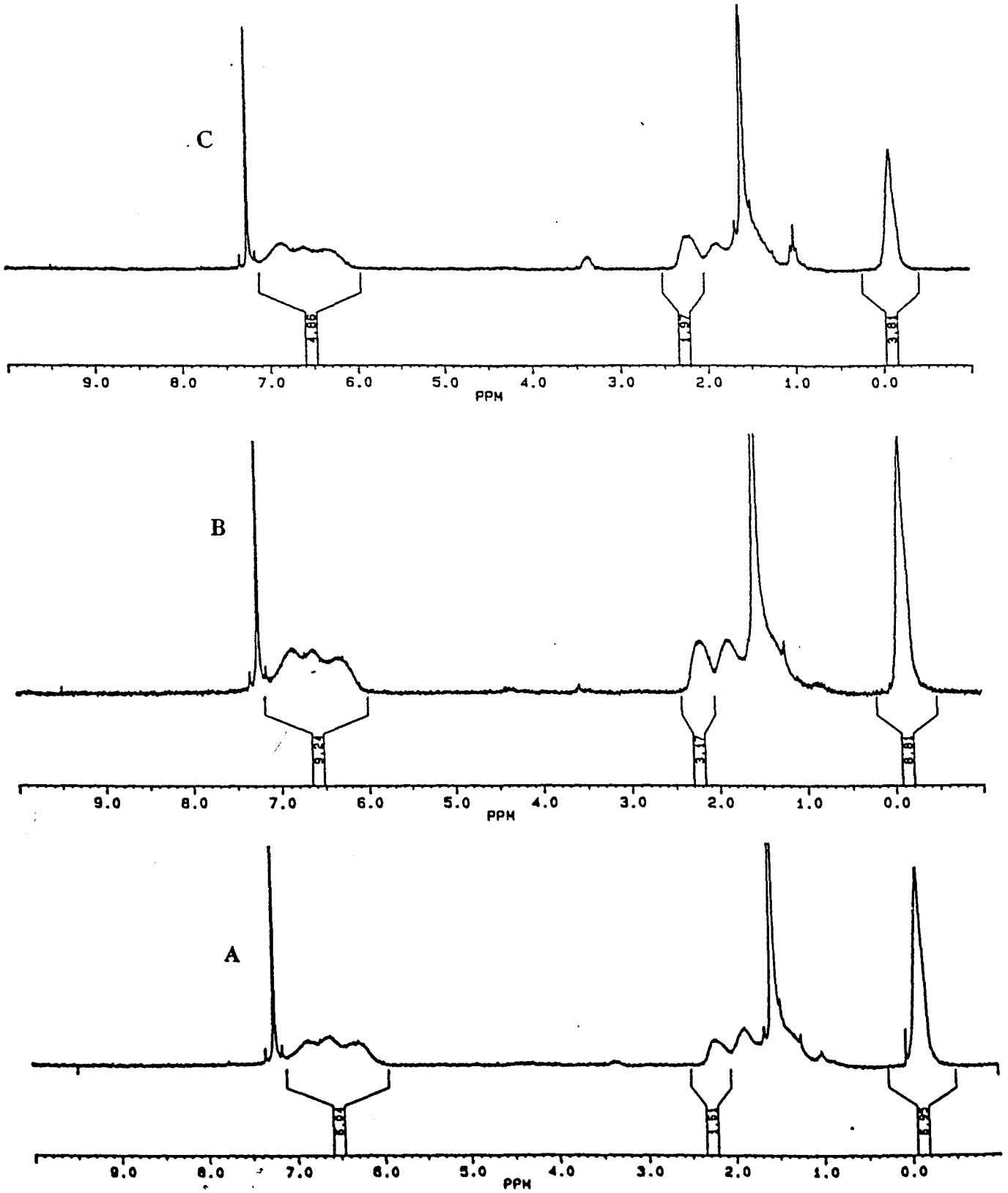

Figure 3.4.3 ^{1}H-NMR spectra of VBTMS oligomer at A) 35.5% B) 46% C) 54% of cleavage by TBAF. Conditions: Oligomer 0.025 Molar, TBAF 0.2 Molar, Solvent THF, Temp. 22 ^{o}C.

Table 3.4.1 Pseudo first-order rate constant data for TBAF cleavage of polymeric substrates.

Substrate	Mn	Linear fit R^2	k x 10^{-3} min^{-1}	
			22 °C	0 °C
VBTMS-Oligomer	3080	0.98	16.4	---
Poly (VBTMS)	13300	0.976	47.0	---
Poly (VBTMS-*co*-sty) VS12	17200	0.99	109.0	---
Poly (VBTMS-*co*-sty) VS11	28000	0.98	95.0	---
Poly (VBTMS-*co*-sty) VS11'	17000	0.974	94.8	---
Poly (VBTMS-*co*-MMA) VM15'	26700	0.99	---	83.0
Poly (VBTMS-*co*-MMA) VM12	26600	0.988	---	78.0
Poly (VBTMS-*co*-MMA) VM11	40800	0.982	286.0	88.0

Conditions: Substrate 0.025 Molar; TBAF 0.2 Molar; Solvent THF; Temp. 22 °C or 0 °C.

On comparing the reaction rates of styrene and MMA copolymers of VBTMS, it can be seen that MMA residue in the copolymer promotes the reaction significantly. Since the reactions on MMA copolymers were very fast at room temperature, the reactions were tried at 0 °C for qualitative comparison. Comparison of the rate constants of MMA copolymers at 0 °C and that of styrenic copolymers at 22 °C shows that MMA can facilitate the fluoride ion cleavage. The rate enhancement from MMA could be due to the increased polarity and the reduced steric hindrance offered by MMA makes an easy access and better solubility for fluoride ion into the MMA copolymer matrix.

Within the copolymer series, there is no significant effect on reaction rate due to an increase in molecular weight (Mn) from 17,000 to 28,000 for VM11' and VM11 and from 26600 to 40800 for VM12 and VM11. This could be due to that the molecular

weights of these copolymers are not widely different that very rapid reaction may not be able to differentiate these copolymers in terms of their reaction rate. With in a particular copolymer series, the effect of composition and molecular weight (Mn) on reaction rate is not significant, as seen from the individual rate constant values for VM15', VM12 and VM11 from MMA copolymer series, and VS12, VS11 and VS11' from styrene coploymer series. The individual copolymers within a copolymer series may be identical for steric factors, coiling tendency, overall copolymer polarity or dielectric constant and their solubility parameters.

3.4.2 Degradation of cross-linked bis(vinylbenzyl)dimethylsilane (BVBDMS) network by TBAF/THF

3.4.2.1 Cleavage of bis(vinylbenzyl)dimethylsilane (BVBDMS) microgel (PP04) by TBAF/THF

The cleavage reaction on the cross-linked system by TBAF/THF was attempted on the microgel (PP04) prepared in 50/50 acetonitrile/toluene mixture. The extent of reaction was estimated by both ^{1}H-NMR and FT-IR spectroscopy. The reactions were carried out under pseudo-first-order condition at 22 °C, keeping the concentration ratio of the silane functionality to fluoride ion as 1:8. The percent cleavage of microgel was estimated based on the relative lowering in the ^{1}H-NMR peak integral of dimethylsilyl group at about 0.0 ppm with respect to that of aromatic peak. The reaction rate was also confirmed from FT-IR data by monitoring the change in the peak integral of the peaks - benzylic-silicon stretch at 1214 cm^{-1} and silicon-carbon stretch of dimethylsilyl group at 1250 cm^{-1}- with respect to an internal standard type peak, 1,3-disubstituted aromatic

ring C-H out of plane bending at 707 cm^{-1}, whose integral is not supposed to change in the reaction. In the reaction with TBAF, the benzylic-silicon stretch and Si-C stretch of dimethylsilyl group are expected to change when either of two benzylic-silicon bonds is cleaved. Figure 3.4.4 shows a schematic representation of a reaction center in the cross-linked network.

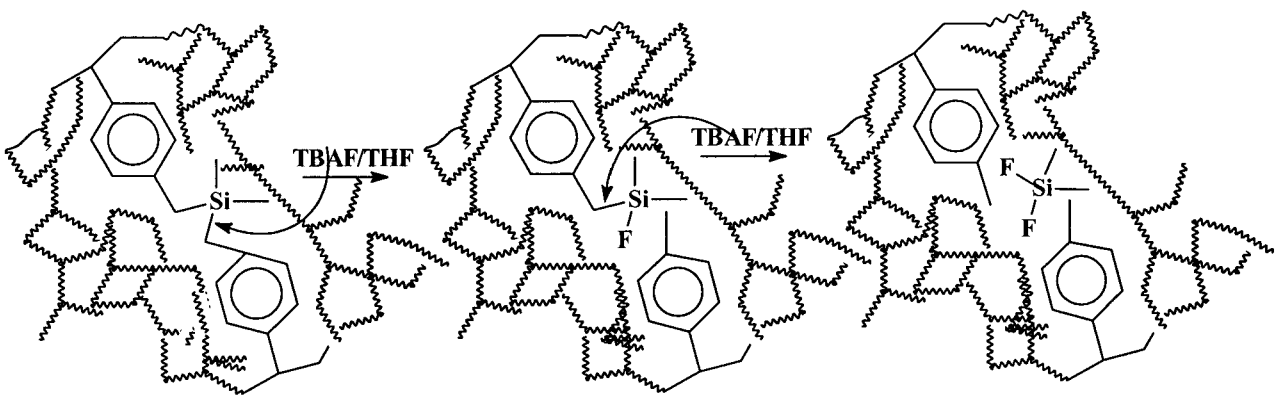

Figure 3.4.4 Schematic representation of reaction site in the cross-linked network of bis(vinylbenzyl)dimethylsilane (BVBDMS) microsphere or microgel.

The kinetic data shown in Table 3.4.2 is likely to be quantitative as the rate constant value obtained from both ^{1}H-NMR and FT-IR based on Si-C stretch at 1250 cm^{-1} of dimethylsilyl group exactly matches with reasonably closer R^2 value of linear fit. However, the rate constant value obtained from FT-IR based on benylic-Si stretch at 1214 cm^{-1} is different with a poor fit of the data.

Table 3.4.2 Kinetic data of TBAF cleavage reaction on bis(vinylbenzyl)dimethylsilane (BVBDMS) microgel (PP04).

Reaction time min.	% Residual dimethylsilyl functionality by ^{1}H-NMR	% Residual dimethyl silyl functionality by FT-IR	% Residual benzylic-silicon functionality by FT-IR
0	100	100	100
5	40.3	33.0	37.3
15	26.0	22.5	30.3
25	17.2	16.1	22.1
35	11.0	10.2	15.8
Pseudo first-order rate constant k min^{-1}	74.1×10^{-3}	73.1×10^{-3}	59.6×10^{-3}
R^2 of linear fit	0.83	0.74	0.68

Conditions: Microgel 0.025 Molar (based on monosilane functionality); TBAF 0.2 Molar; Temp. 22 ^{0}C.

Figure 3.4.5 shows the FT-IR spectra of microgel (PP04) as a function of reaction time. The peaks at 1250 cm^{-1} and 1214 cm^{-1}, shown in Figure 3.4.5, are getting smaller with reaction time, indicating the progress of Si-C bond cleavage. The reaction on the microgel seems to be faster than the corresponding reaction on the linear analogs. Here the cross-links on the microgel do not seem to be a barrier to the access of the small fluoride ion into the microgel matrix, which is completely soluble in the reaction medium THF. At this point, We are not confident to comment about the solubility of the reagent in the microgel matrix to have an enhanced reactivity.

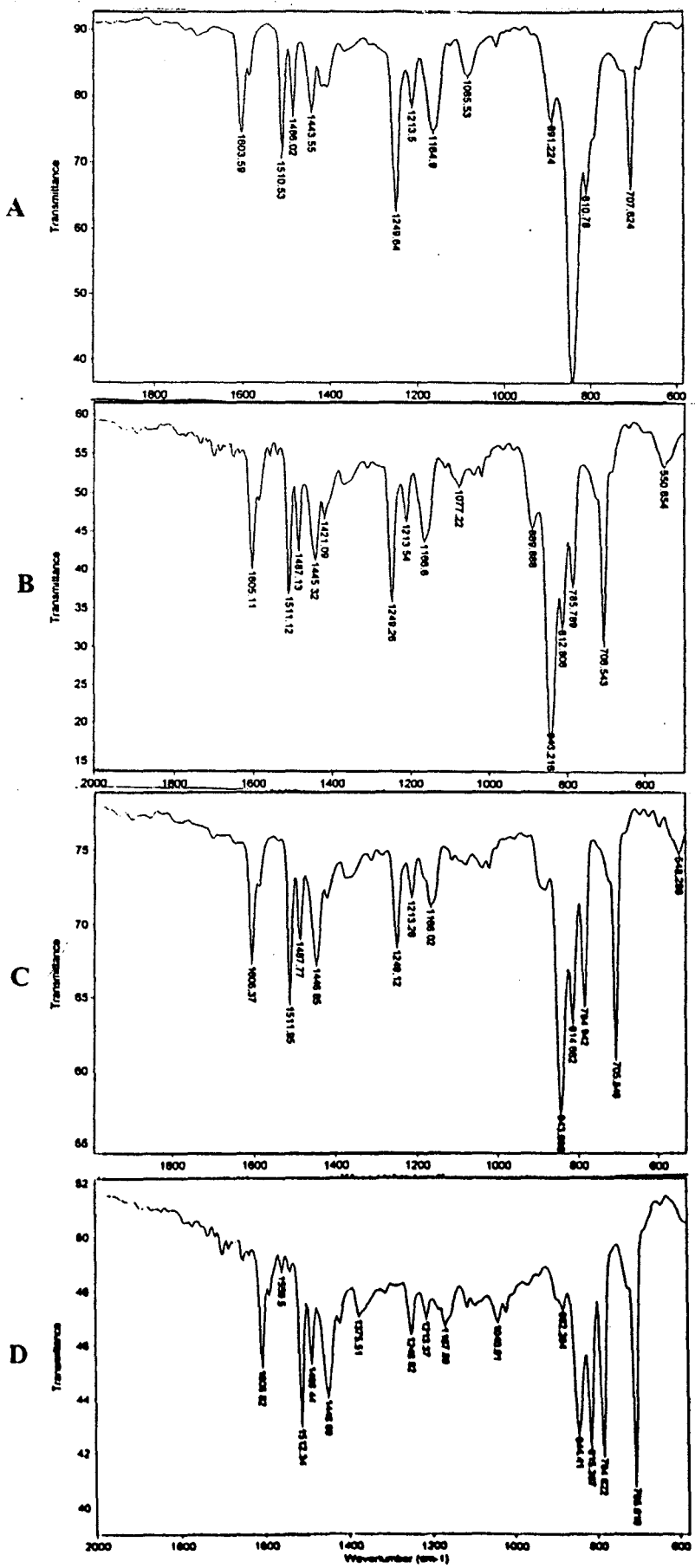

Figure 3.4.5 FT-IR spectra of TBAF cleaved bis(vinylbenzyl)dimethylsilane (BVBDMS) PP04 microgel at reaction time A) 0 min B) 5 min C) 15 min D) 35 min

3.4.2.2 Cleavage of bis(vinylbenzyl)dimethylsilane) microspheres by TBAF/THF

The TBAF promoted cleavage reaction was attempted on cross-linked BVBDMS microspheres (PP01). The reaction rate data was obtained from FT-IR spectra of cleaved particles. The % of cleavage of benzylic-silicon bonds was estimated based on the change in the peak area of benzylic-silicon stretch at 1214 cm^{-1} and silicon-carbon stretch of dimethylsilyl group at 1250 cm^{-1} with respect to an internal standard type peak, 1,3-disubstituted aromatic ring C-H out of plane bending at 707 cm^{-1}). The kinetic data on particle is depicted in Table 3.4.3. The progress of reaction is indicated by the particle size data where the particles are getting progressively smaller as a function of reaction time. As the reaction progresses from the particle surface, cleaving the cross-links, the particle-surface layer starts getting more and more solvated.

Table 3.4.3 Kinetic data of TBAF cleavage reaction on bis(vinylbenzyl)dimethylsilane (BVBDMS) particle (PP01).

Reaction time hrs	% Residual dimethylsilyl functionality by FT-IR	% Residual benzylic-silicon functionality by FT-IR	Particle size μm	CV%
0	100	100	2.289	14.3
6	22.4	25.4	2.239	27.7
15	19.8	21.1	1.810	50.0
26	18.2	17.0	1.576	33.4
36	14.3	13.2	1.392	31.8
112	10.3	-	1.263	49.0
127	8.2	-	1.208	51.5
Pseudo first-order rate constant k hr^{-1}	73.1×10^{-3}	59.6×10^{-3}		
R^2 of linear fit	0.74	0.68		

Conditions: Particle 0.025 Molar (based on monosilane functionality); TBAF 0.2 Molar; Temp. 50 °C.

Mutual merging of particles is an indication of the progressive surface solvation. The particles in the SEM picture (Figure 3.4.7) are merged one another, indicating significant particle-surface reaction.

The pseudo first-order data points derived out of FT-IR data is shown in Figure 3.4.6. The data points based on both the silicon-carbon stretch of dimethylsilyl group and the benzylic-silicon stretch occupy on same type of curves, which are not straight lines. The error in the method stems from the loss of soluble material (cleaved chain fragments containing aromatic residue) from the particles due to the cleavage reaction so that the FT-IR peak of 1,3 disubstituted aromatic ring C-H (out of plane bending at 707 cm^{-1}) would not be an internal type peak as its integral is also susceptible to change with reaction time. Thus, the discrepancy in the data given in the above table is so significant that after 6 hrs of reaction time, about 75-77 % cleavage on particle is shown by FT-IR data with no significant reduction in the particle size. The progression of fluoride etching into the particles needs further study.

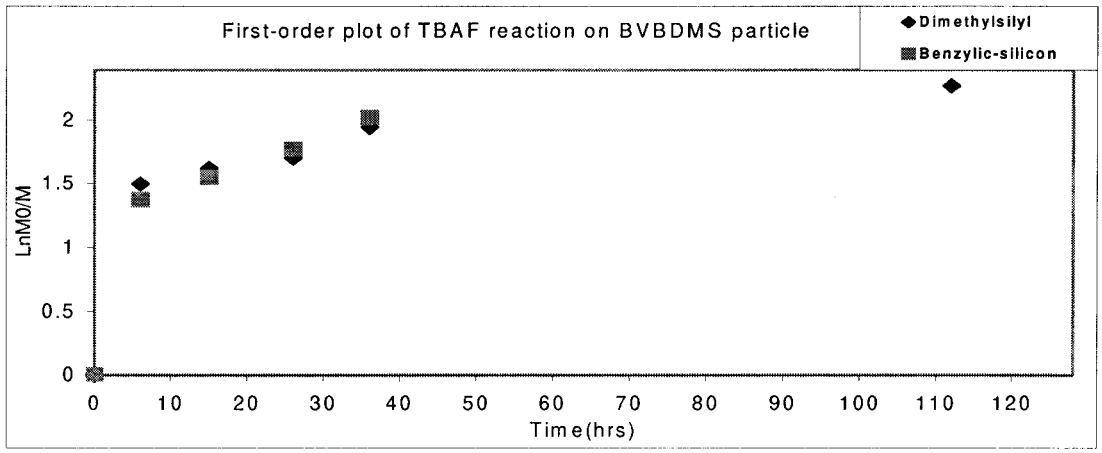

Figure 3.4.6 First-order plot of TBAF reaction on bis(vinylbenzyl)dimethylsilane (BVBDMS) particles (PP01). Particle 0.025 Molar (based on monosilane functionality), TBAF/THF 0.2 Molar; Temp. 50 °C

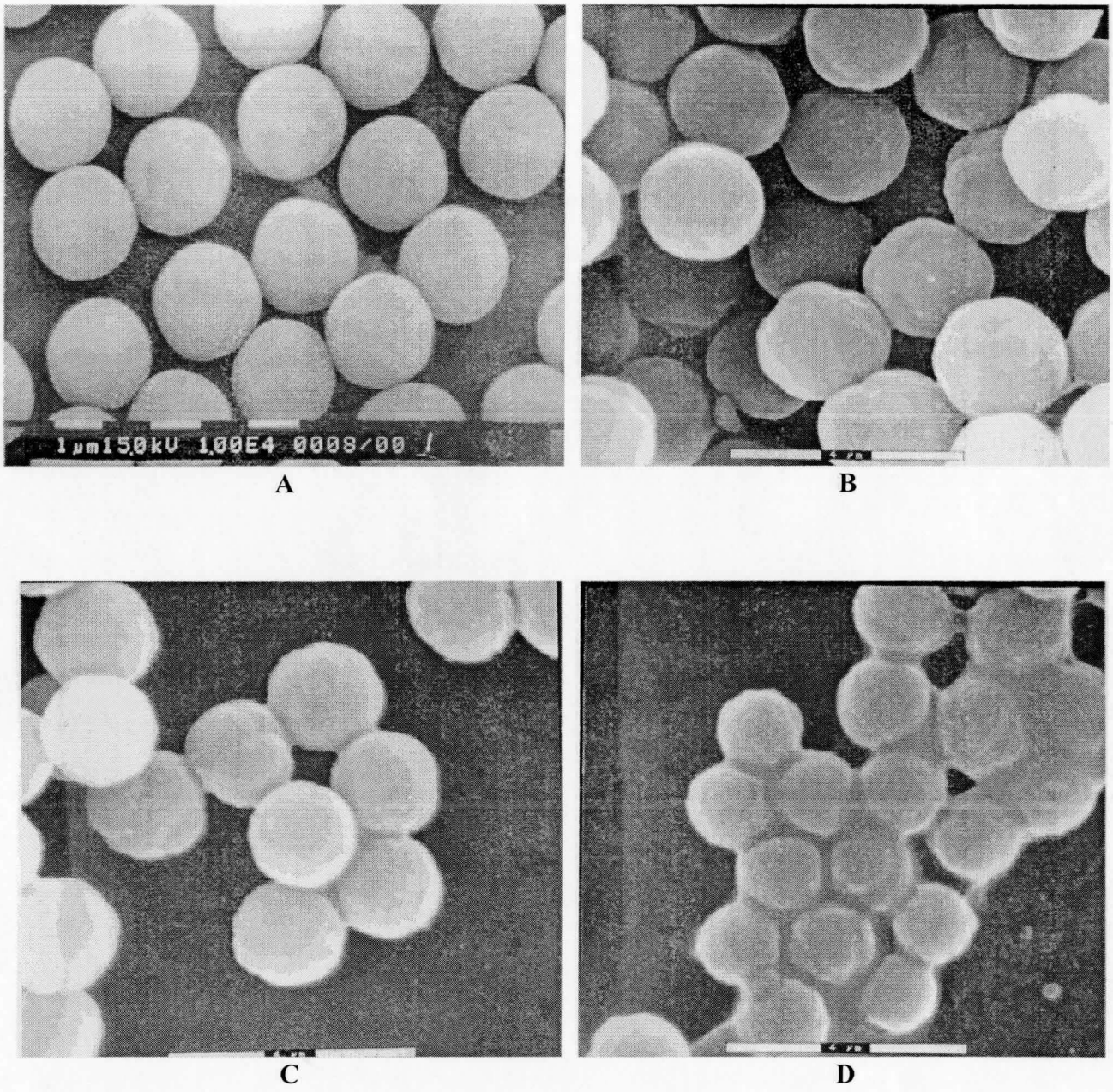

Figure 3.4.7 SEM micrographs of degraded bis(vinylbenzyl)dimethylsilane (BVBDMS) particles by TBAF at reaction time A) 0 hrs B) 6 hrs C) 26 hrs D) 127 hrs. Conditions: TBAF/THF 0.2 Molar; Particles 0.025 Molar (as mono silane functionality); Temp. 22 °C.

3.5 Cleavage of Benzylic-Silicon Bonds by Ceric Ammonium Nitrate / Acetic acid / Benzene (CAN/AcOH/Bz)

The key objective in this part of the thesis is to use ceric ammonium nitrate (CAN) as one-electron oxidant to cleave benzylic-carbon bonds in the substrates. CAN in acetic acid or in aqueous acetic acid has been used as a powerful oxidant[72] for aryl alkanes. Recently, this reagent has been used to selectively oxidize 4-methyl group of poly(4-methylstyrene) to make functional polymers[30]. CAN is only partially soluble ($8x10^{-3}$ mol/l)[73] in acetic acid at room temperature.

Benzene, a good solvent for our polymeric substrates, was used as the co-solvent. The reactions were carried out under nitrogen at different temperatures. Most of the oxidation reactions on the substrates resulted in acetoxymethyl and nitroxymethyl derivatives as the main oxidation products. In few specific cases, chain crosslinking through benzylic radical coupling was observed. The major products of this oxidation are shown in Figure 3.5.1.

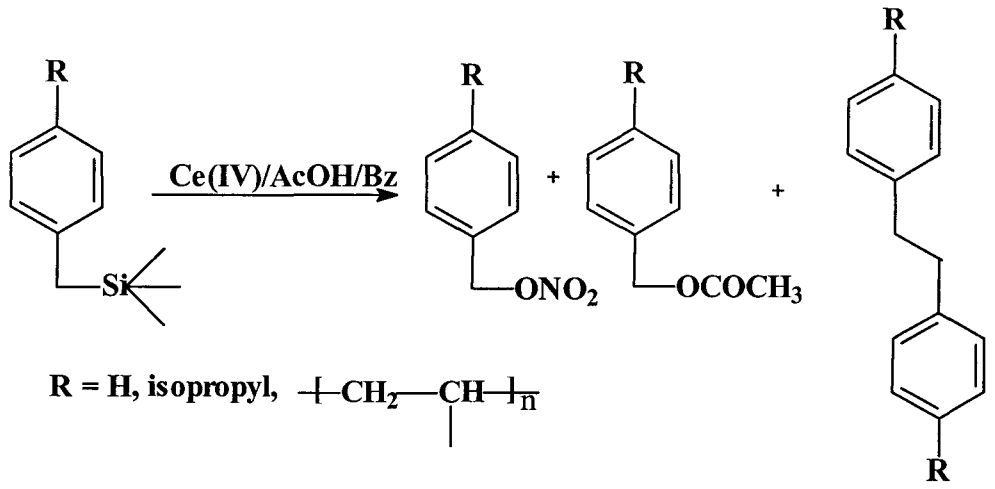

Figure 3.5.1 Major oxidation products of CAN oxidation of a benzylic-silicon substrate.

3.5.1 Oxidation of small molecules and polymer analogs by CAN/AcOH/Bz

Characterization of oxidation: Oxidation yields of the small model molecules including BTMS and ISO-BTMS were measured by GC. The experimental details are given in the experimental section 2.10. The oxidation yields and the corresponding kinetic curves of the polymer analogs are determined from ^{1}H-NMR spectral data of their oxidation products. Figure 3.5.2 shows typical ^{1}H-NMR spectra of the oxidized VBTMS-oligomer, showing all the characteristic peaks. The peaks at 5.3 and 4.9 ppm correspond to the benzylic hydrogens of acetoxy methyl and nitroxy methyl derivatives. The methylene and methine hydrogens of the backbone are at 1.4 and 1.9 ppm, and the aromatic hydrogens at 6.6-6.9 ppm respectively. The peak at 2.03 ppm in the oxidized polymer corresponds to the methyl hydrogens of acetoxy groups formed, and the trimethylsilyl peak is at - 0.03 ppm. A small shoulder at 2.9 ppm is assigned to the ethylene bridge formed by interchain crosslinking. The oxidation yield and the %

cleavage of benzylic-silicon bonds for poly(VBTMS) and poly(VBTMS-*co*-MMA) were calculated from the following equations.

$$\% \text{ acetoxymethyl-} = \frac{\text{Proton integral at 4.9ppm x 4 x100}}{\text{Aromatic integral x 2}} \quad (1)$$

$$\% \text{ nitroxymethyl-} = \frac{\text{Proton integral at 5.3ppm x 4 x100}}{\text{Aromatic integral x 2}} \quad (2)$$

$$\% \text{ cleavage of benzylic-silicon bond} = \frac{\text{Proton integral at -0.03ppm x 4 x100}}{\text{Aromatic integral x 9}} \quad (3)$$

For poly (VBTMS-*co*-Sty), % conversion of trimethylsilyl group can be calculated from the relative change in the peak integral ratio of TMS peak to aromatic peak.

Few of our CAN oxidation reactions involve loss of silicon functionality through cross-linking, though in most cases we observe quantitative conversion to acetoxymethyl and nitroxymethyl products. Hence, the conversion-time plots are drawn in two ways based on a) the relative drop in the ^{1}H-NMR peak integral ratio of trimethylsilyl (TMS) group to aromatic protons (3) (total % cleavage-time plot), b) the relative increase in the ^{1}H-NMR peak integral ratio of combined nitrate and acetate groups formed to aromatic protons [(1)+(2)](total % oxidation-time plot). The rate constants for benzylic-silicon bond cleavage were estimated from the first-order plot of the former data. In order to get some qualitative information about the tendency of the

substrates for cross-linking, a quantity $t_{50}\%$, time required for 50% conversion, was derived from both types of plots. If the reaction strictly obeys first-order kinetics, any difference in $t_{50}\%$ obtained from both plots represents the amount of silicon functionality being lost in crosslinking.

Figures 3.5.3 and 3.5.4 show the total % cleavage-time plots and their corresponding first-order plots for the model small molecules including benzyltrimethylsilane (BTMS) and *p*-isopropylbenzyltrimethylsilane (ISO-BTMS), and the polymer analogs, oligomeric vinylbenzyltrimethylsilane (VBTMS-oligomer) and poly(VBTMS). The % cleavage of benzylic-silicon bonds in the small model molecules was measured by GC, monitoring the disappearance of reactant molecules from the relative change in the ratio of the peak area of reactant to an internal standard, decane. Their $t_{50\%}$ values were estimated from the equations that represent the curves.

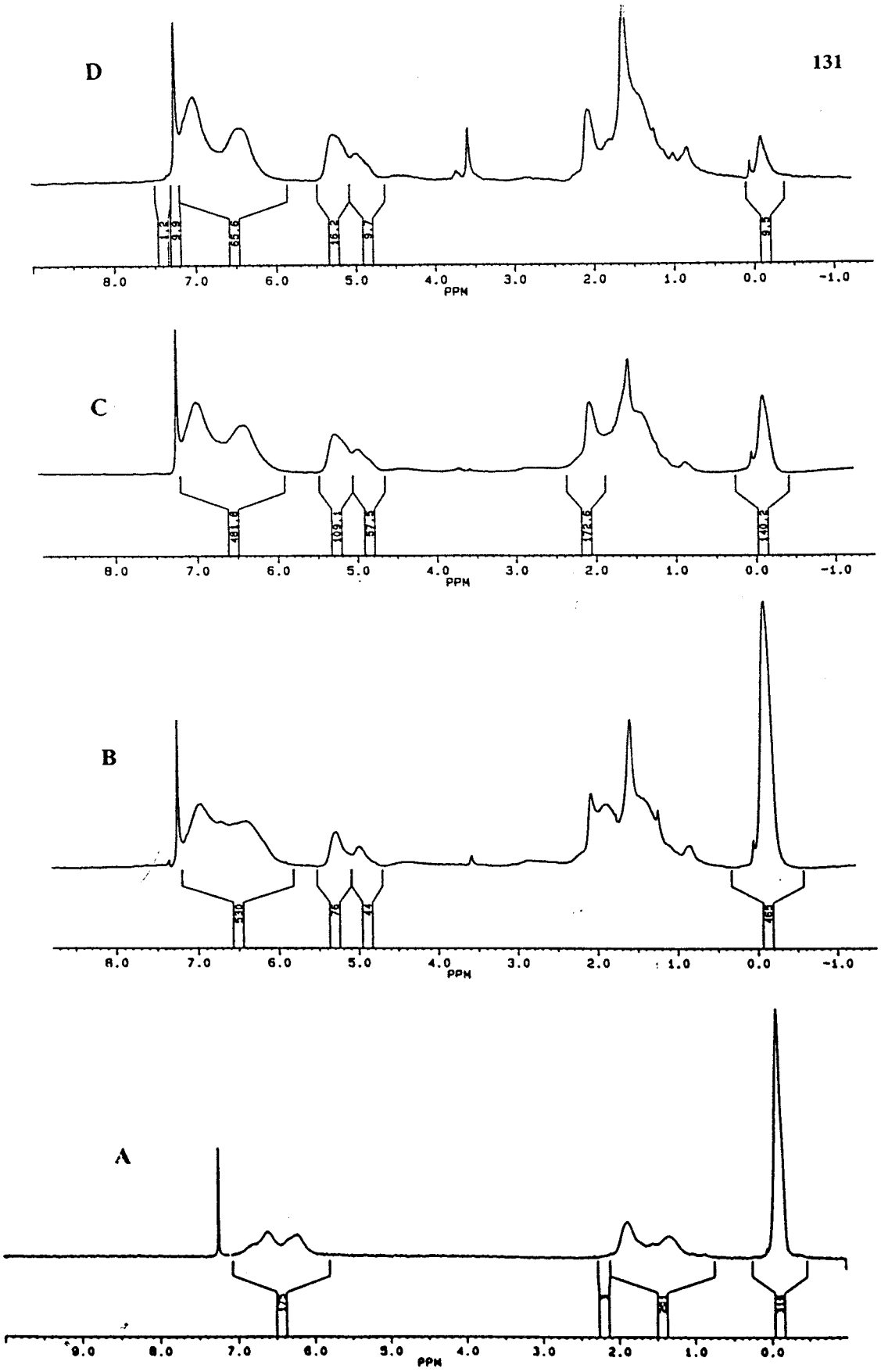

Figure 3.5.2 ^{1}H-NMR spectra of CAN oxidized oligomeric vinyibenzyltrimethylsilane at A) 0% B) 32% C) 53% D) 82% of oxidation. Condition: Oligomer 1 mmol; CAN 3 mmol; Benzene 30 ml; AcOH 30 ml; Temp. 50 °C.

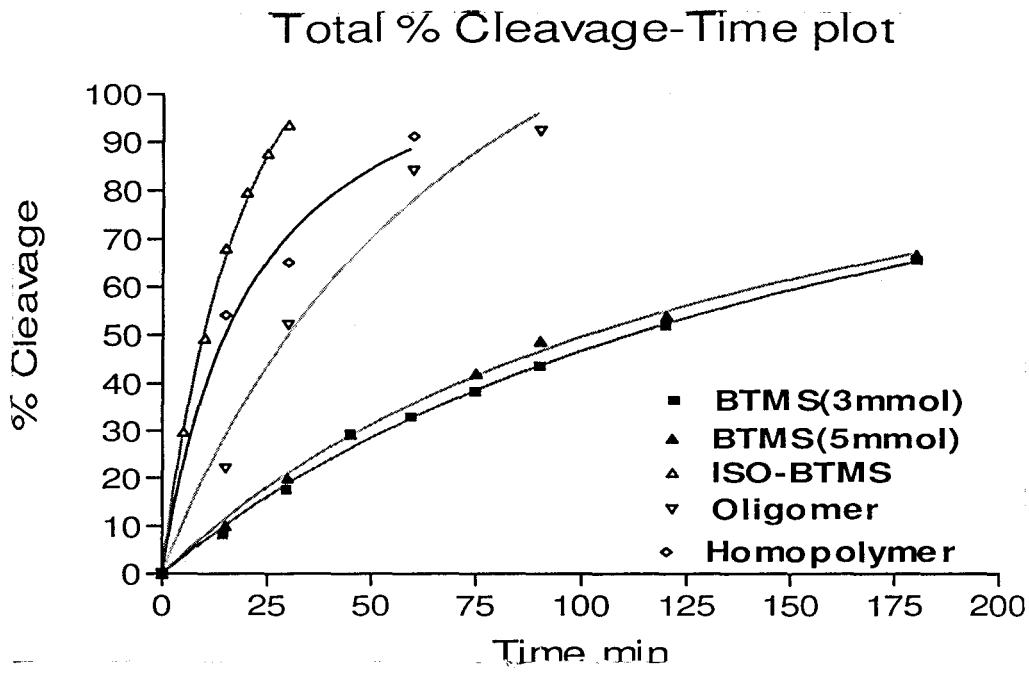

Figure 3.5.3 Total % cleavage-time plot of CAN oxidation reactions of benzyltrimethylsilane BTMS(GC), 4-isopropylbenzyltrimethylsilane-ISO-BTMS(GC), vinylbenzyltrimethylsilane-oligomer(^{1}H-NMR) & poly(*m/p*-vinylbenzyltrimethylsilane-homopolymer(^{1}H-NMR) Conditions: Substrate 1 mmol; CAN 3 mmol; Benzene 30 ml; AcOH 30 ml; Temp. 50 °C.

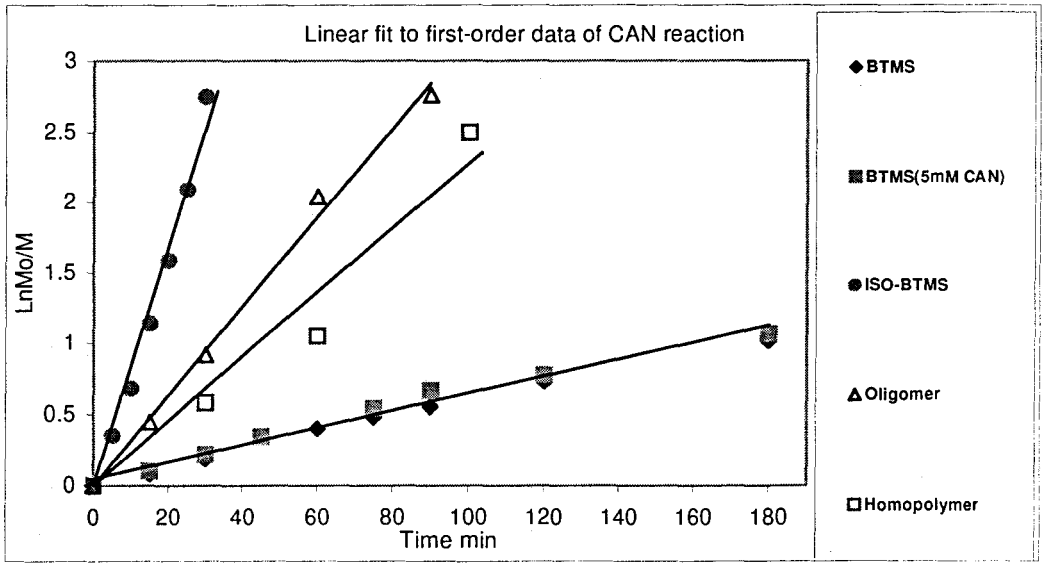

Figure 3.5.4 First-order plot of CAN oxidative cleavage reactions of benzyltrimethylsilane-BTMS(GC), 4-isopropylbenzyltrimethylsilane-ISO-BTMS(GC), vinylbenzyltrimethylsilane-oligomer(^{1}H-NMR), poly(*m/p*-vinylbenzyltrimethylsilane)-homopolymer(^{1}H-NMR), Conditions: Substrate 1 mmol; CAN 3 mmol; Benzene 30 ml; AcOH 30 ml; Temp. 50 °C.

First-order behavior: The pseudo first-order rate constants derived and the experimental observations made on CAN induced oxidation reactions of all the substrates including small model molecules, VBTMS-oligomer and poly(VBTMS), and the copolymers of VBTMS with styrene and MMA are depicted in Table 3.5.1. It is surprising to see all of the substrates obey first-order kinetics up to their complete conversion though the stoichiometric ratio of substrate to CAN is not absolutely in accordance with the first-order condition. Very large excess of reagent in comparison with reactant is considered as the requirement for organic reactions to be in pseudo first-order condition. When the CAN concentration is changed from 3 mmol to 5 mmol, the first-order rate on BTMS is not significantly changed (k = 6.0 and 6.4 x 10^{-3} min^{-1} [entry 1-2 in Table 3.5.1]), keeping the first-order behavior. This must be an indication of the fact that the reaction system containing 1 mmol of substrate and 3 mmol of CAN (stoichiometric ratio 1:3) is most likely to be in a pseudo first-order situation.

Table 3.5.1 Kinetic data of CAN cleavage on different substrates.

Entry	Substrate	temp.°C	Crosslinking/chain degradation tendency	First-order $kmin^{-1}$ / R^2 value of fit	#t_{50}% min
1	BTMS	50	Product recovery and analysis was not done.	6.0×10^{-3} / 0.98	111.6
2	BTMS	50	Product recovery and analysis was not done. (5 mmol of CAN used).	6.4×10^{-3} / 0.97	101.6
3	ISO-BTMS	50	Product recovery and analysis was not done	84.4×10^{-3}/ 0.98	9.7
4	VBTMS-Oligomer	50	No sign of crosslinking and chain degradation as no loss in oxidation yield through crosslinking and no change in molecular weight over entire conversion.	31.6×10^{-3}/ 0.99	29.5 (26.8)
5	VBTMS-homopolymer	50	Significant late crosslinking as about 54% of trimethysilyl (TMS) integral lost during entire conversion. No change Mn until crosslinking starts.	22.8×10^{-3}/ 0.95	14.9 (45.7)
6	VBTMS-homopolymer	50	Severe early crosslinking and the product could not be analysed, being insoluble (powdered CAN used).	----------	---
7	VBTMS-homopolymer	40	No crosslinking up to 19% of oxidation yield followed by severe crosslinking, and the chain degradation from reduction in Mn (1mmol CAN used).	----------	---
8	VBTMS-homopolymer	20	Severe early crosslinking and resulted in insoluble oxidation product.	----------	---
9	VBTMS-homopolymer	65	Severe early crosslinking and chain degradation due to bimodal molecuale weight distribution and a reduction in molecular weight (Mn) from 12500 to 2500.	----------	---
10	VS15	65	No loss in TMS integral for crosslinking and no change in molecular weight over entire conversion	49.2×10^{-3}/ 0.97	10.1 (10.9)
11	VS12	65	No significant loss in TMS integral and no change in molecular weight over entire conversion	46.3×10^{-3}/ 0.99	13.8 (20.1)
12	VM12	65	No significant loss in TMS integral and no change in molecular weight over entire conversion.	88.0×10^{-3}/ 0.99	7.75 (7.74)
13	VM11	65	About 20% loss in TMS integral and no significant change in Mn & Mw over entire conversion.	66.8×10^{-3}/ 0.99	10.3 (17.2)
14	VM11	50	Significant crosslinking as 50% of TMS integral lost in crosslinking during 95% conversion and no sign of chain degradation during early part of reaction.	----------	---
15	VM11	50	Significant crosslinking as 70% of TMS integral lost in crosslinking during 93% of conversion (only 2mmol CAN used).	----------	---
16	VM11	20	No significant oxidation as almost whole TMS integral lost in crosslinking, forming insoluble product.	----------	---
17	VM11	82	Less than 10% of TMS integral lost in crosslinking, without any change in Mn over entire conversion	----------	8.2

Conditions: Substrate 1mmol; CAN 3mmol; Benzene 30ml; AcOH 30ml. (# t_{50}% derived from % cleavage) (t_{50}% in the parenthesis is derived from %total oxidation-time plot of reaction)

Substituent effect: The rate enhancement by more than an order (14 times) for ISO-BTMS compared to BTMS (entry 1-3 in Table 3.5.1) can be explained in terms of the higher electron releasing effect of 4-isopropyl group than a hydrogen that lowers the oxidation potential of ISO-BTMS much more effectively. This observation is in accordance with the results of Baciocchi[31] who proposed an electron transfer mechanism operating through radical cation in the rate-determining step. The kinetic data[31] on ring substituted benzyltrimethylsilanes clearly shows that the reaction rate is strongly influenced by the electronic nature of the ring substituent. The electron donating groups were found to accelerate the reaction with very high negative value (-5.4) for the Hammett reaction constant ρ. High negative ρ value indicates every possibility of the electron transfer mechanism[31]. The plot of rate constant against the oxidation potential of different polymethylbenzenes along with benzyltrimethylsilane (BTMS) was linear with a negative slope. Baciocchi also reported a lower oxidation potential of 1.84v for BTMS compared to toluene of 2.25v and detected no reaction on toluene under the same experimental conditions where BTMS reacted with a much faster rate. This lower oxidation potential resulted in 14 times increase in the first-order rate constant of ISO-BTMS in comparison with BTMS in our CAN promoted oxidation reactions.

Polymer effect: Though 4-isopropylbenzyltrimethylsilane (ISO-BTMS) is the true analogue of poly(VBTMS), their rate constant values differ significantly with substantial rate reduction in polymeric analogs. If the rate-controlling step of the reaction (see reaction mechanism section 3.5.2) is the formation of radical cation, steric

strain experienced by the aromatic ring from the polymer backbone may slow the radical cation formation. This type of situation is not expected in ISO-BTMS.

Dimerization/Aromatic ring oxidation: During the rate study of CAN reactions on the small model molecules (BTMS and ISO-BTMS), the product recovery and their analysis was not done as our particular interest was to measure the rate at which benzylic-silicon bonds are cleaved, and mechanistically, the dimerization/aromatic ring oxidation reactions are found not feasible (see section 3.5.2 Reaction mechanism). Hence, each GC run was not extended to longer residence time to see reaction by-products, if any.

Cross-linking: The cross-linking tendency in the polymer substrates can be qualitatively figured out from the variation in the t_{50}% values derived from total % oxidation-time and % cleavage-time plots (definition and the explanation of t_{50}% values, total % oxidation-time plot, and total % cleavage-time plots are given in section 3.5.1). Figure 3.5.5 shows the two types of plots for all the polymer analogs. Except for the homopolymer, the data points in Figure 3.5.5 were obtained from NMR spectra of oxidation products that were completely soluble in solvents including THF and chloroform. For the CAN reaction of the homopolymer, being insoluble due to crosslinking, the NMR spectrum was taken on dueraterated chloroform-swelled sample of the oxidized homopolymer. Any variation in the $t_{50\%}$ values derived from both kinetic plots indicates the crosslinking and the consequent loss of silicon functionality.

The $t_{50\%}$ values derived from both types of plots for VBTMS-oligomer (29.5 and 26.8 min - entry 4 in Table 3.5.1), are not much different. This small difference in the

t_{50}% values may be attributed to the small shoulder peak appeared in NMR spectra (Figure 3.5.2) at 2.9 ppm corresponding to the ethylene bridge formed by crosslinking.

Very high tendency for crosslinking was observed in the CAN reaction of the VBTMS-homopolymer. The homopolymer was found cross-linked at all attempted reaction temperatures ranging from 20 °C to 65 °C (entry 4-9 in Table 3.5.1). The isolated oxidation products from the reactions carried out at other lower temperatures including 0 °C were also found highly cross-linked and insoluble in most of the solvents. However, we were able to take the NMR spectra of the chloroform swollen crosslinked oxidation product of the reactions carried out at 50 and 65 °C. Figure 3.5.6 is the critical evidence for the crosslinking reaction occurring through benzylic radical coupling to form ethylenic bridge. The spectra of poly(VBTMS) oxidized at 65 °C in Figure 3.5.6 shows a broad peak at 2.9 ppm corresponds to the ethylene bridge, similar to a sharp singlet peak at the same chemical shift observed in the ^{1}H-NMR spectrum of bis(vinylphenyl)ethane[47] (BVPE). The first product-fraction isolated after 10 min of CAN reaction on poly(VBTMS) (Mn=13200) at 65 °C, after being swelled and extracted with THF, showed a bimodal distribution of molecular weight corresponding to Mn of 5600, and a small shoulder peak. The reduction in the molecular weight may be either from backbone degradation originated through backbone methine hydrogen (see section 3.5.2 Reaction mechanism). The acetoxymethyl and nitroxymethyl groups formed from the backbone oxidation can not be separately detected in the proton NMR spectrum as their chemical shifts[30] are identical to those of acetoxymethyl and nitroxymethyl groups attached to an aromatic ring at the *para* position.

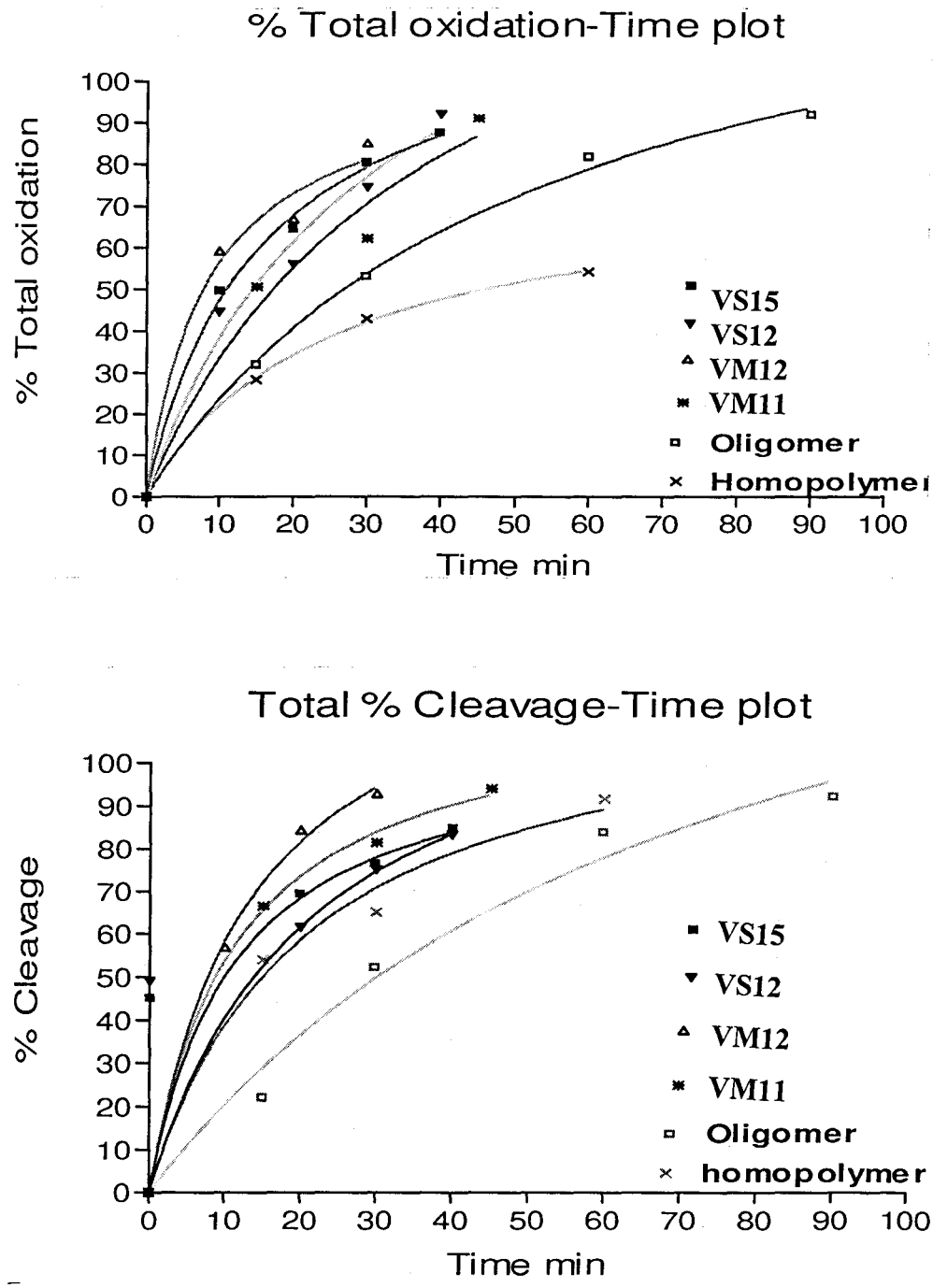

Figure 3.5.5 Total oxidation-time (Top) and % cleavage-time (Bottom) plots of CAN reactions of polymeric substrates (^{1}H-NMR). Conditions: Substrate 1 mmol; CAN 3 mmol; Benzene 30 ml; AcOH 30 ml; Temp. 65 °C. (For oligomer and homopolymer Temp.50 °C).

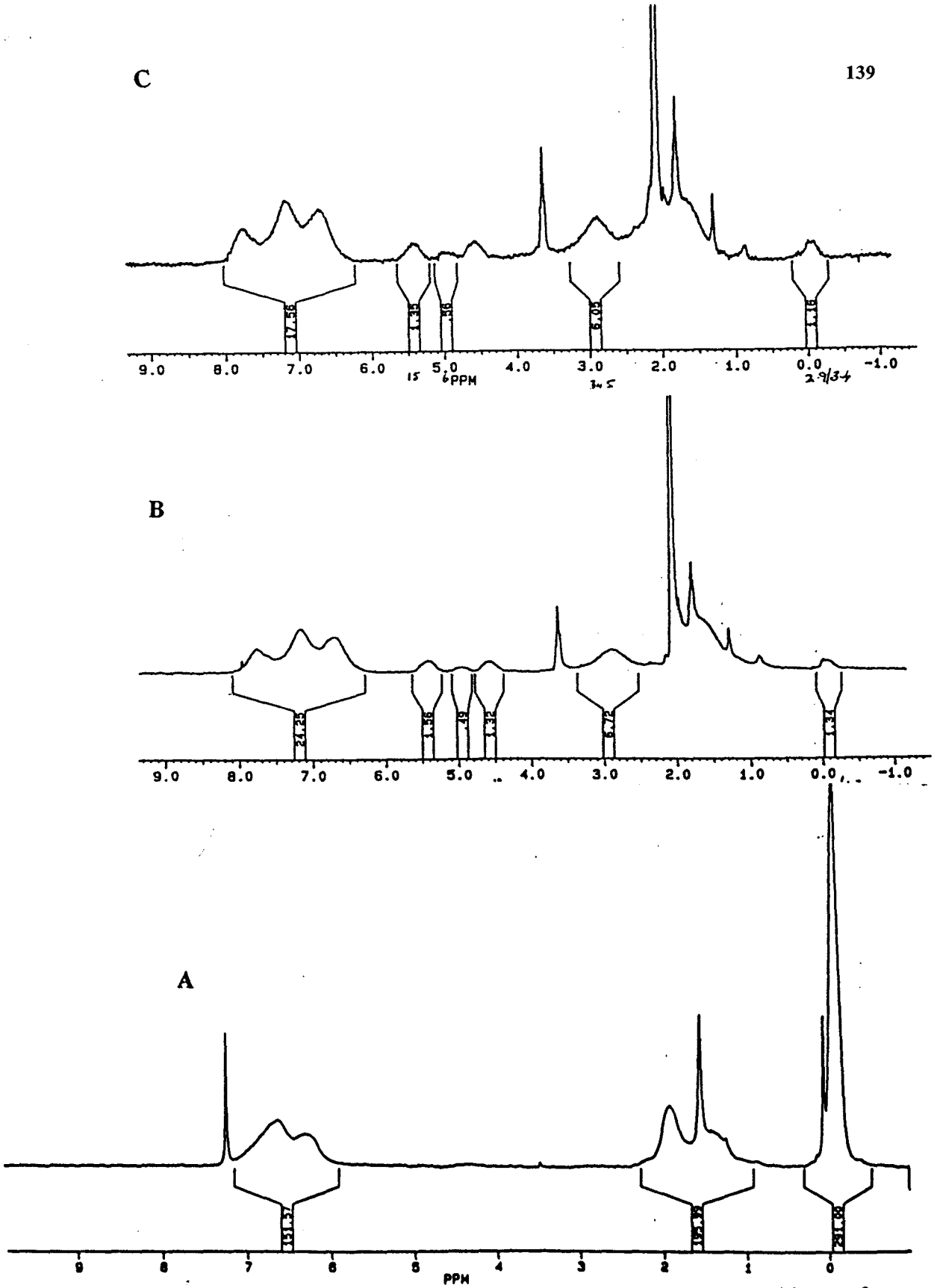

Figure 3.5.6 ^{1}H-NMR spectra of oxidized Poly(VBTMS) as an evidence for crosslinking. A) Poly(VBTMS) Mn = 13200 B) 40 min CAN oxidized Poly(VBTMS) Mn = 2500 C) 50 min CAN oxidized Poly(VBTMS) Mn = 2360 Conditions: Poly(VBTMS) 1 mmol; CAN 3 mmol; Benzene 30 ml; AcOH 30 ml; Temp. 65 °C.

The homopolymer on oxidation at 50 °C shows widely different t_{50}% values of 14.9 and 45.7 min derived from total % cleavage-time and total % oxidation-time plots respectively (entry 5 in Table 3.5.1). This means that the homopolymer takes only 14.9 min for its 50% of silicon functionality to get converted or reacted whereas it needs 45.7 min to achieve 50% of acetoxymethyl and nitroxymethyl functionality in the oxidized product. Thus, the difference in t_{50}% corresponds to the loss of trimethylsilyl functionality in chain to chain crosslinking reactions.

The crosslinking behavior of styrene and MMA copolymers of VBTMS is shown in Figure 3.5.5, which is only applicable to a substrate to CAN ratio 1:3 and the reaction temperature 65 °C. Regarding the oxidized samples used for taking NMR spectra, they were obtained by precipitating the aliquots of the reaction mixture into the nonsolvent methanol. These samples were completely soluble in THF and chloroform and the corresponding NMR spectra were quite clean with only peaks of the substrate and the oxidized functionalities (nitrate and acetate). Since the peak corresponding to ethylene bridge, formed by crosslinking, at 2.9 ppm is not visible in the NMR spectra of oxidized VBTMS-styrene copolymers, it is not likely to expect any significant crosslinking. Unfortunately, for oxidized VBTMS-MMA copolymers, the 2.9 ppm area in the NMR spectra is occupied by MMA peaks so that ethylene bridge formation is not identified from their NMR spectra.

As shown by the in entries 10 and 11 in Table 3.5.1, the cross-linking tendency of styrene copolymers in CAN oxidation increases with decrease in comonomer content (with increase in trimethylsilyl functionality) as evidenced from the increasing variation

in the t_{50}% values derived from both types of kinetic plots. The styrene copolymer VS15 of lowest VBTMS content (13.5%) shows similar values of 10.1 and 10.9 min for both t_{50}% values (entry 10 in Table 3.5.1). This is an indication of the quantitative conversion of trimethylsilyl functionality into acetoxymethyl and nitroxymethyl groups without any significant interchain crosslinking. Also, the styrene copolymers do not suffer any reduction in molecular weight through oxidation reaction. This is an indication of absence of any significant backbone degradation.

The MMA copolymers show a significant tendency to crosslink at lower reaction temperatures and the tendency increases with increase in the VBTMS content of the copolymer. This is evidenced from a significant difference in t_{50}% values 10.3 and 17.2 min for VM11 (entry 13 in Table 3.5.1). The reduced crosslinking tendency with decrease in VBTMS content exhibited by both styrene and MMA copolymers can be explained by the progressive dilution effect of comonomer on the local benzylic radical concentration. MMA[30] can significantly protect the copolymer chain from chain degradation by introducing steric hindrance from backbone methyl groups to the chain CH sites (see section Reaction mechanism 3.5.2), as shown in Structure 6.

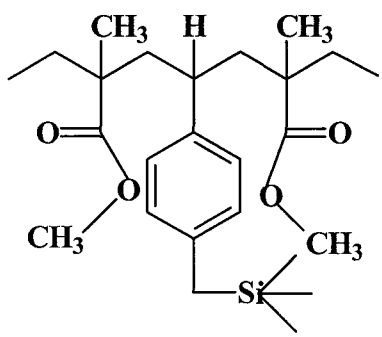

6

The first-order plots for both styrene and MMA copolymers of VBTMS are shown in Figure 3.5.7. The tendency to show a marginal increase in rate constant by MMA-copolymers compared to styrene-copolymers (entry 10-13 in Table 3.5.1) may be due to comparatively higher steric hindrance from the bulky styrene ring so that the rate-determining formation of the radical cation would be retarded.

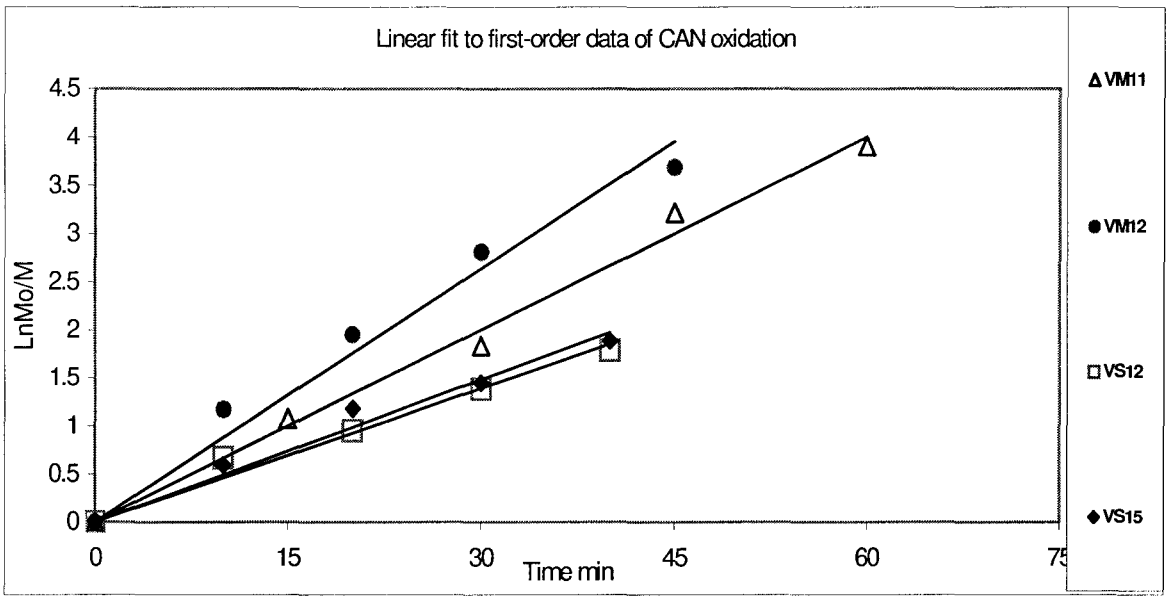

Figure 3.5.7 First-order kinetic behavior of styrene and MMA copolymers of VBTMS (^{1}H-NMR) towards CAN oxidation. Conditions: Substrate 1 mmol; CAN 3 mmol; Benzene 30 ml; AcOH 30 ml; Temp.65 °C.

CAN crystal surface area: The powdered CAN crystals compared to thenormal CAN reagent sample were found to accelerate both oxidation and the cross-linking reactions as observed from the rapid disappearance of Ce(IV). Since the reaction-products were severely cross-linked, and not even swellable in solvents, their analysis by NMR for oxidation yield was found difficult. Since both the dissolved and the solid CAN undergo reaction, the reaction will be faster with powdered CAN of large surface area available as reaction sites. This faster reaction can produce very high instantaneous

radical concentration that results in severe cross-linking reactions (entry 6 of Table 3.5.1).

3.5.2 Oxidation mechanism

CAN/AcOH/N_2 oxidation of benzytrimethylsilane (BTMS) in 2:1 CAN to BTMS molar ratio at 60 °C has been reported by Baciocchi[31] *et al.*, getting benzyl nitrate and benzyl acetate (1:3) in 95% product-yield as the only oxidation products. When the reaction was under pseudo first-order condition with very large excess of BTMS substrate, the kinetic plot was linear up to only 70% of conversion. Showing a varying reaction-order is typical for CAN-oxidation reactions of polyalkylbenzenes[72]. Baciocchi[72] mentioned that CAN oxidation would not follow simple first-order kinetics as the apparent order in cerium(IV) is larger than one due to the involvement of dimeric or polymeric forms of cerium. Baciocchi[72] found the order in Ce(IV) increased as a function of its concentration. Only soluble CAN in acetic acid can undergo ligand exchange reaction between two of its nitrate ligands and acetate anion from the solvent. Insoluble CAN is also reactive in acetic acid through solid state reaction, leading to higher nitrate/acetate product ratio[73]. In addition, he found that two moles of CAN would be needed for one mole of the substrate to be completely oxidized.

The typical reaction mechanism[31] of CAN-oxidation under inert atmosphere in acetic acid involves an electron transfer from the aromatic ring to Ce(IV) to form a radical cation, which breaks off trimethylsilyl cation to form benzyl radical. In an another step, this radical is converted to benzyl cation through one more electron transfer to cerium. The reaction of benzyl cation with nitrate ligands from CAN or with acetate anion from

acetic acid makes the oxidation products, the benzyl acetate and the benzyl nitrate. Baciocchi[31] proposed an electron transfer mechanism, forming radical cation in the rate-determining step. Typical reaction mechanism is shown in Figure 3.5.8.

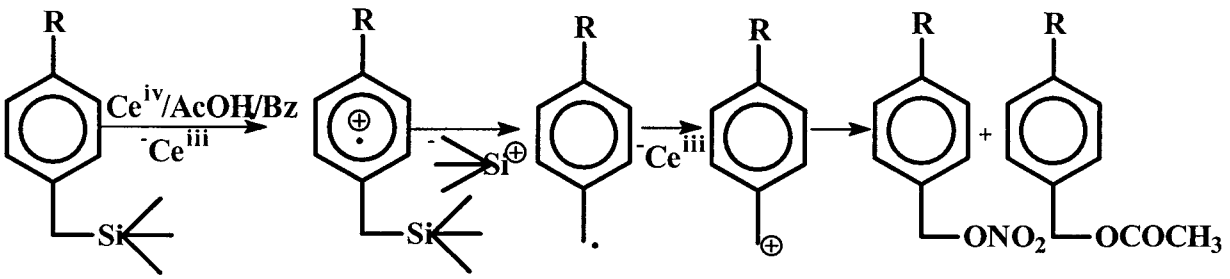

Figure 3.5.8 Typical mechanism of CAN oxidation of a benzylsilyl substrate

Consistent with the observation made by Baciocchi[73,75] and Norman[74] on CAN promoted oxidation of alkylbenzenes, there are some possibilities from our CAN/acetic acid/benzene promoted reactions of benzylsilyl substrates to form biaryls as the ring substitution products, diarylmethanes as the side chain substitution products, aryl acetates and nitrates as the ring oxidation products, and 1,2-diarylethanes as the products of radical coupling. All possibilities, including the functionalization of benzylic carbon[29] and the substituent oxidation[30], are shown in Figure 3.5.9.

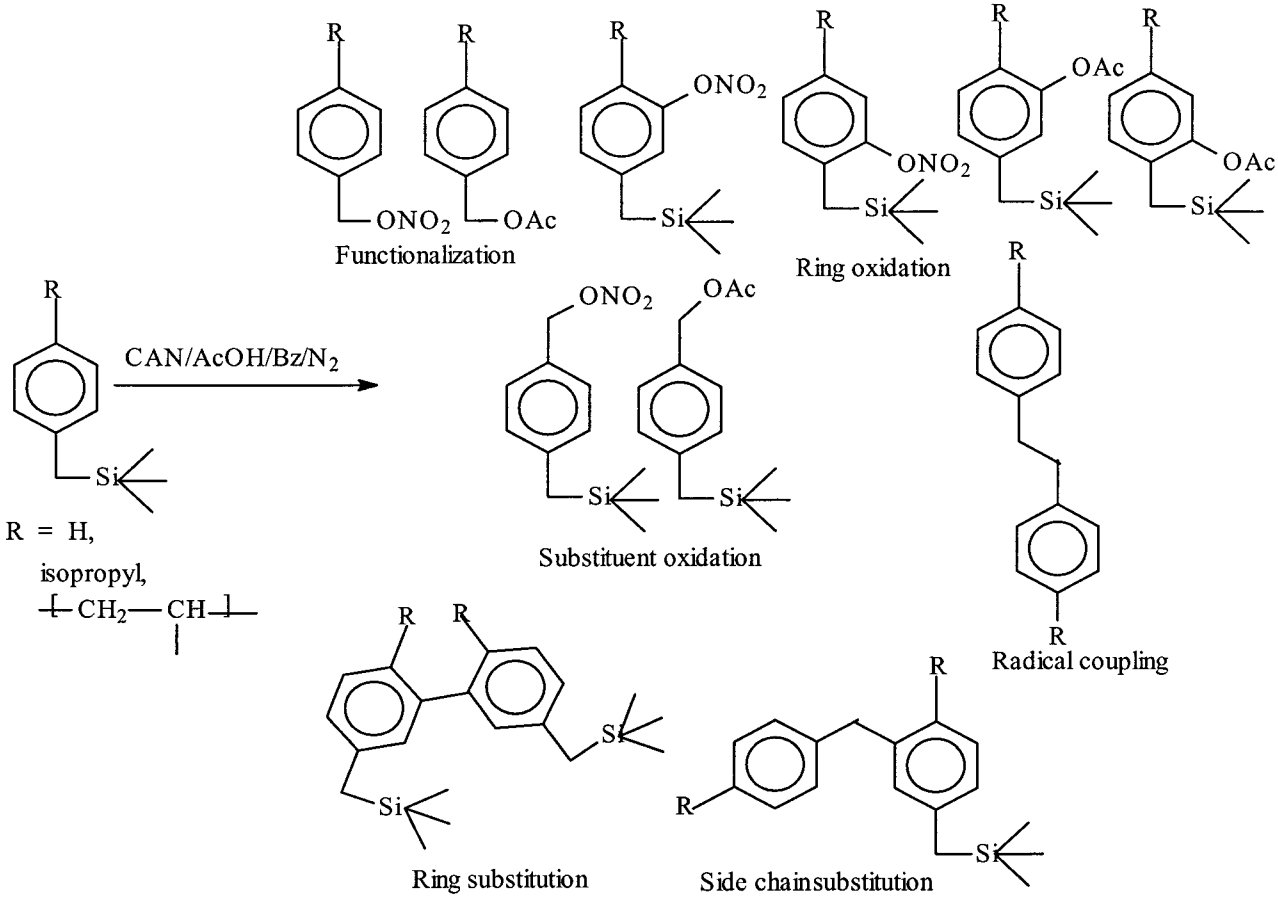

Figure 3.5.9 Possible CAN oxidation products of a benzylsilyl substrate.

Resistance to ring / side-chain substitution: Norman[74] *et al.* reported the formation of biaryls and diarylmethanes as the major oxidation products, and benzylic trifluoroacetates as the minor products in the cerium trifluoroacetate in trifluoroacetic acid promoted oxidation of methylbenzenes including toluene, *p*-xylene, mesitylene and durene The biaryls are formed by the attack of aromatic radical cations on the methylbenzenes followed by the proton loss. The diarylmethanes are formed by the

reaction of benzylic cation with the methylbenzene followed by the proton loss. The % of diarylmethanes formed in their reaction follows the order toluene < *p*-xylene < mesitylene < durene, which is in the order of decreasing oxidation potential or increasing nucleophilic character. However, the formation of these aromatic ring substitution products and the side-chain substitution products are not reported[73] for CAN / acetic acid promoted oxidations of alkylbenzenes. This is attributed to the major basicity and nucleophilicity[74] of acetic acid compared to trifluoroacetic acid so that CAN/acetic acid system results in only benzylic acetates/nitrates, not in diarylmethanes. This rules out the possibility of the diarylmethane formation from our oxidation reaction of BTMS and ISO-BTMS. Similarly, the biaryl formation through the reaction between radical cation and the substrate molecule in our CAN/acetic acid oxidations is also ruled out as the radical cation formed rapidly looses the trimethylsilyl cation (about 100 times faster than corresponding hydrogen) to form benzylic radical.

Resistance to radical coupling: Norman[74] *et al.* clearly mentioned that 1,2-diarylethanes, as the product of dimerization of benzylic radical, are not formed in the CAN promoted oxidation reactions of alkylbenzens as the arylmethyl radicals arising from the radical cations by deprotonation would be expected readily to undergo one-electron oxidation with cerium to carbocation so that radical coupling reactions are prevented. This supports our expectation that no dimer is formed in CAN/AcOH/Bz reactions of BTMS and ISO-BTMS. However, in the polymeric substrates, the radical coupling reactions are quite feasible due to higher local concentation of radicals compared to that with small model molecules. The radical coupling reactions in

polymeric substrates are evidenced by the detected ethylene bridge at 2.9 ppm in their ^{1}H-NMR spectra of oxidation products.

Resistance to nuclear or ring oxidation: Nuclear oxidation has been reported by several authers in CAN/acetic acid promoted oxidation of mesitylene[73], Cobalt(III)acetate/acetic acid/LiCl oxidation of *m*- or *p*-methoxytoluene[76], and Cobalt(III)acetate/acetic acid/KOAc oxidation of 1- or 2-methyl-naphthalene[76]. Nuclear oxidation occures when the nucleophile (X^-) attacks the ring of the radical cation followed by the one-electron oxidation to carbocation that undergoes deprotonation to form products functionalized in the ring, as shown in Figure 3.5.10

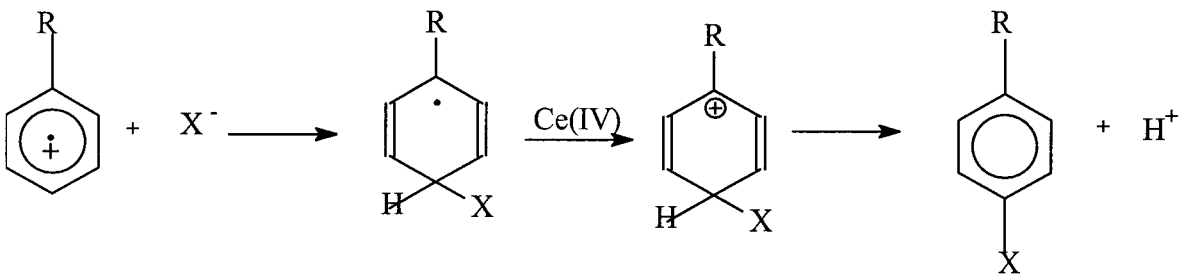

Figure 3.5.10 Ring oxidation mechanism[76].

The relative extent of side chain oxidation to ring oxidation is related to the degree of positive charge adjacent to the side chain (alkyl group) relative to that in other positions of the radical cation. Thus, in 1-methyl-naphthalene[76] and *p*-methoxytoluene, relative extent of positive charge adjacent to the methyl groups in their radical cations are greater than that in 2-methyl-naphthalene[76] and *m*-methoxytoluene respectively. This resulted in no nuclear oxidation products in the former pair, and 12% and 38% of ring oxidation products in the latter pair in addition to their side chain (methyl) oxidation products. Consistent with the above reasoning, mesitylene[72] with CAN/acetic acid gave

25% ring acetoxylated product (2,4,6-trimethylphenyl acetate), and *p*-isopropyltoluene (*p*-cymene) under the same condition[75] gave no nuclear oxidation products.

Baciocchi's observation[29] of formation of only benzyl acetate and benzyl nitrate (3:1 molar ratio) in 95% product yield from CAN/AcOH/N_2 promoted oxidation of benzyltrimethylsilane (BTMS) at 60 °C strongly supports the fact that no ring oxidized, ring substituted or side-chain substituted products are formed from our CAN/AcOH/Bz oxidations of BTMS and 4-isopropylbenzyltrimethylsilane (ISO-BTMS). In addition. the model molecules, BTMS and ISO-BTMS, do not seem to undergo ring acetoxylation reactions.

Reaction stoichiometry: In order to test the stoichiometry of our CAN-oxidation reaction, poly(VBTMS) was oxidized under different polymer to CAN molar ratio at 80 °C. This particular reaction temperature (80 °C) was selected, based on the experiments done at different temperatures, only to avoid the cross-linking reactions. Complete consumption of CAN in the reaction was detected from the complete color change of both the reaction solution and the undissolved cerium from orange Ce(IV) to yellow Ce(III), and the results are entered in Table 3.5.2

Table 3.5.2 Stoichiometry of CAN oxidation reaction on poly(VBTMS)(^{1}H-NMR).

Poly(VBTMS) : CAN mmol	Oxidation yield %	Nitrate/Acetate ratio	Residual TMS %	Appearance
1:1	33	1.76	60	Complete color change to yellow Ce(III)
1:2	94	1.96	0.5	Complete color change to yellow Ce(III)
1:2.5	94	2.1	0.0	Some left over orange Ce(IV)

Conditions: AcOH 30 ml; Benzene 30 ml; Reaction time 1 hr; Temp. 80 °C.

Consistent with Bacciochi's[73] observation, the stoichiometry of our CAN oxidation reaction on poly(VBTMS) is 1:2. The left over cerium(IV) in the third entry of Table 3.5.2 indicates that cerium(IV) in excess of stoichiometric amount is not being consumed for any other side reactions like possible backbone oxidation in the case of polymers or substituent oxidation in the case of ISO-BTMS.

The nitrate to acetate ratio in the CAN oxidation of poly(VBTMS) is found progressively increased with increase in CAN concentration. This trend is attributed to the increasing amount of undissolved CAN in the reaction system with increase in its concentration. It is expected that only soluble CAN[73] can undergo exchange of its two labile nitrate ions with the solvent molecules (acetic acid) and the dispersed CAN in solution predominantly leads to the formation of nitrate in the oxidation products.

Resistance to polymer backbone cleavage and substituent oxidation: Based on the observation made by Baciocchi on CAN oxidation reactions of *p*-cymene[75] and substituted *p*-xylenes,[77] and Ferrari[32] on cobalt(III) diacetate bromide-complex oxidation of 4-methyl group of poly(4-methylstyrene), there is a possibility for substituent oxidation of the model molecule, 4-isopropylbenzyltrimethylsilane (ISO-BTMS), and analogous backbone cleavage for all of the polymeric substrates, as shown in Figure 3.5.10. The electron transer from the ring to cerium(IV) forms the radical cation which looses a proton from chain methine carbon instead of trimethylsilyl cation from benzylic position to form methine radical. The methine radical can transfer another electron to cerium(IV), with simultaneous β-scission, to form polymer chain with end groups containing alkene and a tertiary carbocation, which can form four

addition products as shown in the figure 3.5.11. In the similar way, 4-isopropylbenzyltrimethylsilane (ISO-BTMS) can end up into substituent (isopropyl group) oxidized products.

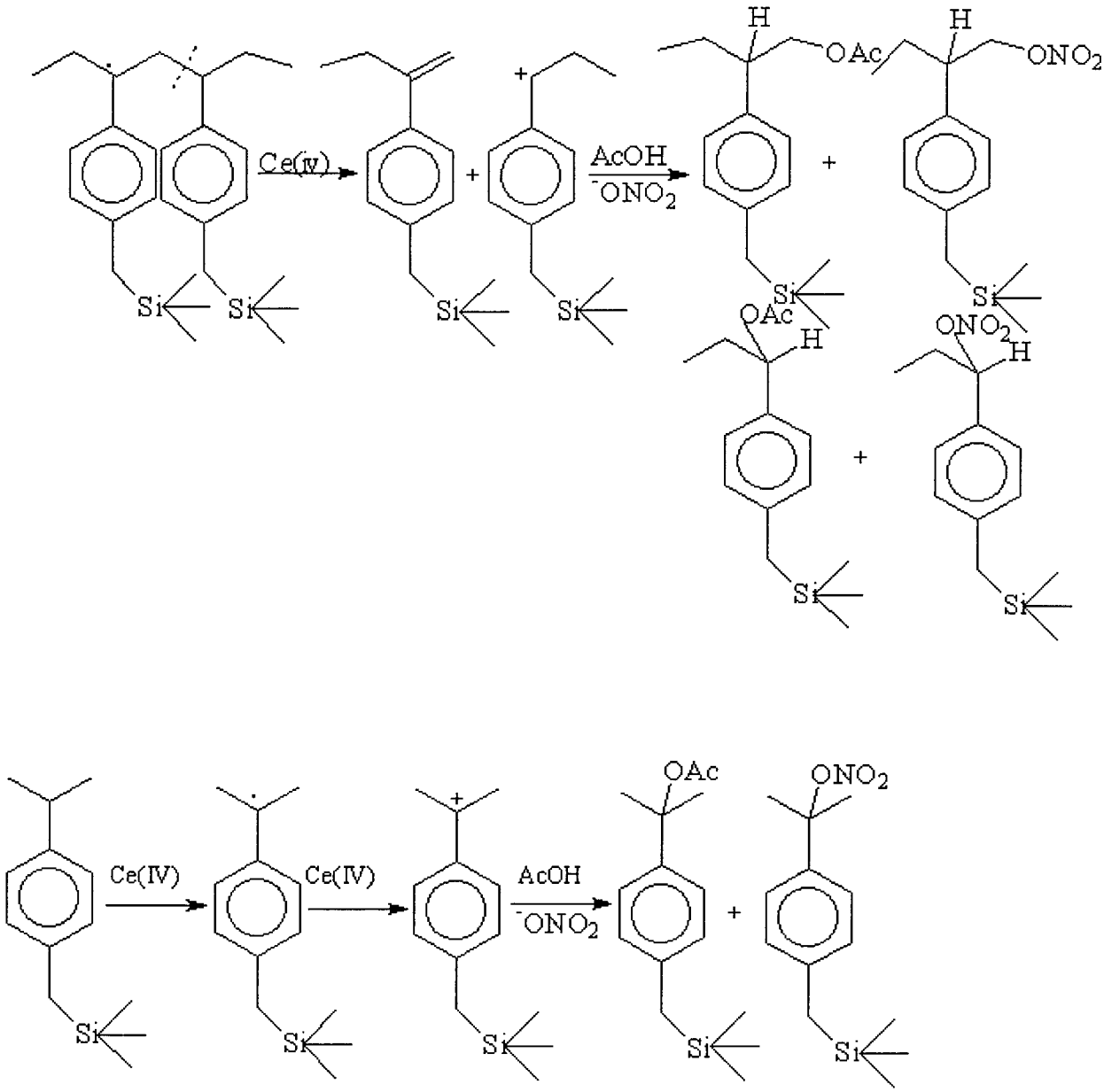

Figure 3.5.11 Possible mechanism of polymer backbone cleavage (Top) and substituent oxidation (Bottom) of 4-isopropylbenzyltrimethylsilane (ISO-BTMS).

The common reactivity scale of hydrocarbons towards hydrogen radical abstraction[78,79] is $3^{o} > 2^{o} > 1^{o}$. Russel *et al.* found the *tertiay* hydrogens of cumene and *p*-cymene to be approximately one order of magnitude more reactive than the primary hydrogens towards hydrogen abstraction by either peroxy radicals[80] or photochemically induced chlorine[81] radicals. In contrast to this rule, Ferrari's oxidation reaction of cobalt(III) on poly(4-methylstyrene) [32] showed a selectivity of 25:1 for oxidation at primary 4-methyl position over *tertiary* methine (C-H) group on the polymer backbone. The former leads to the oxidation products functionalized at 4-methyl group and the latter to oxidative cleavage of polymer backbone. Ferrari proposed two mechanisms for the oxidation. The first one involves a direct hydrogen abstraction step from either primary 4-methyl group or *tertiary* methine (C-H) group to form primary or tertiary radical, followed by an electron transfer to the oxidant, and a reaction with nucleophile to form oxidation products, including poly(4-methylstyrene) functionalized at 4-methyl postion and chain cleaved poly(4-methylstyrene). The second mechanism suggests an electron transfer step from the aromatic ring to (Co(III)) to form a radical cation that looses a proton from either primary 4-methyl group or *tertiary* methine (C-H) group to form primary or *tertiary* radical. These radicals then form the oxidation products as either poly(4-methylstyrene) functionalized at 4-methyl postion or the chain cleaved poly(4-methylstyrene).

The selectivity of 25:1 for forming a primary benzylic radical over tertiary radical is attributed to the fact[30] that during the loss of hydrogen from the primary methyl group, the weakening C-H bond can overlap effectively with the aromatic π-system, reducing the activation energy for the C-H bond cleavage. In contrast, the weakening or breaking

of methine C-H bond is prevented from overlap with the aromatic system by the steric congestion of the neighboring backbone with aromatic *ortho* hydrogens. Voronenkov[82] *et al.*used the same concept to account for the higher stability calculated for the primary compared to the tertiay radical cation of *p*-cymene. During the study of CAN/acetic acid promoted oxidation reaction of α-Z-substituted *p*-xylens (Z = OMe, OH, Me, *t*-Bu, OAc, CO_2Me, CN) to determine the relative reactivity of substituted and the unsubstituted methyl group, k (CH_2Z) / k (CH_3), in the deprotonation of the alkylaromatic radical cation, Baciocchi[77] *et al.* suggested that the rate of deprotonation from the alkylaromatic radical cation is influenced by the relative orientation of C_α-H bond and the aromatic π-system (steroelectronic effect). Their collinearity is expected for better stabilization of the incipient benzylic radical. A value of <0.01 reported by Baciocchi[77] for the ratio, k (CH_2Z) / k (CH_3), when Z = *t*-Bu is attributed to the fact that the interaction between the bulky *t*-Bu group and the ring ortho hydrogens results in a conformation where the C_α-H bond in not collinear with aromatic π-system, so that the stabilization of the benzylic radical formed after deprotonation is not possible.

The benzylsilyl substrates are reported to be oxidized by CAN/acetic acid mainly through the radical cation intermediate.[31] The steric congestion offered by the polymer backbone against methine hydrogen loss together with a 100 times easier loss of trimethylsilyl cation than a proton from the backbone methine (C-H) group eliminate the possibility of backbone cleavage in our polymeric benzylsilyl substrates and the oxidation of isopropyl group in 4-isopropylbenzyltrimethylsilane (ISO-BTMS). The former is supported by the GPC data of the oxidation products, as shown in Table 3.5.3.

The number average molecular weight (Mn) of the oxidized product is not significantly different from that before the oxidation in all cases except in the homopolymer, which suffered from both crosslinking and chain degradation. The data shows that the oligomer is completely free of chain degradation. For styrene copolymers, VS15 (VBTMS:Sty 1:5) and VS12 (VBTMS:Sty 1:2), the molecular weight data measured during the reaction does not support for any chain degradation. Structurely, MMA copolymers are strongly self-protected from chain degradation[30] by the methyl groups in their backbone.

Table 3.5.3 Evidence for absence of backbone degradation of linear polymer analogs

Polymer substrate/ Mn	Reaction condition	Mn of oxidized product at different reaction time
VBTMS-oligomer / 3300	CAN/AcOH/Bz/50°C	3512, 3493, 3553, 3203
VBTMS-homopolymer / 13200	CAN/AcOH/Bz/50°C	12950, 13390, crosslinked
VBTMS-homopolymer / 13200	CAN/AcOH/Bz/65°C	5605, 2500, 2363
Poly(VBTMS-*co*-Sty) VS15 / 10000	CAN/AcOH/Bz/65°C	12100, 11250, 12200
Poly(VBTMS-*co*-Sty) VS12 / 17200	CAN/AcOH/Bz/65°C	17330, 22380, 20030, 22980
Poly(VBTMS-*co*-MMA) VM12 / 26600	CAN/AcOH/Bz/65°C	25700, 28310, 25650, 28700
Poly(VBTMS-*co*-MMA) VM11 / 40800	CAN/AcOH/Bz/65°C	34270, 37490, 30710, 36530

3.5.3 Oxidative degradation of bis(vinylbenzyl)trimethylsilane microspheres

Similar to the small model molecules and the linear polymer analogs, CAN induced reaction was attempted on cross-linked BVBDMS microspheres. The reaction progress was monitored by measuring the particle size reduction of the degraded particles as a function of the reaction time. The particle size data is depicted in Table 3.5.4

Table 3.5.4 Effect of CAN oxidation time on particle size of BVBDMS particles.

Reaction time hrs	0.0	2.0	3.0	4.0	5.0	6.0	9.0
Particle size μm	2.29	1.5	0.725	0.725	0.682	0.68	0.52
CV%	14.3	28.2	31.35	30.38	59.8	27.7	57.8

Conditions: BVBDMS particles 0.5 mmol (1 mmol in monosilane functionality); CAN 3 mmol; AcOH 30 ml; Benzene 30 ml; Temp. 50 ^{o}C.

Figure 3.5.12 shows the SEM pictures of the oxidation products of BVBDMS particles. The particle size reduction as a function of reaction time is clearly seen in the SEM pictures. The morphological change on the particles during the reaction indicates for a random reaction starts at the particle surface and slowly advances into the interior of the paticles. The merging of particles is a sign of significant cleavage of cross-links at the particle surface and subsequent surface layer solvation. Since, the particles have very high crosslink density, the reaction is slow compared to that on the linear analogs. As the CAN reaction is extremely fast, and there is no gradient in crosslink density from particle-surface to particle-center due to the two double bonds of BVBDMS are isolated and of similar reactivity, the SEM pictures of degraded particles indicate a random reaction on the particles. Apart from taking the particle size reduction data and the corresponding SEM pictures of degraded particles, an attempt was made to quantify Si-C bond cleavage by following the FT-IR spectrum of both degraded particles and of corresponding soluble fraction from the reaction. However, both spectra gave very broad peaks, likely due to a multitude of functional groups, and were impossible to interpret.

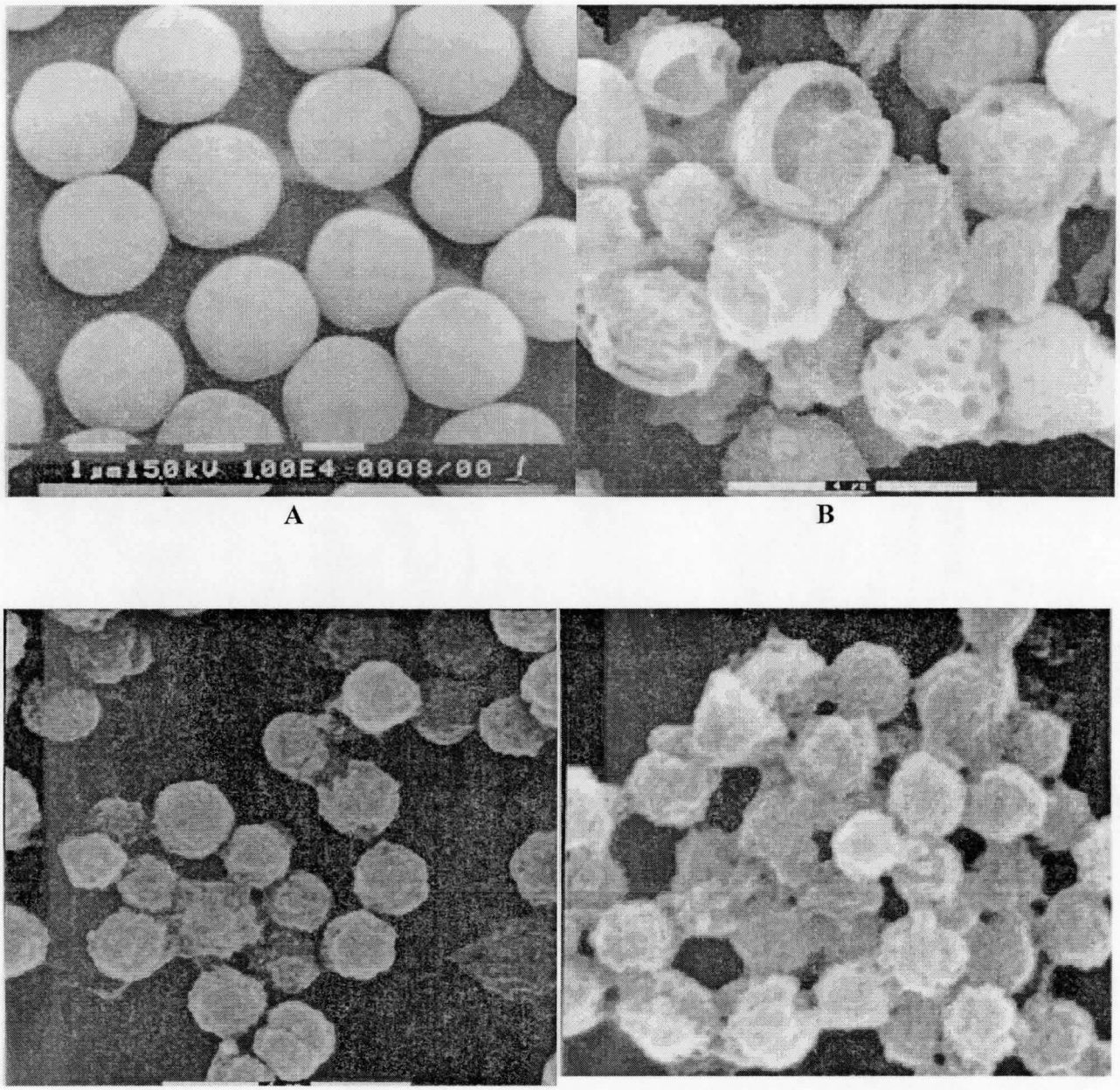

Figure 3.5.12 SEM micrographs of degraded bis(vinylbenzyl)dimethylsilane (BVBDMS) microsphers by CAN at the reaction times A) 0 hr B) 2 hrs C) 4 hrs D) 9 hrs. Conditions: CAN 3 mmol; AcOH 30 ml; Benzene 30 ml; BVBDMS Particles 1 mmol (as mono silane functionality); Temp. 50 ^{o}

3.6 Conclusions

Chemical cleavage of several substrates containing benzylic-silicon bonds was successfully carried out using hydroxide ion and fluoride ion as nucleophilic reagents, and ceric ammonium nitrate as an oxidative reagent. Small substrate molecules including benzyltrimethylsilane (BTMS), *p*-isopropylbenzyltrimethylsilane (ISO-BTMS) and bis(vinylbenzyl)dimethylsilane (BVBDMS) were synthesized by Grignard reaction. Vinylbenzyltrimethylsilane-oligomer, poly(vinylbenzyltrimethylsilane), and styrene and methyl methacrylate copolymers of vinylbenzyltrimethylsilane were prepared using free radical solution polymerization. Crosslinked network polymers including microspheres and microgels of bis(vinylbenzyl)dimethylsilane were synthesized using free radical precipitation polymerization.

Narrow dispersed microspheres were synthesized from bis(vinylbenzyl)dimethylsilane (BVBDMS) by precipitation polymerization in acetonitrile solvent. The reactivities of *para/para, meta/meta,* and *meta/para* isomers of BVBDMS cross-linker in precipitation polymerization were found to be similar and to obey first-order kinetics. Their apparent rate of polymerization is comparable with that of *meta* and *para* divinylbenzene (DVB) isomers under identical polymerization conditions. FT-IR analysis of BVBDMS microspheres shows that there are only few pendant double bonds in the particles. This is likely due to the similar reactivity of isolated double bonds in BVBDMS.

The cleavage reactions were quantitavely monitored by ^{1}H-NMR / ^{29}Si-NMR or FT-IR to derive the reaction kinetic parameters. Si-C bonds in the series of substrates were

successfully cleaved by hydroxide ion using the reagent KOH/THF/EtOH. Among the series, the small molecules and the oligomeric analog obeyed first-order kinetics, but the homopolymer and the copolymers showed an anomalous behavior of deviation from first-order kinetics. This could be due to lower concentration of hydroxide ion in the polymer matrix, arising from the exclusion of polar hydroxide ion from the hydrophobic polymer matrix. ISO-BTMS exhibited a lower first-order rate than BTMS. This is attributed to the electron releasing substituent effect. MMA was found to accelerate the reaction in poly(VBTMS-*co*-MMA) by increasing the overall copolymer polarity. The reverse is true with the corresponding styrene copolymers owing to the steric hindrance offered by the phenyl ring and the enhanced hydrophobic repulsion against the access of hydroxide ion into the polymer matrix. An electrophilically assisted process was proposed as a principal reaction mechanism for this cleavage reaction. It was found that the only nucleophile attacking on silicon would be the hydroxide ion in KOH/EtOH/THF promoted reactions.

The fluoride ion initiated cleavage reactions on the substrates containing Si-C bonds were found to follow first-order kinetics. The reaction on the small molecules was not studied due to their very rapid reaction at room temperature The homopolymer of vinylbenzyltrimethylsilane exhibited a higher rate of reaction than the corresponding oligomer. However, the change in the reaction rate within a copolymer series, differing in molecular weight and composition, was not significant. Poly(VBTMS-*co*-MMA) exhibited a higher rate than styrene copolymers for polarity or steric reasons.

The oxidative cleavage of benzylic-silicon bond by ceric ammonium nitrate (CAN) was found to obey first-order kinetics at 1:3 substrate to cerium(IV) molar ratio and did not show any deviation in reaction-order even at higher CAN concentration. The electron releasing isopropyl group reduces the oxidation potential of *p*-isopropylvinylbenzyltrimethylsilane (ISO-BTMS), resulting in an enhanced reaction rate compared to benzyltrimethylsilane (BTMS). This rate accelerating substituent effect, together with a much higher negative value (- 5.4) of Hammett reaction constant ρ is in accordance with the radical-cation mechanism operating in ceric ammonium nitrate promoted oxidation reactions. Significant loss of silane functionality was observed in reactions with polymeric substrates. This is attributed to the benzylic radical coupling reactions. The possibility of polymer backbone cleavage is ruled out for the following reasons: A) lack of significant molecular weight reduction in the oxidation products of polymeric substrates. B) 100 times faster breaking of benzylic-silicon bond as trimethylsilyl cation than a hydrogen from carbon as proton, and the steric congestion offered by the polymer chain favors the benzylic radical formation only at the primary carbon, not on *tertiary* methine (C-H) on the chain.

3.7 REFERENCES

1. E. W. Colvin, *Silicon in organic synthesis*, Butterworths, London (1981), chapter 2 & 3.

2. E. AV. Ebsworth, in *Organometalic Compounds of the group 4 Elements*, Ed. A. G. MacDiarmid, Vol.1, Part 1, New York (1968).

3. E. Alan Pierce, in *Silylation of Organic Compounds*, Pierce chemical company, Rockford, Illinois, chapter 4.

4. J. R. Hwu and J. M. Wetzel, *J.Org.Chem.*, **50**, 3946 (1985).

5. I. Fleming, *Chemi.Soci.Rev.*, **10**, 83 (1981).

6. T. H. Chan, *Tetrahedron Lett.*, 171 (1974).

7. L. H. Sommar and F. C. Whitmore, *J.Am.Chem.Soc.*, **68**, 485 (1946).

8. L. H. Sommar and F. C. Whitmore, J. Gold and R. E. Van Sterien, *J.Am.Chem.Soc.*, **68**, 1551 (1947).

9. D. Grafstein, *J.Am.Chem.Soc.*, **77**, 6650 (1955).

10. J. P. Pillot, B. Bennetae, J. Dunogues and R. Calas, *Tetrahedron Lett.*, **22**, 3401 (1981).

11. F. K. Cartledge and J. P. Jones, *J.Organomet.Chem.*, **67**, 379 (1974).

12. S. Patai, in *The chemistry of organic silicon Compounds.*, John Wiley & Sons, An Interscience Publications, Part-1, chapter 14.

13. A. G. Brook, J. M. Duff and W. F. Reynolds, *J.Organomet.Chem.*, **121**, 293 (1976).

14. I. Fleming, in *Comprehensive Organic Chemistry*, Vol. 3, Pergamon Press, Oxford, 1979, chapter 13.

15. A. C. Hopkinson, *J.Org.Chem.*, **46**, 998 (1981).

16. C. G. Pitt, *J.Organomet.Chem.*, **61**, 49 (1973).

17. G. R. Buell, R. Corriu and L. Spialter, *J.Am.Chem.Soc.*, **92**, 7424 (1970).

18. W. F. Reynolds and G. K. Hamer, *J.C.S. Perkin II.*, 971 (1977).

19. W. Hanstein and T. G. Tayler, *J.Am.Chem.Soc.*, **92**, 7476 (1970).

20. W. Hanstein and T. G. Tayler, *J.Am.Chem.Soc.*, **92**, 829 (1970).

21. T. Schaefer, R. Sebastian and G. H. Penner, *Can.J.Chem.*, **69**, 496 (1991).

22. T. Schaefer, G. H. Penner and C. S. Takeeuchi, *Can.J.Chem.*, **67**, 1283 (1989).

23. C. Eaborn, in *Organosilicon Compounds,* Butterworths, Scientific Publications, London (1960).

24. C. R. Hauser, *J.Am.Chem.Soc.*, **73**, 5846 (1951).

25. H. Gillman, *J.Am.Chem.Soc.*, **75**, 4531 (1953).

26. C. Eaborn and Parker, *J.Am.Chem.Soc.*, **73**, 126 (1955).

27. H. H. Szmant and O. M. Devlin, *J.Am.Chem.Soc.*, **73**, 3059 (1951).

28. C. Eaborn and R. W. Bott, *J.Chem.Soc.*, 1971 (1964).

29. R. A. Benkeser, *J.Am.Chem.Soc.*, **74**, 253 (1952).

30. Q. Sheng, *Functional polymers derived from 4-methyl styrene,* PhD thesis, McMaster University (1996).

31. E. Baciocchi, *Tetrahedron Lett.,* **30**, 3573 (1989).

32. L. P. Ferrari, *J.Polym.Sci.,Polym.Chem*, **33**, 957 (1995).

33. J. Yoshida and T. Murata, *Tetrahedron Lett.,* **27**, 3373 (1986).

34. P. J. Flory, in *Principles of Polymer Chemistry*, Cornell University Press, Ithaca, NY (1953) Chapter 3.

35. M. Lazar, 'Characteristic feactures of chemical reactions of macromolecules' in *Chemical reactions of natural and synthetic polymers*, chapter 2.

36. J. C. Bevington, 'Chemical modifications of synthetic polymers' in *Comprehensive Polymer Science*, Pergamon Press, Oxford. Vol.6, P.24.

37. R. W. Lenz, 'Polymer reactions' in *Organic Chemistry of Synthetic High Polymers,* Interscience Publishers, Chapter 17.

38. A. Hvidt and R. Corett, *J.Am.Chem.Soc.*, **92**, 5546 (1970).

39. D. D. Muller, *J.Am.Chem.Soc.*, **89**, 6024 (1967).

40. J. C. Bevington, *'Chemical modifications of synthetic polymers'* in *Comprehensive Polymer Science*, Pergamon press, Oxford. Vol.6, p.30.

41. L. Segel, 'Influence of Morphology on Reactivity', in *Chemical reactions of polymers,* E. Fetters, Mir, Moscow (1967), Vol.1, p.46.

42. S. P. Rowland, 'Solid-liquid interactions', in *Applied Fibre Science.* F. Happey, Academic Press London, 1979, Vol. 2, p.205.

43. H. Morawetz, in *Chemical Reactions of Polymers*, E. Fetters, Mir, Moscow 1967, Vol.1, p.16.

44. D. Bernard, *J.Am.Chem.Soc.*, **77**, 5472 (1955).

45. I. Sakurada, *Pure Applied Chem.*, **16**, 263 (1968).

46. N. A. Plate, *Pure Appli.Chem.*, **46**, 49 (1976).

47. H. D. H. Stover and W. H. Li, *J.Polym.Sci., Part A: Polym.Chem.*, **32**, 2023 (1994).

48. Y. Nagasaki and T. Tsuruta, *Makromol.Chem.*, **190**, 1855 (1989).

49. K. Li, *Functional crosslinked polymer microspheres*, PhD thesis. McMaster University.

50. J. S. Doweny, R. S. Frank and H. D. H. Stover, *Macromolecules,* **32**, 2838 (1999).

51. R. S. Frank, *Crosslinking copolymerization of divinylbenzene and maleic anhydride*, PhD thesis. (2000), McMaster University.

52. M. Imoto, M. Kinoshita and M. Nishigaki, *Makromol.Chem.*, **86**, 217 (1965) .

53. Y. Nagasaki, S. B. Han and M. Kato, *Makromol.Chem.,* **193**, 1633 (1992).

54. Y. Nitadori and T. Tsuruta, *Makromol.Chem.,* **179**, 2069 (1978).

55. V. Bandrup and E. H. Immergut, *Polymer Hand book*, Wiley-Interscience Publications (1989).

56. A. Willey, *J.Macromol.Sci-Chem.,* **A4(7)** 1453 (1970)

57. C. Eaborn and R. W Bott, *J.Am.Chem.Soc.*, 2342 (1963).

58. C. Eaborn, *J.C.S. Perkin II.*, 203 (1979).

59. J. F. Bunnett, *J.Am.Chem.Soc.*, **76**, 3011 (1954).

60. R. Alexander and C. Eaborn, *J.Organomet.Chem.*, **21**, 65 (1970).

61. R. Alexander, W. A. Asomaning, C. Eaborn, I. D. Jenkins and D. R. M. Walton, *J.C.S. Perkin I.,* 490 (1974).

62. C. Eaborn and W. A. Stanczyk, *J.C.S. Perkin Trans.II.,* 472 (1991).

63. I. D. Jenkins and C. Eaborn, *J.Organomet.Chem.*, **69**, 185 (1974).

64. C. Eaborn, R. Eastmond, and M. Walton, *J.C.S.(B),* 127 (1971).

65. C. Eaborn, R. W. Bott and B. M. Rushton, *J.Organomet.Chem.*, **3**, 448 (1965).

66. C. Eaborn and F. M. S. Mahmoud, *J.Organomet.Chem.,* **206**, 49 (1981).

67. H. Morawetz and CHIN-PAO SU, *J.Polym.Sci., Polym.Chem.*, **15**, 185 (1977).

68. M.Talu and H. B. Ozgun, *Eur.Polym.J.,* **26**, 5 (1990).

69. V. Bohmer, H. E. Sauerbrey, and H. Kammerer, *Makromol.Chem.*, **175**, 391 (1974).

70. S. E. Rankin, S. J. Kirchner and A. V. McCormick, *J. Non-Cryst.Solids.*, **258**, 187-197 (1999).

71. E. F. Caldin and G. Long, *Nature.*, **172**, 583 (1953).

72. E. Baciocchi, L. Mandolini and C. Rol, *Tetrahedron Lett.*, **37**, 3343 (1976).

73. E. Baciocchi and C. Rol, *J.Org.Chem.*, **42**, 3682 (1977).

74. O. C. Norman, C. B. Thomas and P. J. Ward, *J.C.S. Perkin Trans.II.*, 2974 (1973).

75. E. Baciocchi and C. Rol and R. Ruzziconi, *J.Chem.Research.*, 334 (1984).

76. E. I. Heiba, R. M. Dessau, and W. J. Koehl, *J.Am.Chem.Soc.*, **91**, 6830 (1969).

77. E. Baciocchi, M. Mattioli and R. Romano, *J.Org.Chem.*, **56**, 7154 (1991).

78. C. Walling, *Free radicals in solution*, J. Wiley & Sons, Inc., New York, 1957.

79. R. A. Sheldon and J. K. Kochi, Metal-Catalized Oxidations of Organic Compounds, Academic Press, New York, 1981, chapter 10.

80. G. A. Russel, *J.Am.Chem.Soc.*, **78**, 1047 (1956).

81.G. A. Russel, A. Ito, and D. G. Hendry, A. N. Bourns *J.Am.Chem.Soc.*, **85**, 2976 (1963).

82. V. V. Voronenkov and V. N. kokorev, *J.Org.Chem. USSR*, 2302 (1990).